

Aus dem Fachbereich Biophysik
Theoretische Medizin und Biowissenschaften
der Medizinischen Fakultät
der Universität des Saarlandes, Homburg, Saar

Migration of Primary Human Lymphocytes in 3D matrices

Dissertation zur Erlangung des Grades eines Doktors der Naturwissenschaften

der Medizinischen Fakultät
der Universität des Saarlandes

2018

Vorgelegt von Rouven Schoppmeyer
Geb. am 11.03.1984 in Lindlar, Deutschland

Tag des Promotionskolloquiums: _____

Dekan: _____

Vorsitzender: _____

Berichterstatter: _____

Table of Contents

List of Figures.....	7
List of Tables	8
List of Abbreviations	9
1. Abstract / Zusammenfassung.....	11
1.1 Abstract.....	11
1.2 Zusammenfassung	13
2. Introduction	15
2.1 Innate and adaptive immune system.....	15
2.1.1 Adaptive immune system	16
2.2 Immune killer cells: natural killer cells and cytotoxic T lymphocytes.....	17
2.2.1 Target recognition by killer cells.....	18
2.3 Cytotoxic T lymphocytes	19
2.3.1 The T cell receptor.....	20
2.3.2 <i>In vitro</i> T cell populations	21
2.3.3 Killing machinery of CTL	22
2.3.3.1 Immunological synapse	22
2.3.3.2 CTL cell-mediated cytotoxicity.....	23
2.4 How killer cells find their battleground.....	24
2.5 The extracellular matrix.....	25
2.5.1 ECM proteins.....	26
2.5.2.1 Collagens	26
2.5.2.2 Fibronectin.....	27
2.5.2 Hyaluronic acid.....	28

2.5.3 Integrins and the extracellular matrix	28
2.6 Cell migration	30
2.6.1 Modes of migration	31
2.6.2 2D vs. 3D migration systems.....	32
2.6.3 Cell polarization	36
2.6.3.1 Polarization - Small GTPases	38
2.6.3.2 Polarization and migration - Leading edge and uropod	39
2.6.3.3. Polarization maintenance in T cells.....	39
2.6.5 Cytoskeleton	40
2.6.5.1 Actin	40
2.6.5.2 Microtubules and microtubule organizing center (MTOC).....	42
2.6.6 Analyzing cell migration	43
2.5.6.1 Advantages of SPIM for 4D imaging.....	44
2.7 Profilin and actin dynamics	45
2.7.1 Profilin expression in humans	47
2.7.2 Profilin regulation.....	48
2.8 Project aims	50
3. Materials and methods.....	52
3.1 Reagents and antibodies	52
3.2 Cell Culture	53
3.2.1 Continuous cell culture of suspension cell lines.....	53
3.2.2 Isolation and culture of primary human lymphocytes	54
3.2.2.1 PBMC isolation	54
3.2.2.2 Staphylococcal enterotoxin A (SEA) stimulation of human PBMC	55
3.2.2.3 Positive isolation of CD8 ⁺ from PBMC	55

3.2.2.4 Negative isolation of CD8 ⁺ or NK cells from PBMC	55
3.2.2.5 Cell culture of primary cells	56
3.2.2.6 Bead stimulation of untouched isolated CD8 ⁺ cells using α CD3/CD28 antibody coated beads.....	56
3.3 Electroporation (plasmids and siRNA) of primary human CTL	57
3.3.1 siRNA	57
3.4 Real-time killing assay (Kummerow et al. 2014).....	58
3.4.1 Staphylococcal Enterotoxin A pulsing of Raji cells for real time killing.....	59
3.5 Live cell imaging	59
3.5.1 Cell labeling for fluorescence microscopy	59
3.5.2 Preparation of “Nutragen” and “Fibricol” collagen solution	59
3.5.5 Epifluorescence Microscopy	60
3.5.7 Fixation of cells in collagen	60
3.5.8 IF staining of CTL in collagen droplets on coverslips / μ dishes.....	61
3.5.9 Height measurement of 2D matrix	61
3.6 Single plane illumination microscopy	61
3.6.1 Sample preparation for SPIM imaging and tracking analysis	61
3.6.2 Single plane illumination microscopy (SPIM)	62
3.6.3 Fixation of primary CTL in collagen rods.....	63
3.6.4 Automated cell detection and tracking of SPIM data using Imaris.....	63
3.7 2D matrix migration	63
3.8 Data Analysis.....	64
3.9 Statistics and graphing.....	64
3.10 Ethics	64
4. Results	66

4.1 Development of 3D migration assays.....	66
4.1.1 3D Biology	66
4.1.2 Automated cell tracking and analysis	67
4.1.2.1 Parameters for quantification of migration.....	68
4.1.3 Choosing a fluorescent dye for automated tracking analysis	70
4.1.3.1 Testing fluorescent small molecule dyes for cell tracking	70
4.1.3.2 H33342 nuclear labeling does not affect primary human lymphocyte migration	72
4.1.4 The 2D matrix migration system	74
4.1.5 3D matrix migration system - Single plane illumination microscopy (SPIM).....	76
4.1.5.1 Imaging primary lymphocytes in 3D matrices using SPIM	76
4.1.5.2 Collagen concentrations and CTL migration in 3D and 2D matrix systems (data courtesy of Dr. Renping Zhao, University of Saarland, Biophysics, Homburg, Germany).....	78
4.1.6 Migration parameters of primary human lymphocytes in collagen type I	79
4.1.6.1 Bead stimulated CTL migrate with higher persistence than unstimulated CTL or NK in collagen	79
4.1.6.2 Matrix modifications using ECM components to modulate CTL and NK migration.....	81
4.1.6.2.1 Non-crosslinked modification of a collagen matrix	81
4.1.6.2.1.1 Fibronectin modulates migration of bead stimulated CTL by altering persistence and velocity	81
4.1.6.2.1.2 Hyaluronic acid modulates persistence of bead stimulated CTL	82
4.2 Profilin-1, pancreatic cancer and CTL	84
4.2.1 PFN1 dysregulation can result in CTL dysfunctionality and induce cancer	86
4.2.2 Profilin-1 expression in primary human CTL	86

4.2.3 Profilin-1 is a negative regulator of CTL cytotoxicity	87
4.2.4 Profilin-1 in cell migration	88
4.2.4.1 CTL migration in 3D depends on PFN1 binding to poly-L-proline ligands and PIP ₂	88
5. Discussion.....	92
5.1 Migration of lymphocytes	92
5.1.1 Imaging 3D volumes	93
5.1.2 3D Migration	93
5.1.2.1 Choosing a matrix system	94
5.1.2.2 Methods for analysis of lymphocyte migration.....	95
5.1.2.2.1 2D matrix	96
5.1.2.2.2 3D SPIM.....	96
5.1.4 Tracking cells in 3D	97
5.1.5 A fluorescent label for migrating cells	98
5.1.6 Migration of lymphocytes in a collagen matrix	98
5.2 Migration tuning by extracellular matrix components	100
5.2.1 Fibronectin and CTL migration.....	101
5.2.2 Hyaluronic acid and CTL migration.....	101
5.2.3 Matrix modifications and experimental design	103
5.2.4 Mechano-sensing by CTL	103
5.3 Conclusion on lymphocyte 3D migration.....	103
5.5 Profilin and CTL.....	104
5.5.1 Profilin1, CTL and cancer	105
5.5.2 Profilin characterization in human CTL.....	105
5.5.3 Profilin1 function in primary human CTL	106

5.5.3.1 Profilin1 and CTL cytotoxicity	106
5.5.3.2 Profilin1 and CTL migration	107
5.5.4 Conclusion on PFN1 function in CTL.....	109
6. References	111
7. Publications	121
8. Acknowledgements	122

List of Figures

Figure number	Title	Page
Figure 1	Mechanism of leukocyte extravasation from a blood vessel	25
Figure 2	Integrin $\alpha\beta$ heterodimers define the adhesion molecule binding of a T cell	30
Figure 3	The mode of migration of lymphocytes is tuned by extracellular cues	32
Figure 4	2D and 3D amoeboid motility are defined by substrate, substrate binding strength, cell contractility and protrusive forces	34
Figure 5	General aspects of cell polarization during migration of a eukaryotic cell	38
Figure 6	Schematic of a simple SPIM setup	44
Figure 7	Profilin promotes elongation of nucleated actin filaments	47
Figure 8	Cell morphology in 3D collagen	67
Figure 9	Migration analysis using automated tracking software (Imaris, Bitplane AG)	69
Figure 10	A fluorescent label for analysis of migration	71
Figure 11	H33342 does not alter migration parameters of primary human bead stimulated CTL in collagen	73
Figure 12	The 2D matrix system generates a thin matrix that allows cells embedded in a matrix to be imaged within a single imaging plane	75
Figure 13	Substrate concentration affects migration parameters	77
Figure 14	Increasing collagen concentration effectively reduces average velocity and maximal velocity in 3D SPIM and 2D matrix	79
Figure 15	Bead stimulated CTL migrate with higher persistence than unstimulated CTL	80
Figure 16	Fibronectin modulates velocity and persistence of bead stimulated CTL in 3D	82
Figure 17	Hyaluronic acid modulates persistence of CTL in 3D	83
Figure 18	Expression of PFN1 is decreased in peripheral CD8 ⁺ T cells from patients with pancreatic cancer	85
Figure 19	PFN1 is a negative regulator for CTL-mediated cytotoxicity	88
Figure 20	PFN1 regulates CTL persistence and velocity via phospholipid and poly-L-proline interactions	90

List of Tables

Table number	Title	Page
Table 1	ECM components used in this work	27
Table 2	Material list	52
Table 3	Antibody list	52
Table 4	Plastic and glass ware	53
Table 5	Continuous cell lines and corresponding culture conditions	53
Table 6	Continuous cell line sources	53
Table 7	Cell culture reagents	54
Table 8	Primary cell isolation/stimulation kits	54
Table 9	Primary cell culture supplements	56
Table 10	siRNA used in experiments	57
Table 11	Colibri LEDs equipped in the Cell Observer Z.1	60
Table 12	Objective list of the Cell Observer Z.1	60
Table 13	Filter sets of the Cell Observer Z.1	60
Table 14	Solid state laser used in experiments of the Lightsheet Z.1 system	62
Table 15	Detection and illumination objectives of the Lightsheet Z.1	62
Table 16	Equipped beam splitters of the Lightsheet Z.1	62
Table 17	Migration parameters determined for primary human lymphocytes	81
Table 18	Coefficients of correlation from the average MSDs (Fig. 11) and the correlating mode of migration	91

List of Abbreviations

ADP	Adenosine diphosphate
AIMV	Proprietary serum free lymphocyte proliferation medium
APC	Antigen presenting cell (incl. macrophages, B cells and dendritic cells)
Arp2/3	Actin related protein 2/3 complex
ATP	Adenosine triphosphate
CD XXX (where X is a number)	Cluster of differentiation - surface proteins of immune cells
CD107a aka LAMP1	Lysosomal membrane protein 1
CD4 ⁺ T cell	CD4 expressing T cells - helper T cells
CD8 ⁺ T cell	CD8 expressing T cells - cytotoxic T cells
CTL	Cytotoxic T lymphocyte
CTLbs	CD8 ⁺ T cells <i>untouched</i> isolated from PBMC and α CD3/ α CD28 <u>be</u> ad <u>st</u> imulated
CTLus	CD8 ⁺ T cells <i>untouched</i> isolated from PBMC <u>un</u> stimulated
Ctrl	Control
DPBS	Dulbecco's Phosphate buffered saline
EBP	End binding protein
ECM	Extracellular matrix
F-actin	Filamentous actin (polymer)
FN	Fibronectin
G-actin	Globular actin (monomers)
H33342	HOECHST 33342 bis-benzimide blue fluorescent nuclear dye
HA	Hyaluronic acid
HEV	High endothelial venules
ICAM-1	Intercellular adhesion molecule 1
IL-2	Interleukin 2 - a potent leukocyte chemokine
IL2R $\alpha/\beta/\gamma$	Interleukin 2 receptor $\alpha/\beta/\gamma$ subunits
IS	Immunological synapse
kDa	Kilo Dalton (molecular weight)

LED	Light emitting diode
LFA-1	Leukocyte functional antigen 1 - a cell adhesion molecule
LG	Lytic granule
mENA	Mammalian Enabled
mL	Milliliter
mM, nM, μ M	Milli-, nano-, micromolar
mRNA	Messenger RNA
MSD	Mean squared displacement
MTOC	Microtubule organizing center
MW	Molecular weight
NK	Natural killer cell
PBMC	Peripheral blood mononuclear cells
PCR	Polymerase chain reaction
PFN	Profilin
Pi	Inorganic phosphate
PRW	Persistent random walk - a migration strategy
qRT-PCR	Quantitative real time PCR
SBP	Side binding protein
SEA	Staphylococcal enterotoxin A
siRNA	Small interfering ribonucleic acid
SPIM	Single plane illumination
SYTO X	SYTO green fluorescent nuclear dye (x = number)
TBP	TATA box binding protein
TMBN	Tandem monomer binding nucleator
TSM	Track speed mean ($\mu\text{m s}^{-1}$)
VASP	Vasodilator stimulated phosphoprotein
WASP	Wiskott Aldrich syndrome protein
WAVE	WASP-family verprolin-homologous protein

1. Abstract / Zusammenfassung

1.1 Abstract

Cytotoxic T cells protect us from viruses and tumors and move large distances within the body to find infected or transformed target cells. Their migration is an interplay of their intrinsic ability to migrate and to sense their environment and adapt to it. The composition of extracellular signals and physical contact to connective tissue fibers modulates the migration of T cells. To be able to analyze lymphocyte behavior in 3D I first developed new imaging methods in 3D environments for epifluorescence and Single Plane Illumination Microscopy (SPIM) using collagen as matrix. As a natural non-toxic substrate that is biologically active and can form sponge-like porous matrices that are homogenous and stable under physiological conditions collagen is a perfect starting point to remodel basic tissue architecture and determine basic migration parameters of lymphocytes. Using this collagen based system with a flattened matrix to avoid out of focus migration of cells (2D matrix) I could determine the basic migration parameters of primary human cytotoxic T lymphocytes (CTL) and natural killer cells (NK) in a 3D environment using epifluorescence microscopy. In 0.25 % collagen, representing normal tissue interstitial matrix, lymphocytes migrate in a random walk at average speeds $\sim 5 \mu\text{m min}^{-1}$ (range $\sim 0.6 - 18 \mu\text{m min}^{-1}$) and low average persistence. Bead stimulation of CTL that enriches effector and effector memory subtypes, increases average persistence while average velocity is nearly unchanged. By adding extracellular matrix (ECM) compounds the matrix can easily be modified and cell behavior can be modulated. E.g. fibronectin can modulate cell velocity and persistence while fragmented hyaluronic acid, mimicking inflammation or injury, can modulate persistence of CTL. Transferring the collagen system to selected plane illumination microscopy (SPIM) for long term imaging of large 3D volumes SPIM is highly advantageous as it reduces potential toxicity from illumination of the sample and is unraveled in acquisition speed. Additionally the high resolution and frame rate of SPIM systems allows imaging large volumes of containing hundreds of cells or large organoids / spheroids while at the same time catching subcellular dynamic structures like filopodia or actin waves. A system to analyze CTL biology in SPIM experiments was developed and established successfully. Having set up 3D imaging methods we aimed to elucidate the function of a protein central to CTL dynamics governed by actin polymerization: profilin. Many cytosolic proteins are involved in cytoskeletal remodeling yet not much is known about the dynamic control in human CTL.

Profilin1 (PFN1) an actin binding protein that lies at the border of cytoskeletal dynamics and signaling pathways, was found, by our Chinese collaborators in Shanghai, to be downregulated in CTL from pancreatic cancer patients. Using overexpression systems of PFN1 (and mutations) with fluorescent fusion proteins and siRNA downregulation we could show that PFN1 is a negative regulator of CTL cytotoxicity and that interactions with phospholipids and regulatory proteins are important for proper regulation of migration. Interestingly actin polymerization rates appear almost unaffected by changes of the relative PFN1:G-actin concentration as is the case for overexpression of PFN1, the Y59A (abolished actin binding) mutant and CTL with siRNA downregulation of PFN1. Apart from this we could show that PFN1 in primary human CTL modulates the protrusion pattern during migration and the release of LGs at the IS via actin structure modulation at the IS. This shows that especially the interplay with phospholipid pathways is an important function for PFN1 apart from supplying actin monomers to polymerizing actin filaments. The results of the profilin study were published in 2017 (Schoppmeyer et al. 2017).

1.2 Zusammenfassung

Zytotoxische T Zellen beschützen uns vor Viren und Tumorzellen und müssen dafür große Distanzen im Körper und Gewebe zurücklegen um infizierte oder transformierte Zellen zu finden und eliminieren. T-Zell Migration ist ein Zusammenspiel von extrazellulären Signalen, physischem Kontakt zu Fasern der extrazellulären Matrix, zytoskeotaler Dynamik und dem intrazellulärer Signalwege. Um das Migrationsverhalten von Lymphozyten zu analysieren habe ich zuerst neue Imaging-Methoden entwickelt in 3D Umgebungen für die Epifluoreszenz- und Lichtblattmikroskopie (Selected Plane Illumination Mikroskopie oder SPIM) mit Kollagen als grundlegender Matrix. Diese Methoden werden in dieser Arbeit als 2D Matrix (Epifluoreszenz) und 3D SPIM (Lichtblattmikroskopie) benannt. Die natürliche und nicht toxische Kollagenmatrix ist biologisch aktiv und polymerisiert unter physiologischen Bedingungen zu schwamm-artigen, porösen, homogene und stabilen Matrizen. Dies macht Kollagen zu dem perfekten Startpunkt zur Remodellierung einer grundlegenden Gewebearchitektur und Bestimmung der Grundlegenden Migrationsparameter von Lymphozyten. Mit Hilfe des Kollagen basierten Systems und einer verflachten Matrix (10 - 15 μm) um eine „out of focus“ Migration der Zellen zu verhindern konnte ich Grundlegende Parameter von primären humanen Lymphozyten von gesunden Spendern mit Hilfe des 2D Matrixsystems bestimmen. Lymphozyten migrieren mit einer Zufallsbewegung mit einer Durchschnittsgeschwindigkeit von etwa 5 $\mu\text{m min}^{-1}$ und niedriger Persistenz in 0.25 % Kollagen. Bead Stimulation von CTL, welche Effektor und Effektor-Gedächtniszellen in der Population anreichert, erhöht die durchschnittliche Persistenz der Population während die Durchschnittsgeschwindigkeit sich kaum verändert. Durch das Hinzufügen von Komponenten der Extrazellulären Matrix (Fibronektin und Hyaluronsäure) ist es relativ einfach möglich die Matrix und damit das Verhalten der darin migrierenden Zellen zu modulieren. Fibronektin z.B. beeinflusst sowohl die Durchschnittsgeschwindigkeit als auch die Persistenz während Hyaluronsäure nur die Persistenz beeinflusst. Zur Langzeitbeobachtung von Zellen unter physiologischen Bedingungen reicht das 2D Matrix System nicht aus auf Grund seiner Limitationen. Der Transfer des kollagen-basierten Systems zu SPIM erlaubt Langzeitaufnahmen von Zellpopulationen in 3D Volumen unter probenschonenden Bedingungen bei gleichzeitiger subzellulärer Auflösung. Das Aktin-Zytoskelett steht zentral zu dynamischen Prozessen in T Zellen und die Polymerisation von Aktinfilamenten ist die treibende Kraft für die Zellbewegung. Eine Vielzahl an Proteinen sind in der Remodellierung

des Zytoskeletts involviert aber wie dieser Prozess in CTL reguliert wird ist weitgehend unbekannt. Unsere Chinesischen Kooperationspartner in Shanghai fanden heraus, dass Profilin1, ein aktin-bindendes Protein welches die Brücke zwischen Aktindynamik und zellulären Signalwegen spannt, in CTL von Patienten mit malignem Pankreaskarzinom herunterreguliert ist. Mithilfe von Überexpression von Fluoreszenzprotein getagtem PFN1 (und bekannten Mutanten) und siRNA Knock-Down von PFN1 in primären humanen Lymphozyten konnten wir zeigen, dass PFN1 ein negativer Regulator der Zytotoxizität von CTL ist und dass Interaktionen mit Phospholipiden und Poly-L-Prolin Liganden essentiell sind für die einwandfreie Regulierung der Migration von CTL. Interessanterweise scheint die Aktinpolymerisationsrate nur marginal beeinflusst von Änderungen der relativen Konzentrationen von PFN1 und G-actin wie es sich bei Experimenten mit PFN1 und PFN1_Y59A (keine Aktinbindung durch PFN1) und siRNA Knock Down Experimenten gezeigt hat. Zusätzlich konnten wir zeigen, dass PFN1 in primären humanen CTL das Muster der generierten aktin-angetriebenen Vorstülpungen während der Migration beeinflusst, die Exozytose von lytischen Granulen sowie Aktinstrukturen an der immunologischen Synapse moduliert. Dies zeigt, dass Profilin nicht nur Aktin für die Polymerisation bereitstellt sondern auch an Lipidsignalwegen beteiligt ist und darüber die Polarisation beeinflussen.

2. Introduction

Humans represent a large nutrient source and comfortable habitat for many pathogenic agents, some of which rely on our species to be able to replicate or thrive. Although not all infections are fatal or cause disease, it is necessary to prevent or eliminate an infection wherever possible. This becomes especially important as asymptomatic, persistent infections can be related to certain neoplastic changes (Epstein-Barr-Virus (EBV), Human Papilloma Virus (HPV)) (Bosch et al. 2002, Ferber 2003). To fight pathogens, our body developed a cellular and molecular system, the immune system, to either prevent pathogens and parasites to enter the body, to repel them (parasites) or kill them prior to entering the body (Parkin and Cohen 2001). Ultimately pathogens or pathogen infected cells have to be eliminated in specific or unspecific ways once they managed to invade the body (Murphy et al. 2008). Pathogens can enter the body in various ways and the human body has developed protective measures to physically and/or chemically deter them from entry into the sterile inner part of the human body. The main barrier towards the external world is the skin. Skin provides a protective barrier against entry of pathogens. The oral cavity, the gastrointestinal system, the lungs and sinuses and also eyes and ears are weak spots for pathogen entry due to their permeability that is necessary for proper nutrient and gas exchange. If pathogens manage to break these barriers, a series of immune responses will be initiated to contain the infection if possible and eliminate the invader from the system. Molecular and cellular systems have been evolved in the constant arms race against pathogens. Thus the immune system is actually a combination of different levels of protection that complement each other. The immune system is grouped into two main categories, namely the innate immune system (unspecific, fast) and the adaptive immune system (specific, slower) both include cellular and molecular mechanisms described below (Parkin and Cohen 2001, Murphy et al. 2008).

2.1 Innate and adaptive immune system

The innate immune system reacts immediately after the physical and chemical barricades have been breached and is activated by recognizing molecular pattern, so called pathogen associated molecular patterns (PAMPs), present on bacteria or viruses (Kumar et al. 2011). Cells of the innate immune systems are natural killer (NK) cells, dendritic cells (antigen presenting cell (APC)), phagocytes (macrophages and neutrophils), eosinophils, basophils and mast cells (Parkin and Cohen 2001). NK cells are cytotoxic against early neoplasms and cells infected with certain viruses and use invariant genes as receptors that detect common changes

that occur in e.g. in viral infections (Kumar et al. 2011). Dendritic cells are antigen presenting cells of the innate immune system and activate T cells (Alberts et al. 2002). Distributed in peripheral tissues dendritic cells take up foreign material and process it to present peptide antigens on their surface using a protein complex named major histocompatibility complex (MHC). After endocytosis of antigenic proteins they travel from peripheral sites of infection or inflammation to local lymph nodes where mature T cells pass by during their search for their activating antigen after leaving the thymus. Via their TCR T cells can scan APCs for their specific antigen. Because of this specificity that allows an immune response to be adapted to a certain antigen or pathogen T cells are classified as part of the adaptive or acquired immune system. Next to T cells the adaptive immune system includes also B cells that launch antibody responses. B and T cells are produced in large quantities in the bone marrow with each mature cell showing its own specificity to a specific antigen via its B or T cell receptor (Parkin and Cohen 2001, Murphy et al. 2008). Lymphocytes mature in primary lymphoid organs: B cells mature in the bone marrow, T cells mature in the thymus (Parkin and Cohen 2001, Zhang and Bevan 2011). Humoral or non-cellular adaptive immunity responses (= antibody responses) are mediated by B cells that once activated by their antigen will proliferate and develop into plasma cells that produce large amounts of antibody molecules. Antibodies secreted by B cells opsonize pathogens or pathogenic cells marking them for killing by NK cells (antibody dependent cell-mediated cytotoxicity, ADCC) or phagocytosis (Murphy et al. 2008). T cells on the other hand orchestrate humoral responses, activate the innate immune system or become killer T cells that eliminate virus infected cells or tumor cells. Lymphocytes generate memory cells that will keep watch in the bodies tissues and reactivate quickly if their antigen is encountered again (Parkin and Cohen 2001, Zhang and Bevan 2011).

2.1.1 Adaptive immune system

T cells comprise a large group of cell types and associated subsets that function in different immunological context. A main category of T cells are CD4⁺ (also T_h or T_{helper}) and CD8⁺ T cells (also cytotoxic T lymphocytes (CTL), referred to in this work as CTL) which express an αβ T cell receptor (TCR) (Parkin and Cohen 2001, Murphy et al. 2008). CD4⁺ T cells include helper T cells (T_{h1} /T_{h2}), regulatory T cells and T_{h17} (Parkin and Cohen 2001, Zhang and Bevan 2011). CD4⁺ T cells are mediators of adaptive immune responses by regulating B cells antibody production stimulating and enhancing functions of CTL and secretion of cytokines

that destine the immune response. CD4⁺ and CD8⁺ T cells develop from the same precursor cells and during maturation in the thymus are thoroughly screened for functional T cell receptors and lack of auto-reactivity to self-antigen (Jameson and Bevan 1998, Sebzda et al. 1999). T cells, once matured, are exclusively CD4⁺ or CD8⁺ and this expression defines the interactions with APCs and target cells. Lymphocytes use a set of genes that are somatically rearranged to produce a sheer infinite amount of surface receptors, with each naïve T cell having their own specific ligand that will activate only that specific T cell through its TCR (T Cell Receptor) (Arstila et al. 1999, Ebert et al. 2010). The adaptive immune response is slower but highly specific towards a certain pathogen or tumor (Janeway and Medzhitov 2002, Murphy et al. 2008). As mature T cells are not primed for effector functions, first a T cell must find its cognate antigen by scanning APCs in secondary lymphoid organs (SLOs) (Parkin and Cohen 2001, Murphy et al. 2008, Zhang and Bevan 2011). T cells that have not been activated by antigen are referred to as naïve. There is extensive crosstalk between the innate and the adaptive immune system. Especially activation of lymphocyte by APCs and cytokine profiles to large a part defined by cells of the innate immune system, modulate adaptive immune responses (Shanker et al. 2015). Considering the complexity of cell types, effector and regulatory functions and the cross-talk between innate and adaptive immune system poses difficulties in defining specific functions of T cells in experimental populations (Shanker et al. 2015). The final effector cells to kill tumor cells or pathogen infected cells are named killer cells, as they are able to eliminate host cells they contact without harming the surrounding cells. Their potential to fight tumor cells makes them an important target for medical applications and understanding their complex functionality will help to use and manipulate a patient's own T cells to make them more fit to fight the cancer that was able to avoid their surveillance so far. To do this reliably and successfully one needs to understand the mechanisms that define T cell behavior and those that orchestrate their functions in as many details as possible.

2.2 Immune killer cells: natural killer cells and cytotoxic T lymphocytes

To eliminate intracellular pathogens or tumor cells from the body, the immune system must attack its own kind in favor of survival of the rest. In humans there are two main killer cell types that show cytotoxicity. Natural killers (NK) are cells of the innate system and cytotoxic T cells (CTL) are cells of the adaptive immune system. NK represent the initiate quick response towards infected or abnormal cells whereas CTL are specific for a certain peptide

antigen that must be presented to them in a complex manner to activate them into effective killer cells. After activation this antigen will serve as recognition signal for a target to be killed by the CTL. To avoid unwanted killing by NK and CTL several levels of security for recognition of a target exist. An important mechanism in this regard is immune tolerance by tumor cells that can modulate immune check points inducing tolerance of the immune system towards the antigens generated by neoplastic cells (Makkouk and Weiner 2015). This can occur at different stages of the immune response e.g. by altering the immune cell and cytokine concert that governs the outcome of an immune response towards an antigen. An important step in killer cell clearance of tumor cells is recognition of the tumor as “renegade”.

2.2.1 Target recognition by killer cells

NK cells detect targets for elimination using a variety of surface receptors that can either be inhibitory to NK cell cytotoxicity or activating. NK can also bind to major histocompatibility complex class I (MHC I) molecules that are expressed on all healthy, nucleated cells and present intracellular derived antigens resulting in an inhibitory signal. Lack of MHC I expression on a cells surface, as it occurs in neoplastic changes or viral infections will activate NK cells (Pegram et al. 2011) resulting in cell-mediated killing by release of granzymes and perforin into the contact zone with the target cell named immunological synapse resulting in apoptosis of the target cell (Topham and Hewitt 2009). Another mechanism of NK cell target elimination is antibody dependent cell-mediated cytotoxicity (ADCC). This process establishes a link between adaptive and innate immune system. Antibodies produced by the adaptive immune system opsonize virus infected cells to be eliminated by NK cells (Chung et al. 1999). ADCC is also used for immunotherapy of neoplasms expressing unique antigens (B cell lymphoma, neuroblastoma) (Wang et al. 2015) and can be exploited for *in vitro* cytotoxicity screening of NK cell populations using target cells with downregulated MHC I or using IgG antibodies against surface markers of the target cells. T cells show a much more complex control over specific target cell recognition. Antigen-activated CTL detect suitable target cells via interaction of their TCR via specialized molecules that are expressed on all nucleated cells and present peptides as antigens (major histocompatibility complex I, MHC I) (Murphy et al. 2008). CTL will roam homed tissues applying a migration mode strategy that is defined by activation state, chemokines and extracellular matrix (ECM) factors, scanning cells they contact for surface exposed antigens. Contact of a CTLs TCR with its cognate peptide-loaded MHC I causes a CTL to form a stable contact to the target cell, an

immunological synapse (IS), and kill the cell. Each naïve T cell has its own cognate antigen meaning its own specificity and after activation CTL will only, but effectively, kill target cells presenting their specific antigen. The next section will describe T cell functions in detail.

2.3 Cytotoxic T lymphocytes

The power of T cells lies in their specificity and efficiency. Initially described as “cellular antibodies” observed in kidney transplants that were cytotoxic to the transplant and they were soon identified as bone marrow originating cells that mature in the thymus and are distinct from “soluble-antibody producing cells” (B cells) (Govaerts 1960). The life time of a T cell is highly controlled as they are efficient and dangerous killers yet they are as essential to host survival. T and B cells are crucial for every individual. Different pathologic genetic conditions are known to cause defects in T and B cell development which renders the individual prone to many infections and usually results in death at early age (Cole and Cant 2010). The destiny of a CTL narrates as follows. Naïve cells are generated in vast numbers each with their own specific cognate peptide antigen. In search for their antigen they circulate through blood and lymph until specialized cells of the immune system present antigens derived from pathogens or tumor cells in secondary lymphoid organs. If a T cell is specific for a presented antigen it is referred to as “activated” and will proliferate generating many clones with different fate in the ongoing infection / inflammation (effector cells, memory cells). The activated cells will reenter the blood stream and ride along until they reach an area of inflammation or their homing tissue. Inflamed tissue presents molecular “warning signs” on its surface to T cells. Endothelial cells near inflamed tissue express adhesion molecules and chemokines that allow CTL to halt at this site and transmigrate into the inflamed tissue (Campbell and Butcher 2000, Mora and von Andrian 2006). Here CTL migrate within the matrix, contacting cells they encounter. If a cell displays a CTLs cognate antigen it will be recognized and killed. This is an important task as dysfunctional T cells result in different yet often severe to fatal conditions rendering the person highly susceptible to certain pathogens. A complete dysfunction of T (and B) cell development referred to as severe combined immunodeficiency (SCID) can be due to mutations in enzymes crucial for gene rearrangement during T cell development or the common cytokine receptor gamma chain and also defects downstream of TCR signaling. SCID is fatal early after birth (Dosch et al. 1978, Cole and Cant 2010). The processes underlying the “curriculum vitae” of a T cell are highly complex

and not fully understood in their orchestration. The following paragraphs describe in more detail what is known about how T cells function.

2.3.1 The T cell receptor

Specificity of a CTL is mediated via the TCR. During T cell selection in the thymus the functionality of the TCR of a T cell and low reactivity to self is ensured (Jameson and Bevan 1998). A T cell receptor binds to peptide loaded MHC on APCs or target cells depending on location and activation state. The mechanism of rearranging the immunoglobulin receptors of T cells (and also B cells) can produce receptors that allow recognition of virtually any molecular structure. Yet T cells are dependent on peptide derived antigens for activation. As pathogens can adapt to immune detection by altering their proteins through mutation or expression of different proteins having the same function the invariant receptors of the innate immune system can be rendered ineffective. A pathogen able to evade the innate system causes a severe threat yet breaking the first line of defense is not the end. As long as an APC can take up pathogen-derived peptides or gets infected by the pathogen, followed by proteasome-processing of its proteins, and present them on the cell surface T cells can be activated. T cell generation is exhaustive but this energy trade-off allows creating a repertoire of T cells with a diversity of the TCRs of 10^6 with the mathematical possibility of up to 10^{15} distinct specificities (Arstila et al. 1999). This results from (1) random combination of discontinuous $\alpha\beta$ TCR genes which bind to MHC class I and II on APCs, and (2) random nucleotide addition or deletion during gene rearrangement (Arstila et al. 1999). This system allows T cells to be produced with various specificities for peptide ligands, despite being totally oblivious about which specificity might be necessary, hence the exhaustive brute force approach of T cell receptor specificity (Arstila et al. 1999, Murphy et al. 2008). That every T cell has its own specificity poses an experimental difficulty as each T cell (cells of different specificity) requires a different MHC:peptide to be activated physiologically. If a cell encounters its antigen on an APC an activating cascade will be initiated (Murphy et al. 2008, Masopust 2013). Recently the long time paradigm that only non-self-reactive T cells will leave the thymus might have to be revised as self-reactive T cells have been found in the periphery in mice and it has been shown that MHC:self-peptide interaction with resting naïve T cells can provide a survival signal (Brownlie and Zamoyska 2013). As a security measure naïve T cells need three signals to be activated: (1) Peptide antigen via APCs, (2) a costimulatory signal represented by CD80/CD86 on APC which will bind to CD28 on T cells,

and (3) an autocrine signal by activated T cells, interleukin-2 (IL-2) (McDonald and Nabholz 1986, Murphy et al. 2008, Smith-Garvin 2009). For our experiments *in vitro* primary human T cells are activated unspecifically via antibodies directed against CD3 and CD28 on isolated T cells. This method has been proven to be sufficient to yield a large number of activated T cells (Li and Kurlander 2010, Teschner et al. 2011). Although T cells will secrete IL-2 in an autocrine fashion in this primary culture additional recombinant IL-2 is added to aid proliferation and survival. *In vitro* stimulation as in this case will result in a heterogeneous population of T cell subtypes mainly consisting of effector and effector memory type T cells (Li and Kurlander 2010, Teschner et al. 2011). Experimentally, CTL specificity can be overcome by using antibodies that bind to the signaling subunits of the TCR, CD3 (for killing), and additionally to the costimulatory receptor CD28 (for activation/stimulation) plus IL-2 application to culture. This is sufficient for *in vitro* stimulation (microbead immobilized α CD3/ α CD28) or target cell recognition (soluble α CD3). This activation is achieved as the used antibodies will “crosslink” TCR complexes via binding to CD3 through its two antigen binding domains.

2.3.2 *In vitro* T cell populations

Isolated lymphocytes from whole blood or leukocyte reduction chambers (the source of cells used in this thesis) show a variable subtype composition. Upon activation naïve CD8⁺ T cells start proliferation and produce large amounts of clones that will take up different functions. Cells of different function produced this way are categorized into subtypes depending on cytotoxicity, migration behavior, homing tissue, cytokine profile and surface molecule expression (Sallusto et al. 1999). Subtypes of CD8⁺ T cells include naïve cells (no cognate antigen contact), effector memory (immediate effector functions), central memory cells (reside in lymph nodes) and effector cells. CTL used in this work were isolated from PBMC using magnetic beads (Dynal system, Thermo Fisher). To avoid pre-activation of CTL during isolation by isolation-antibodies the “untouched” system was used (Dynal Dynabeads Untouched Isolation of CD8⁺ T cells/ NK cells, Fisher Scientific). “Untouched” refers to a method where peripheral blood mononuclear cells (PBMC) are treated using an antibody cocktail targeting surface molecules of all other present leukocytes, effectively removing the unwanted cells. As this method is not 100 % efficient the CTL populations after isolation may contain a few percent of non-CD8⁺ cells. α CD3/ α CD28 bead stimulated CTL (primarily used in this work) differentiate preferentially into effector and effector memory subtypes which

have highest cytotoxic and migration potential and thus are ideal for analyzing killing, migration and related processes (Sallusto et al. 1999, Duarte et al. 2002, Geginat et al. 2003, Li and Kurlander 2010, Teschner et al. 2011).

2.3.3 Killing machinery of CTL

If an activated T cell found a suitable target a complex process forming a tight membrane to membrane contact named the immunological synapse is initiated. Forming this close contact is essential for specific target cell killing as it allows to secret e.g. lytic substances into the cleft between the T cell and its target without affecting possible healthy surrounding cells.

2.3.3.1 Immunological synapse

The immunological synapse (IS) is a cell:cell membrane contact area initiated by recognition of the target by NK or CTL via NK receptors or the TCR (Alarcón et al. 2011, Angus and Griffiths 2013). CTL will form a close contact with cells presenting T cell specific MHC:peptide on their surface which is the execution signal for the activated CTL (Stinchcombe and Griffiths 2003). IS formation is a controlled and complex process that reorients cytoplasmic structures and that can be maintained for several hours during activation (Stinchcombe and Griffiths 2003). Migrating CTL will consecutively contact local cells and scan their surface for peptide:MHC. If a T cell encounters its antigen presented on a cells surface migration is halted and TCR signaling is induced, activating Src family kinases (Stinchcombe and Griffiths 2003, Dustin 2014). Initial TCR signaling results in rapid actin accumulation followed by actin depletion at the IS, which is essential for functional cytotoxicity via lytic granules (LG) (de la Roche and Asano 2016). This is followed by enrichment of TCR clusters in the actin depleted area and microtubule organizing center (MTOC) relocation towards the IS, the latter tags along LGs and vesicles containing additional TCRs to the IS (Gomez et al. 2007, Martín-Cófreces and Robles-Valero 2008, de la Roche and Asano 2016, Obino et al. 2016). A hallmark of this polarization during killing is the reorientation of the MTOC towards the IS (de la Roche and Asano 2016). Upon IS formation the cytoskeleton is remodeled near the contact site and supramolecular structures (supramolecular activation complex or SMAC) are formed at the contact site (Sasahara et al. 2002, Brown et al. 2011). The SMAC has distinct zones, central, peripheral and distal, termed cSMAC, pSMAC and dSMAC respectively (Dustin 2014). In the cSMAC signaling proteins are concentrated while in the pSMAC high concentrations of adhesion proteins and

cytoskeletal organizing proteins like talin can be found (Dustin 2014). These organized structures and their maintenance over extended periods of time, resulting in the concentration of signaling proteins, is essential for activation of T cells.

2.3.3.2 CTL cell-mediated cytotoxicity

Different things can happen if a T cell meets its cognate MHC:peptide ligand. If the cell is naïve it can be activated if it is an already activated effector the result of TCR ligand binding is death of the antigen bearing cell. CTL mediated cytotoxicity follows two mechanisms:

1. Perforin-granzyme pathway - LG release (TCR-mediated, specific)
2. Fas/FasL pathways - activation induced cell death (AICD) (FasL-mediated, unspecific)

Release of LGs is the main mechanism of specific killing of target cells via CTL. After physical contact of the CTLs and its targets membrane an immunological synapse is formed. This is followed by cytoplasmic rearrangement of organelles towards the IS. LGs are relocated towards the IS along with the MTOC (Stinchcombe et al. 2001, Stinchcombe and Griffiths 2003, Quintana et al. 2007, Bertrand et al. 2013). The IS of CTL has a distinct secretory domain within its SMAC where LG exocytosis occurs (Stinchcombe and Griffiths 2003). TCR activation by target cell contact results ultimately in LG release which occurs within minutes after TCR activation (Stinchcombe et al. 2001, Stinchcombe and Griffiths 2003). Perforin and granzymes cause CTL cytotoxicity by initiating apoptosis in target cells. Long it was thought that perforin forms pores in the target cell membrane through which granzymes enter and initiate apoptosis by cleaving effector caspases (Russell and Ley 2002). But perforin pores are too small for granzymes and granzymes can enter cells without perforin but then require additional signals to be able to initiate apoptosis (Russell and Ley 2002). Combined targeted release of perforin and granzymes will kill a target by initiating apoptosis. The cell surface protein Fas belongs to the tumor necrosis factor family of proteins (Waring and Müllbacher 1999). Fas is expressed in immune and non-immune cells. The Fas/FasL pathway is mainly used to regulate lymphocyte numbers via activation induced cell death (AICD). Binding of FasL to Fas causes the Fas bearing cell to undergo apoptosis (Waring and Müllbacher 1999). Activated CTL express Fas and FasL and interaction of Fas:FasL on lymphocytes are important for terminating proliferation of lymphocytes after clearing of an infection or tumor (Murphy et al. 2008). Activated T cells upregulate FasL and can kill cells expressing Fas. There is also evidence supporting an increase of LG mediated cytotoxicity of CTL correlating with the level of Fas expression (Kagi et al. 1994). Fas is

upregulated in cells with damaged DNA or lesions marking them as targets to be killed by activated CTL (Waring and Müllbacher 1999).

2.4 How killer cells find their battleground

Estimating a human being as 70 L and a T cell as 250 fL poses a similar challenge than asking a human to find a few bad apples in the earth's volume in a reasonable time frame. The task to find a few specific targets appears unachievable. To effectively relocate T cells to a site of antigen activation, pathogen infection, neoplastic changes or inflammation, the immune system uses a simple system of circulation (blood and lymph), guidance (homing receptors) and rallying points (secondary lymphoid tissue) where information about invaders or neoplastic cells is gathered and presented to T cells (Mora and von Andrian 2006). During their life time CTL will migrate for various reasons, including searching for antigen and finding a target post-activation. To eliminate target cells, one big challenge for activated killer cells is to locate the inflamed tissue and once there kill the pathogenic cells. To achieve this activated CTL travel in the bloodstream until encountering post capillary vascular endothelial cells primed to express homing receptors and chemokines on their surface that target CTL of different subtype (Mora and von Andrian 2006, Vestweber 2015). Tissue distribution of memory cells, localization of activated effectors to sites of ongoing inflammation and naïve T cell circulation are regulated by surface molecules of vascular endothelial cells. Vascular cells will induce expression of cell adhesion molecules and chemokines upon inflammation or infection that attracts activated effector T cells (Murphy et al. 2008, McEver and Zhu 2010, Vestweber 2015). Following the rolling and adhesion mechanism CTL will be arrested at the vascular endothelial surface followed by transendothelial migration (McEver and Zhu 2010). Next CTL will encounter the interstitial matrix of the target tissue and have to migrate within to detect their targets and eliminate them. A T cell searching for either antigen or a site of inflammation is guided by its homing receptors (Mora and von Andrian 2006). The expression profile of selectin binding proteins, chemokine receptors and adhesion molecules thus defines the target tissue of T cells (Masopust 2013, Vestweber 2015) (**Fig. 1**). NK cells, once matured do not need antigenic activation, and can be found in blood, tissues and organs (Grégoire et al. 2007, Carrega and Ferlazzo 2012). As much as is known about T cell homing, only few data on NK cell trafficking are available (Grégoire et al. 2007, Carrega and Ferlazzo 2012) and human NK express many different chemokine receptors and expression differs for NK subsets (Grégoire et al. 2007, Carrega and Ferlazzo 2012). Crossing the endothelial

barrier CTL encounter the ECM, non-cellular components providing structure, elasticity, nutrients, survival and proliferative signals, among many other functions.

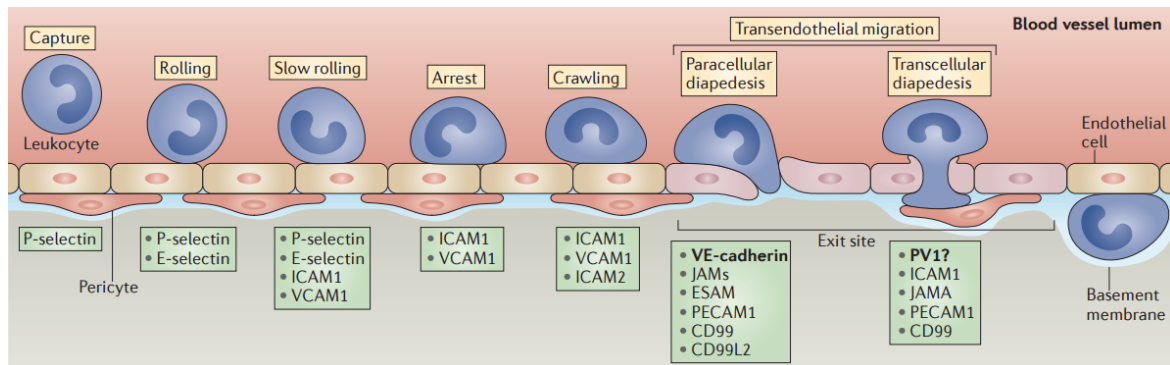


Figure 1 - Mechanism of leukocyte extravasation from a blood vessel. Lymphocytes traveling in the blood stream leave the circulation in a cascade of rolling along the side of the vessel walls mediated by selectins and cell adhesion molecules (surface proteins on lymphocytes and endothelial cells). Rolling along the wall of activated endothelium CTL are slowed and finally arrested through interaction with cell adhesion proteins like VCAM. This is followed by arrest of movement in presence of chemokine signals and finally initiation of transendothelial migration: the process of traversing the endothelial cell barrier. **Legend** - P/E-selectin: cell adhesion molecules, glycoproteins; ICAM1/2: intercellular adhesion molecule 1/2; VCAM1: vascular adhesion molecule 1; JAM: Junctional Adhesion Molecule; ESAM: endothelial cell adhesion molecule; PECAM: Platelet endothelial cell adhesion molecule / CD31; CD99: single-chain type-1 glycoprotein; PV1: Plasmalemma vesicle-associated protein (from *Vestweber 2015*).

2.5 The extracellular matrix

The life of a T cell is 3-dimensional. Born in the bone marrow, matured in the thymus and after activation, roaming interstitial matrices of tissue, T cells encounter during all developmental stages in their lifespan a complex 3-dimensional environment that affects or defines their behavior. Reaching their battleground, activated T cells will migrate within the tissues interstitial space, made up of extracellular matrix (ECM). ECM is a generic term also referred to as connective tissue as it physically holds organs in place at the same time allowing flexibility of the tissue through elasticity in certain fibers making up the ECM (Schulz 2005). Although composition differs depending on location, the functions of the ECM are similar in different contexts: mechanical signals to cells, cell adhesion through cell adhesion molecules, stability, elasticity and strength of the ECM and also signals that can tune migration behavior, cell proliferation and differentiation (Mouw et al. 2014). ECM also supports and separates organs (Schulz 2005). There are two main categories of ECM namely basal membranes and interstitial fibrous matrices (a combination of features from both groups can be found in the reticular network in secondary lymphoid organs) (Sorokin 2010). Basal membranes separate tissue surfaces from the connected interstitial matrix. The connective

tissue making up the interstitial matrix of most tissues, where CTL migrate within, contains mainly collagens of Type I/III/V/XI, glycoproteins like fibronectin, proteoglycans like chondroitinsulfate, non-proteinated glycans (hyaluronic acid) and non-glycosylated proteins (elastin) (**table 1**). Once arrived at the site of inflammation cues through extracellular matrix factors like collagen, fibronectin, glycosaminoglycans, growth factors and/or chemotactic/haptotactic gradients define CTL migration and directionality. Next to structural stability and flexibility the ECM offers various signals to cells including proliferation, differentiation and survival (e.g. hyaluronic acid via CD44 to activated T cells, ensuring survival of killer cells when reaching their target tissue to elicit effector functions) (Hynes et al. 2009, Baaten et al. 2010).

2.5.1 ECM proteins

2.5.2.1 Collagens

Collagens are extracellular proteins that make up most of the ECM and are the most abundant proteins in animals. Collagens in solution turn the liquid into a colloid (“*kolla*” from greek glue and “*gen*” English to produce), hence the name. A human being consist about one third of collagens and so far 28 types of collagens have been identified in humans (Ricard-Blum et al. 2011). Collagen consists of a triple helix formed from 3 individual collagen strands called tropocollagen (Chattopadhyay and Raines 2014). From these tropocollagen molecules larger structures are formed. Different types of collagen produce different forms of 3D structure ranging from fibrillary structures over networks to filaments (Ricard-Blum et al. 2011). Collagens show low immunogenicity due to the highly conserved primary protein structure. Type I being the most abundant collagen in animals and the type of collagen mainly used in research or medical applications (Chattopadhyay and Raines 2014). Under the right conditions *in vitro* (pH, temperature and osmolarity) isolated pepsinized collagen type I can polymerize and form stable sponge-like matrices that can serve as 3D matrix for scientific experiments (Prockop et al. 1995, Gelse et al. 2003, Artym and Matsumoto 2011). The structure of a collagen matrix with regard to pore size and diameter depends on the source of the collagen and the method of extraction (Wolf et al. 2009). Pepsinized bovine collagen, polymerized *in vitro*, as used in this work produces homogenous collagen structures with pore diameters in the lower μm range depending on formulation (Wolf et al. 2009). Isolated T cells do not adhere to collagen type I and for this collagen type I is used as a control for adhesion

assays (Gorski and Kupiec-Weglinski 1995). Apart from integrin mediated signaling collagen can provide biological signals to cells via the CD45 receptor. Protein tyrosine phosphatase receptor type C (CD45) participates in TCR signaling targeting Src family kinases resulting in a lower activation threshold for TCR antigen recognition via MHC binding (Saunders and Johnson 2010). Apart from TCR signaling modulation CD45 can bind to collagen and it was shown that this interaction provides a survival signal to Jurkat T cells by modulating integrin signaling via the focal adhesion kinase and extracellular-signal regulated kinase pathways (FAK / ERK) (Bijian et al. 2007).

2.5.2.2 Fibronectin

Initial studies on T cell fibronectin interaction showed that CTL bind to fibronectin only after antigenic activation and that this binding provides a costimulatory signal for degranulation of CTL contacting surface bound MHC I (Campbell and Butcher 2000). Fibronectin is a glycoprotein found in the ECM with diverse functions. Functions include induction of cell migration and proliferation and it aids in cell adhesion. Fibronectin can induce directional motility in a chemokinetic and haptotactic fashion in different cell types (Somersalo and Saksela 1991, Hautzenberger et al. 1994). T cells express two integrin dimer pairs that bind to fibronectin: $\alpha 4\beta 1$ (VLA-4) and $\alpha 5\beta 1$ (VLA-5) that bind to different domains of fibronectin (Hautzenberger et al. 1994). Fibronectin is commonly used as coating for culture ware or for imaging applications to induce migration, increase attachment and cell survival. The source of fibronectin used in this work is human plasma which contains fibronectin dimers and can be found in tissue when blood plasma enters the interstitial space as is the case upon vasodilation caused by acute inflammation.

Table 1 - ECM components used in this work.

Compound	Protein	Polysaccharide	Function (Schulz 2005, Gandhi et al. 2008)
Collagen	x		Structure, integrin signaling
Fibronectin	x		Integrin signaling - proliferation, migration
Hyaluronic acid		x	Cell signaling, inflammation, counteracts compression of tissue

2.5.2 Hyaluronic acid

Hyaluronic acid (HA) is a complex carbohydrate or glycosaminoglycan (GAG) with various functions. GAGs are linear polymers of repetitive disaccharide units. HA is a prominent compound of the ECM and is a polymer of repetitive disaccharide units consisting of β_{1-4} -D-glucuronic acid and β_{1-3} -N-acetyl-D-glucosamine. HA contains no protein moiety and due to the large molecular weight of HA fragments of over $>10^6$ Da it is synthesized extracellularly (Kogan et al. 2007). The receptor for HA is CD44 and is expressed in T cells (De Grendele et al. 1998, Baaten et al. 2010). Activated T cells use CD44 as an alternative to C-type lectins as initial rolling adhesion receptor as CD62L is downregulated upon T cell activation (Baaten et al. 2010). CD44 itself has no cytoplasmic signaling domain but its cytoplasmic tail can associate with other membrane proteins to hijack their downstream signaling pathways. HA also functions as regulator of T cell development and survival of certain subtypes (T_{H1} and T_{Reg}) (Baaten et al. 2010). Enzymatic or chemical digestion of HA polymers produces fragments of different sizes upon inflammation or injury and these fragments have been shown to signal pro-inflammatory (low MW fragments) or anti-inflammatory (high MW fragments) signals (Cyphert et al. 2015).

2.5.3 Integrins and the extracellular matrix

Next to affecting ECM stability, elasticity and structure, proteins, proteoglycans and non-protein polysaccharide also transfer extracellular signals to cells in contact with these ECM factors, through specific surface receptors. For proteins like fibronectin and collagen they are referred to as integrins. Integrins are membrane proteins and functional integrins are heterodimers of each one α and β subunit (see **Fig. 2**). On leukocytes integrins are limited to a specific expression pattern which is itself depending on activation state, cellular subtype and extracellular signals (Harris et al. 2000). T cell migration is thought to be integrin-independent (Lämmermann et al. 2008, Pinner and Sahai 2009) yet this depends on context and the integrins in question. In mice *in vivo* during skin inflammation blocking integrin fibronectin interaction via RGD-peptides suppressed T cell motility and antibodies against $\beta 1$ and $\beta 3$ also suppressed T cell motility (Kim et al. 2014). Notably migration of T cells in this inflammatory context happens along thick ECM fibers. In this context migration is integrin-dependent whereas random migration in a homogeneous 3D collagen matrix environment is integrin-independent haptokinetic migration. Integrin ligand-binding activates Rho family GTPases that establish polarization of the cell. Integrins are linked to complex signaling

pathways further described in the next section (Hautzenberger et al. 1994, Hyun et al. 2009, Chen et al. 2012). The severity of outcome of integrin deficiencies in humans ranging from susceptibility to bacterial infections over impaired wound healing to defects in immune cells highlights their importance for immune functions (Abram and Lowell 2009). Integrins mediate adhesion and diverse signal transduction and leukocytes express specific integrin pairs that aid in homing leukocytes to their target tissues. Integrins are linked to different pathways which are defined by the types of integrins expressed by the cell (Harris et al. 2000, Abram and Lowell 2009). Integrin signaling is separated in two mechanisms named “inside-out” or “outside-in” signaling. “Inside-out” signaling refers to processes where conformational changes occur resulting in higher affinity binding of integrins to their substrates and clustering of integrins increasing avidity for substrate binding (Abram and Lowell 2009). These signals can be extracellularly derived yet originate not directly via integrin ligand interactions but via extracellular signals through chemokine receptors or activation of the TCR which will activate phospholipase γ (PLC γ) and protein kinase C (PKC). This in turn activates small GTPases like Rap1 that induce conformational changes in targeted integrins thus activating them into a high affinity state for their ligand (Abram and Lowell 2009). “Outside-in” signaling describes signaling events following clustering of integrins after ligand binding and is with regard to T cells of importance during TCR activation (Abram and Lowell 2009). Signaling pathways associated with outside-in signaling are mediated by Src and Syk family kinases which are linked via Rho-GTPases to actin cytoskeletal reorganization (Abram and Lowell 2009). Outside-in is the actual signaling via integrins binding their ligands.

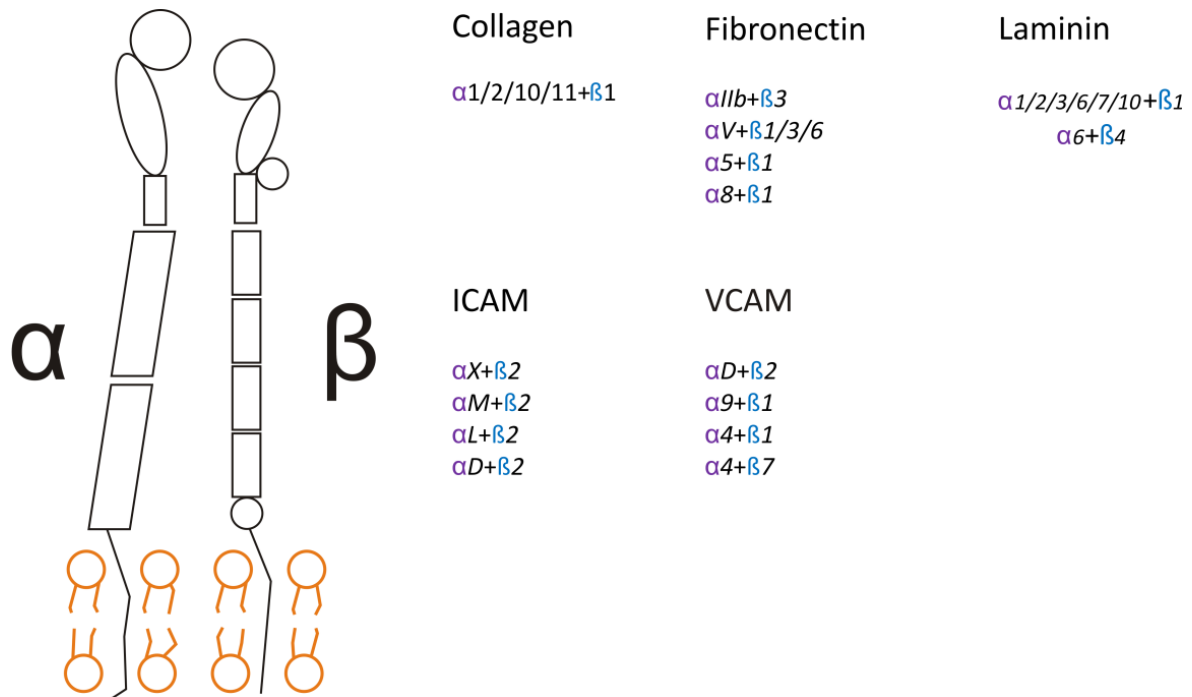


Figure 2 - Integrin $\alpha\beta$ heterodimers define the adhesion molecule binding of a T cell. Functional integrins are heterodimers of one α (18 in humans) and one β (8 in humans) subunit each (schematic on the left) that show high affinity binding to specific ligands where one integrin heterodimer is not generally limited to bind only one but may also bind several ligands. Shown on the left is a schematic of integrin structure formed by one α and β subunit both being transmembrane bound with ligands binding at the top. The combination of α and β subunits defines the integrin ligand e.g. $\beta 1$ and $\alpha 5$ will bind fibronectin whereas $\beta 1$ and $\alpha 1$ bind collagen. Integrins of the ICAM-binding group (e.g. $\alpha L\beta 2$ in T cells) may also bind collagen (Adapted from Humphries 2006, Chen et al. 2012, Zhang et al. 2012).

2.6 Cell migration

Encountering an interstitial matrix of target tissue activated CTL will migrate and start to fulfil their duty. To effectively find a (mainly rare) target among many healthy surrounding cells CTL can adapt different modes of migration which anyways occur during T cell development. The next paragraph describes the different modes and how and when a T cell switches its mode. Tuning of migration occurs through modulation of actin polymerization rate (speed) and polarization which defines persistence time and thus directionality of migration. It is possible to quantify migration via velocity and (directional) persistence (Petrie et al. 2009). Persistence is a simple dimensionless parameter to describe the straightness of movement and is calculated as follows: $\frac{\text{Euclidean distance (start-end of track)}}{\text{Track length}}$. To reduce

artifacts through analysis time intervals should be kept as low as possible to avoid loss of information e.g. if a cell changes direction several times between intervals.

2.6.1 Modes of migration

When placed inside a homogeneous collagen matrix T cells apply a random walk. The collagen fibers provide haptokinetic signals to CTL that can guide migration in this otherwise unguided environment. Cell migration can be categorized as Brownian, random, persistent random or Lévy walk (differing in certain parameters or directionality of movement) or highly directional or ballistic (Krummel et al. 2016). Persistent random walk (PRW) mathematically describes a walk strategy, where phases of persistent movement are followed by phases of localized more Brownian type of migration (Harris et al. 2006). A Lévy walk strategy is similar to a persistent random walk yet the persistence time (the time a cell moves straight) is increased compared to PRW. This is a common strategy e.g. also employed by predators when hunting for prey that allows scanning a large area in least time. CTL do not apply only a single mode of migration yet can switch between certain migration behavior depending on context of location, cytokines, gradients and extracellular signals which tune the migratory behavior in different ways (see **Fig. 3**). Migratory cues for T cells differ depending on cell differentiation and inflammatory context and are specific for each environment of T cell activation (Krummel et al. 2016). Also T cells migrate with different “motivation”. In search for their antigen, in lymphoid tissue with densely packed APCs, naïve T cells apply a Brownian or random walk strategy and once activated shift their motility strategy towards more defined (more persistent) movements (Krummel et al. 2016). This more ballistic movement can change the search efficiency as faster and/or more persistent cells might miss possible targets or contact them too briefly yet it allows the cell also to cover a larger area (Gérard et al. 2014). The mode of migration applied always has trade-offs for the resulting advantages and T cells adapt their mode of migration intrinsically (Gérard et al. 2014). Exemplary for adaptation of the mode of migration, is the different migration mode applied by CD4⁺ or CD8⁺ cells when scanning APCs for antigen. This means the cells need to locate their cognate antigen on disperse distributed APCs in lymphatic tissue. Here CD4⁺ and CD8⁺ T cells apply different strategies. CD4⁺ contact more APCs within a lymph node in a given time frame compared to CD8⁺ T cells (Krummel et al. 2016). This results from shorter contact times with the APCs, thought to result from the higher affinity antigens presented to CD4⁺ T cells. CD8⁺ T cells antigens are often low affinity antigens and need longer cell-to-cell contact

times to initiate activation (Krummel et al. 2016). Modulation of their migration mode allows $CD4^+$ and $CD8^+$ to compensate for these differences.

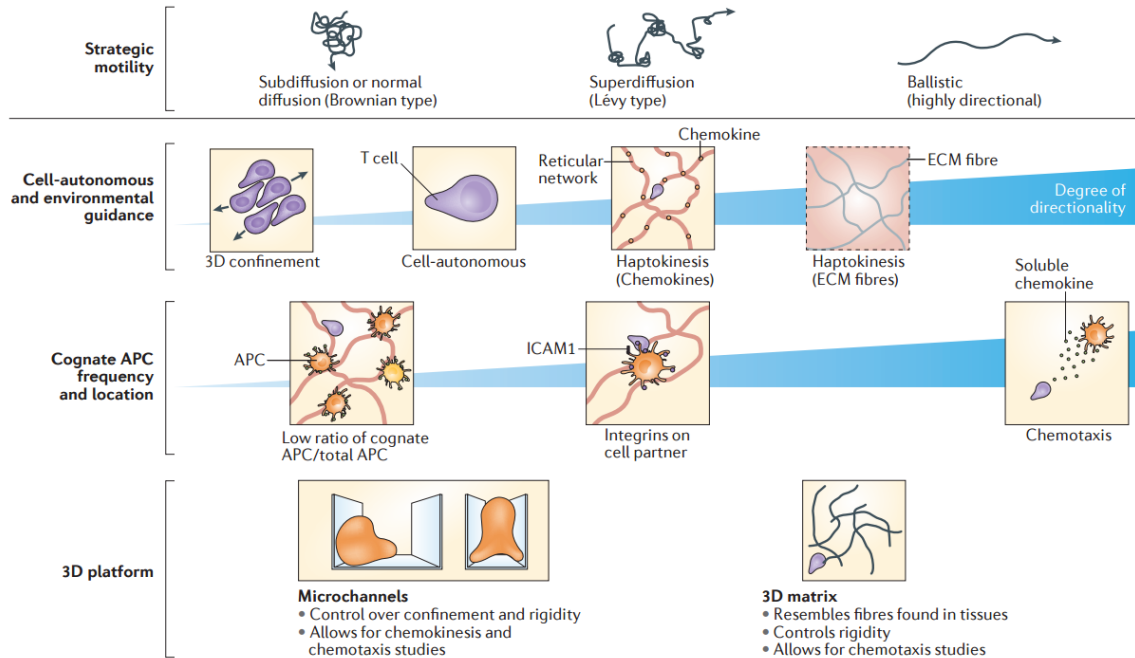


Figure 3 - The mode of migration of lymphocytes is tuned by extracellular cues. The migration strategy applied by lymphocytes depends on local context. Confinement of movement causes a sub-diffusive walk whereas unguided autonomous migration or chemo- and haptokinesis further increase the degree of directionality (upper row). When searching for antigens presented by densely packed antigen presenting cells at secondary lymphoid organs CTL apply a more sub-diffusive mode of migration that lowers search time for rare antigens as they are common for $CD8^+$ T cells. Interaction with cell adhesion molecules like intercellular adhesion molecule 1 (ICAM1) can cause an arrest of migration of otherwise more directional movement resulting in local Brownian type motion followed by more persistent migration periods, which is referred to as Lévy walk. Highly persistent or directional migration occurs upon chemotactic or haptokinetic signals to the cells that will follow the gradient or the ECM fiber. Chemotaxis, haptokinesis and the extracellular signals that define lymphocyte migration can be screened for using different experimental setups including microchannels and 3D systems. Microchannels are advantageous for chemokinetic or chemotactic experiments and allow precise definition of channel parameters. 3D systems are more complex but will represent a more physiological environment representing more realistic cellular behavior. **Legend:** APC: antigen presenting cell; ICAM1: intercellular adhesion molecule 1; ECM: extracellular matrix (from Krummel et al. 2016).

2.6.2 2D vs. 3D migration systems

So far most analysis of migration of mammalian cells has been performed in 2D systems (Decaestecker et al. 2007, Doyle et al. 2013, Krummel et al. 2016). The “2D on-a-glass” systems necessary for microscopy techniques to function can nowadays be challenged by new technologies. Although coated ECM factors can transfer signals to cells it has often been

demonstrated that 2D and 3D behavior of cells and expression profiles are different, especially cancer cells and immune cells (Luca et al. 2003, Lämmermann and Sixt 2009, Petrie et al. 2012, Myungjin et al., 2013, Imamura et al. 2015). Migration in 2D generally uses lamellipodia extension and contraction. 2D systems lack the biophysical matrix interactions and resistance that induce changes in cellular behavior. Stimuli provided by a matrix depend on the matrix structure and composition and can be physical (haptokinetic, durotactic) or biological. Most cells (especially T lymphocytes) depend on survival signals which are offered by ECM factors (Gorski and Kupiec-Weglinski 1995). 2D has been the standard for microscopy experiments for a long time. In 2D migration experiments, cells settled on ECM-protein coated surfaces will form focal adhesions (FA) which are dynamic multi-protein complexes that participate in adhesion and signaling. Focal adhesions link integrins, the ECM proteins and the cytoskeleton and function in integrin binding modulation, induction of cell migration and proliferation and can serve as mechano-sensors (Wozniak et al. 2004). Migration in 2D uses lamellipodial extension driven by actin-polymerization and contraction of FA linked actin fibers and this is the dominant mode of migration in 2D yet represents only one many mechanisms of cell migration in 3D (Petrie and Yamada 2012). T cells encounter both conditions *in vivo*. Rolling on endothelial cells to cross the endothelial barrier into the interstitial matrix would represent a kind of 2D migration whereas interstitial matrix migration would represent a 3D system. For primary human T cells it was shown that migration in 2D is integrin-dependent and relies on actin-myosin contractility yet in 3D T cells move using an actin tread milling process further tuned by matrix properties and kinetic or tactic cues (Gough et al. 2010). Comparing migration in 2D and 3D environments active Ras was found more important for migration in 3D systems than in 2D. Downstream of Ras lays dephosphorylation of the actin depolymerizing protein cofilin resulting in its activation. Knocking down cofilin had no effect on 2D actin-myosin mediated migration yet reduced 3D protrusive-based migration. Blocking myosin activity in 2D resulted in migrating cells that are more sensitive to inhibition of cofilin activation (Gough et al. 2010). Cell behavior thus can differ on multiple levels ranging from gene expression to cell morphology and motility when analyzing cells in 2D system compared to 3D systems.

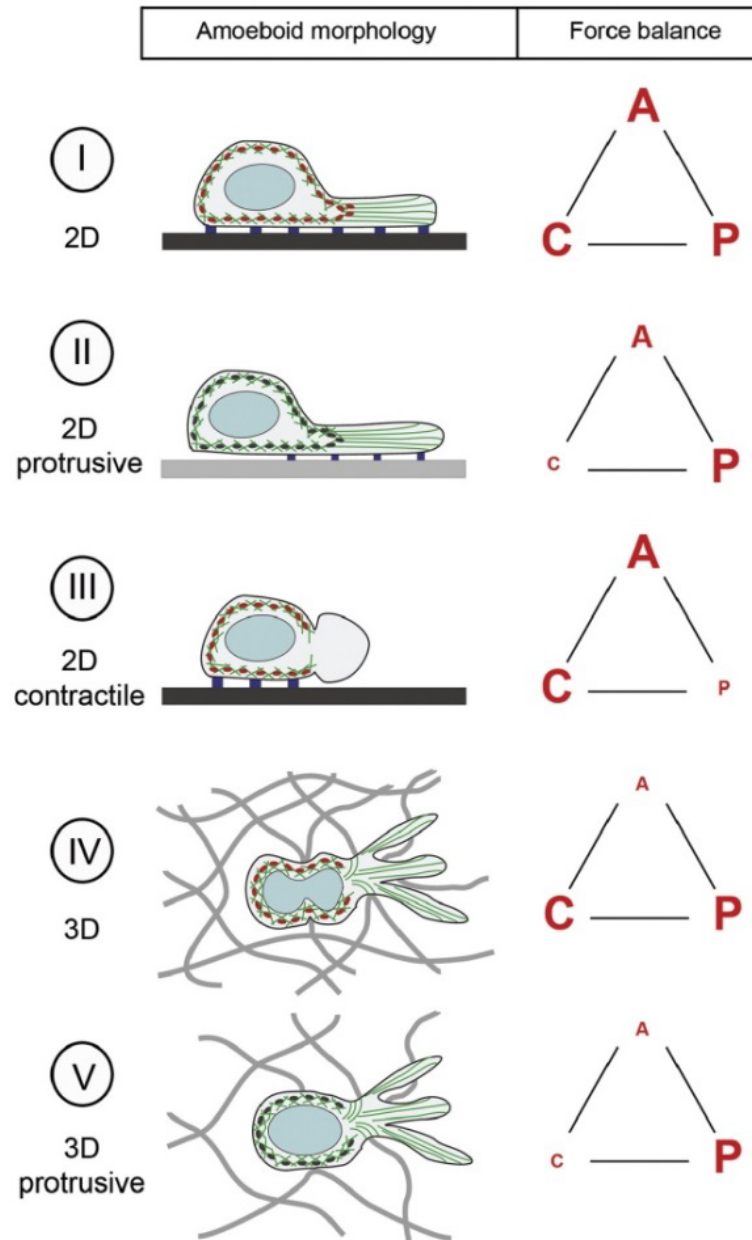


Figure 4 - 2D and 3D amoeboid motility are defined by substrate, substrate binding strength, cell contractility and protrusive forces. The main forces driving and defining cell migration are adhesion strength (A), contractility (C) and polymerization driven protrusions (P). The different modes of 2D and 3D migration are caused by imbalances between these three forces. Low adhesive substrates as depicted in (II) are not depending on contractile forces at the uropod whereas in (I) on highly adhesive substrates the forces must be balanced to favor migration. In 3D environments amoeboid migration does not require contractility in low adhesive matrices except if the nucleus must be squeezed through a narrow pore of the matrix (IV). In low density matrices (V) migration is mainly polymerization driven (adapted from **Lämmermann and Sixt 2009**).

Transferring the benefits of ECM interactions to the physiologically more relevant 3D environment will help to define cellular functions and behavior. 3D systems offer several benefits that cannot be accounted for in 2D:

1. Local microdomains can be retained in 3D matrices whereas in 2D systems secreted/produced factors will diffuse into the vast overlaying medium
2. Physical interactions with a matrix supply haptokinetic information depending on matrix stiffness and not stiffness of the culture substrate (glass, plastic) which has a high elastic modulus
3. Modifiability (by cells and the experimenter) of the matrix allows altering physical properties

The migration experiment “standard cell”, fibroblast, switches to a protrusive migration when contractility is reduced either by reducing matrix stiffness or inhibiting RhoA signaling reducing myosin II activity in the cells rear (Petrie and Yamada 2016). Fibroblasts depend on extracellular signals to induce migration and in general move in a chaotic way, produce thick stress fibers and form many and large focal adhesions to the substrate they are migrating on/in. CTL on the other hand appear to intrinsically migrate even when encountering a collagen matrix without chemokinetic cues (Harris et al. 2006, Le Clainche and Carlier 2008, Lämmermann and Sixt 2009, Krummel et al. 2016). As the 2D matrix system, used for migration analysis in this work, uses non-crosslinked collagen in a lower concentration range, protrusive migration is favored over contractile but because of the small average pore size of bovine derived pepsinized collagen contractility is still important for CTL to migrate within the matrix and should gain importance with increasing matrix stiffness (=higher collagen concentrations). As well in 2D as 3D experimental setups the mode of migration and the dominant forces driving migration can differ depending on substrate, substrate concentration and other factors. Overall migration is result of the force balance between attachment, protrusion and contraction. Matrix substrates that bind only with low affinity and with large pores will favor protrusive based migration that is independent of contraction, whereas upon high affinity binding to the substrate migration will depend on contraction through myosins to detach the cell:substrate interactions (**Fig.4**) (Lämmermann and Sixt 2009). In lymph nodes in mice *in vivo* acto-myosin contraction functions in detachment of the uropod and inhibition of myosin contractility resulted in impaired migration and less effective target search (Munoz et al. 2014). Another study showed that mouse lymphocytes upon chemotactic stimulation show impaired migration when treated with ROCK or myosin inhibitors and this effect was dependent on pore size of the matrix. Smaller pore sizes shift the dependence of migration towards contractility (Soriano et al. 2011). A general statement that contractility or attachment

is negligible is highly context specific and T cells can adapt to different ECM compositions, rigidity and fiber network density. Studies on leukocyte migration showed that enzymatic fragments of ECM constituents were produced by migrating leukocytes, yet this could not be reproduced *in vivo*. T cells move in an amoeboid fashion through a matrix, and this migration is generally independent of matrix degrading proteases (Sorokin 2010). Another important difference of 3D to 2D systems is microdomains within the matrix. Substances secreted by cells (e.g. cytokines) in 2D will diffuse away into the overlaying medium quickly reducing local concentrations or even abolishing the effect by dilution. The fibers of the collagen matrix can deter substances from diffusing into the surrounding allowing cells to modulate the surrounding matrix. For NK cells it was shown that in 2D NK velocity and persistence increase if “bystander” cells (non-target cells) are present whereas in 3D only velocity increases (Zhou et al. 2017). This increase in velocity of NK was found to result from H₂O₂ production of the bystander cells. Healthy cells in the interstitial matrix thus also influence the behavior of lymphocytes by modulating the local microenvironment.

Signals that modify migration can be classified as haptokinetic (physical interaction / mechanical sensing; migration along fibers), haptotactic (haptokinesis with additional gradient producing cues, e.g. ECM fiber-bound chemokines), chemokinetic (soluble factors that induce migration, no guidance), chemotactic (gradient of chemokines defines directionality of migration towards higher concentrations of the chemotactant) and durotactic (migration along ECM gradients e.g. from a thinner part to a thicker part of a collagen fiber) (McCarthy and Furcht 1984, Harris et al. 2006, Plotnikov et al. 2012). Collagen fibers can deliver mechanical signals to cells through mechano-sensory proteins or stretch activated cation channels (Runnels et al. 2002, Feske et al. 2012).

2.6.3 Cell polarization

Polarization of a cell occurs in different contexts yet for a cell to migrate it has to establish polarity (**Fig. 5**). Generally this refers to the polar distribution of cell organelles and differential activation of signaling molecules or signal mediators (PLC activity, Rho/Rac activity) and is generated by extracellular stimuli that induce differential activity of polarization inducing proteins e.g. Rac and Rho GTPases (Ridley et al. 2003, Hyun et al. 2009). CTL polarize after engagement of the TCR towards the contacted cell and during migration yet activated T cells and NK cells are intrinsically polarized without chemokinetic

induction (Sánchez-Madrid and del Pozo 1999). The polarity during migration (protrusions at the front uropod at the rear) is maintained during target cell contact but migration is halted via TCR-mediated signaling. Polarization defines migration direction and allows the cell through its shape to transfer forces generated within the cell into movement (Sánchez-Madrid and del Pozo 1999). When a T cell polarizes for killing an important step is the relocation of the microtubule organizing center (MTOC) which controls relocalization of organelles towards the immunological synapse (Gomez et al. 2007, Martín-Cófreces and Robles-Valero 2008). Polarized cells also show a gradient distribution of Ca^{2+} ions in the intracellular space with high $[\text{Ca}^{2+}]$ at the rear end and low $[\text{Ca}^{2+}]$ at the front end (Wei et al. 2009). Additionally transient localized increases in $[\text{Ca}^{2+}]$ could be observed in lamellipodia in different cell types during migration (Wei et al. 2009). As many cytoskeletal proteins require Ca^{2+} for function, yet the gradient of Ca^{2+} results in a decreased $c[\text{Ca}^{2+}]$ at the cell front, localized calcium flickers can deliver the Ca^{2+} necessary for these proteins to function without globally disturbing the polarity gradient (Wei et al. 2009). Polarity of a T cell can be defined by different cellular components that distribute relative to the direction of movement (Krummel and Macara 2006). These include the cytoskeleton (actin and tubulin), surface receptors, vesicle polarization (microtubule dependent) and so called polarity proteins. These polarity inducing proteins include e.g. scribbled (Scrib) and lethal giant larvae (Lgl) and were identified as mediators of apical versus basal epithelial cell polarity and evidence indicates a function in polarity maintenance of T cells (Krummel and Macara 2006).

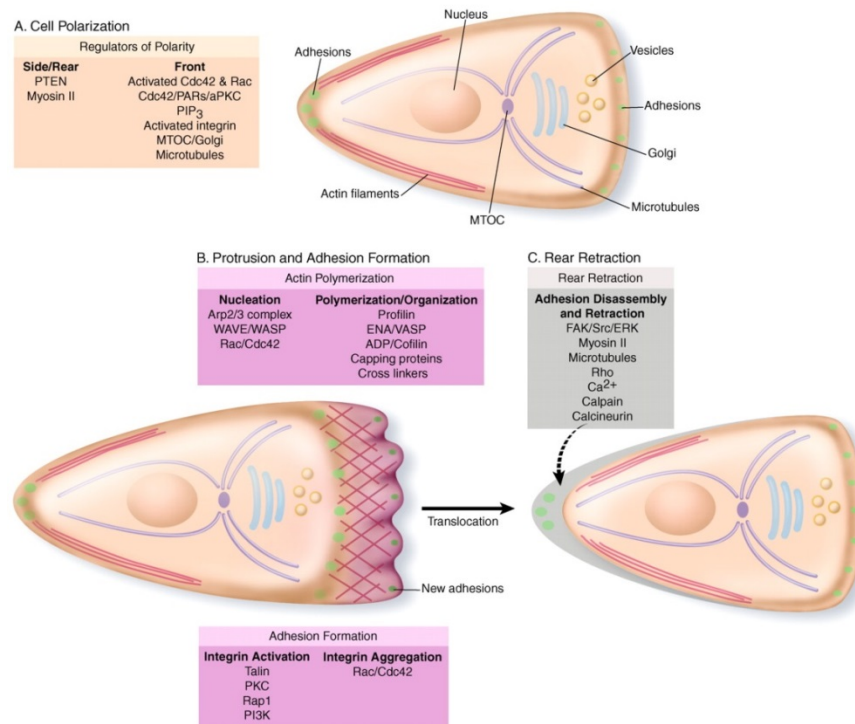


Figure 5 - General aspects of cell polarization during migration of a eukaryotic cell. (A, C) A polarized cell can be identified by the distribution of cell organelles and the activation state of polarization controlling proteins. The cell front is defined by the activated form of the small GTPases Cdc42 and Rac, presence of activated integrins and as a hallmark the relocation of the MTOC towards the front. Myosin II can be found at the rear where its activity is favored by Ca²⁺ influx resulting in contraction and cell translocation. (B) Cellular locomotion is driven by actin polymerization which requires nucleation by e.g. Arp2/3 via WAVE proteins which themselves are activated by Rho-GTPases like Rac. Polymerization itself is highly controlled. Profilins deliver polymerization ready ATP-G-actin monomers, mENA/VASP proteins compete with capping protein for binding to the barbed end and also favor formin mediated polymerization over Arp2/3 mediated polymerization. Cofilin aids in depolymerization of older filaments. Adhesion formation is controlled via integrin dynamics including activation downstream of Rac/Cdc42 and focal adhesion initiators like talin or vinculin. **Legend:** PTEN: Phosphatase and Tensin homolog; PARs: Protease-activated receptors; aPKC: activated protein kinase C; PIP₃: phosphatidylinositol triphosphate; MTOC: microtubule organizing center; Arp2/3 actin related protein complex 2/3; WAVE/WASP: Wiskott-Aldrich syndrome proteins (WASP) / WASP-family verprolin-homologous proteins (WAVE); Ena/VASP: enabled/vasodilator stimulated phosphoprotein; ADP: actin depolymerizing protein; FAK: focal adhesion kinase; ERK: extracellular-signal regulated kinases; Src: tyrosine kinase Src; PKC: protein kinase C; PI3K phosphatidylinositol 3 kinase; Rap1: Ras-related protein 1 (from **Ridley et al. 2003**).

2.6.3.1 Polarization - Small GTPases

Cell polarity was mainly studied via activity of small GTPases (Krummel and Macara 2006). The Ras family of small GTPases includes Rho-GTPases which participate in signal transduction and regulation of gene expression. Rho-GTPases bind GTP or GDP with high affinity, GTP bound Rho representing the active state (Tanizaki et al. 2010, Saoudi et al. 2014, Ridley 2015). The activation switch (GDP exchange to GTP or vice versa) is controlled

via two groups of proteins guanine nucleotide exchange factors (GEF) and guanine nucleotide dissociation inhibitors (GDI) adding multiple levels of control to GTPase activity (Saoudi et al. 2014). GTP bound activated Rho-GTPases serve as binding sites for a variety of different signaling-related molecules. In T cells diverse functions ranging from cytoskeletal reorganization to activation and migration are controlled by Rho protein family members (Heasman and Ridley 2008, Tybulewicz and Henderson 2009, Rougerie and Delon 2012). A cell's polarity is defined by spatially differential activation of different members of the Rho-GTPase family: Rac at the front, Rho at the rear of a cell (Ridley 2015). Different members of this protein family regulate differential actin polymerization dependent processes e.g. Cdc42 participates in induction of formin mediated linear actin filaments. T cells polarize for two main reasons: migration and target cell killing with certain differences in a polar migrating and target cell contacting polar CTL.

2.6.3.2 Polarization and migration - Leading edge and uropod

During migration polarization is defined by differential spatial organization of the cellular components (Sánchez-Madrid and del Pozo 1999). Migrating CTL have distinct features that define front and rear. The leading edge of the cell is enriched with receptors for chemokines and proteases and this enrichment of tactic receptors at the leading edge is unique for lymphocytes (Sánchez-Madrid and del Pozo 1999). Actin is enriched in protrusions and filopodia at the leading edge and in migrating lymphocytes a cortical actin array is evenly distributed around the cell body. The polarized localization of tactic receptors to the front and the concentration of adhesion molecules at the uropod appear to be endogenous to lymphocytes. This means activated lymphocytes have an intrinsic polarity defined by differential presence of receptors and adhesion molecules and are not defined in their general polarity by extracellular signals. CTL thus have a head and a tail. During CTL migration the MTOC is localized at the uropod (Ratner et al. 1997) where also adhesion molecules are concentrated that can aid in interaction with other lymphocytes (memory cells) and serve as an anchor for the cell in 3D environments (Sánchez-Madrid and del Pozo 1999).

2.6.3.3. Polarization maintenance in T cells

Polarization of T cells is generally best defined by cytoskeletal remodeling especially during migration and this is located downstream of the complex activity of Rho family GTPases (Krummel and Macara 2006). Downstream of Rho GTPases, the Arp2/3 complex and

WASP/WAVE proteins act in mediating actin remodeling. One interaction partner of WASP/WAVE proteins are profilins. Via its interaction with phospholipid pathways profilins can affect maintenance of cell polarity despite being mainly considered a protein that mediates actin polymerization by delivering actin monomers (Nürnberg et al. 2001, Behnen et al. 2009). This shows that polarity and cytoskeletal dynamics are closely entwined.

2.6.5 Cytoskeleton

Dynamic movements of a cell are possible through control of the cell cytoskeleton. This generic term refers to globular proteins that can polymerize to form linear and / or branched filaments and those proteins associated with them. Cytoskeletal proteins or filaments participate in a multitude of cellular processes starting with cellular structure, transport of organelles and migration. Filamentous proteins are grouped into three basic groups: microfilaments (filamentous actin), intermediate filaments (vimentin, keratin, desmin etc.) and microtubules ($\alpha/\beta/\gamma$ - tubulin) (Alberts et al. 2002). Concerning migration actin filaments are most important as they generate protrusive forces (Fletcher and Mullins 2010).

2.6.5.1 Actin

Actins are cytoplasmic proteins and are among the most abundant proteins in eukaryotes. The human genome encodes three isoforms: α (muscle cells), β and γ (muscle and non-muscle cells) yet they differ only in few amino acids located at the N-terminus (Dominguez and Holmes 2011). Actins can be ATP or ADP bound and are ATPases that work with higher efficiency when in filamentous form (F-actin) compared to globular actin (G-actin) (Korn et al. 1987). ATP-actin polymerizes more readily than ADP-actin and proteins like profilins aid in ADP-to-ATP-actin conversion. This process ensures a pool of readily polymerizing ATP-actin units that once polymerized will intrinsically cleave ATP to ADP after a certain time resulting in destabilization of the filament. Actins are globular proteins that can polymerize in a linear fashion. Branched filaments need aid from other proteins e.g. Arp2/3 (actin related protein complex 2/3) to be initiated. Before polymerization there is need for nucleation of actin filaments which refers to small F-actin strands of few monomers that can form in different context connected to different proteins (Uribe and Jay 2009, Paul and Pollard 2010). Cell motility depends on actin polymerization and actin dynamics are under complex control via a vast network of interacting proteins. Spontaneous polymerization of actin filaments is valueless for cells because of the lack of control over actin dynamics and the slow rate of

elongation of unguided polymerization. Thus cells evolved different pathways that integrate extracellular and intracellular signals, control nucleation, elongation, branching and depolymerization to form or move the cell body. These pathways comprise of a vast number of proteins. The proteins participating in actin dynamics can be grouped in two categories defined by their binding to F-actin: *End-binding proteins* (EBP) that control polymerization rate and can serve as attachment points for actin filaments and *side-binding proteins* (SBP) include severing proteins (actin depolymerizing factor ADF/cofilin), myosin motors and filament crosslinkers (filamin, α -actinin) (Crevenna et al. 2015). Depending on the protein in question, *in vitro* polymerization analysis of actin filaments showed, that side binding proteins can modulate elongation rate, halt elongation and cause changes in the flexibility of the filament resulting from structural alteration (Crevenna et al. 2015). Before polymerization a nucleus, a multimer of several actin monomers, must be present to initiate a new filament or branch (Korn et al. 1987, Mogilner and Oster 1996, Lee and Dominguez 2010, Nürnberg et al. 2011, Bovellan et al. 2014). The *de novo* formation of actin filaments requires nucleation by either of three groups of proteins: formins, Arp2/3 depending nucleation promoting factor proteins (NPFs) and tandem monomer binding nucleators (TMBN). Nucleation of actin filaments, the stable formation of multimeric actin, is the main rate limiting step of polymerization as on the one hand intermediate actin dimers are unstable and the sequestering of actin monomers by monomer-sequestering proteins prohibits spontaneous polymerization (Korn et al. 1987, Mogilner and Oster 1996, Firat-Karalar and Welch 2011, Nürnberg et al. 2011, Bovellan et al. 2014). The Arp2/3 NPFs can nucleate new filaments only on already existing filaments introducing a branch in the filament by inserting itself at the filament end. *Formins* can nucleate actin filaments and serve at the same time as elongation factors inhibiting binding of capping protein to the filament barbed end. Formins produce unbranched actin filaments (Paul and Pollard 2010, Firat-Karalar and Welch 2011). The last group of nucleators (TMBN) comprises proteins that contain repeated G-actin binding motifs. Binding of actin to these motifs draws the monomers close together allowing formation of an otherwise unstable actin nucleus (Firat-Karalar and Welch 2011). An additional kind of nucleation is performed by filament severing proteins like cofilin, which can introduce nicks in a filament that can serve as a nucleus for new filament elongation or branching via the Arp2/3 pathway (Wioland et al. 2017).

Actin filament elongation has been extensively studied *in vitro*. Polymerization of actin filaments has three basic phases in solutions containing only G-actin.

1. Formation of a nucleus, 2. Elongation, 3. Steady state or equilibrium

Reaching the third state or equilibrium the remaining G-actin concentration is referred to as critical concentration that *in vitro* for a G-actin containing solution lays around 0.1 μM . This means at concentrations above 0.1 μM G-actin will polymerize and below F-actin will depolymerize. Actin polymerization of pure monomers *in vitro* is non-covalent and reversible (Korn et al. 1987). Actin monomers are non-covalently bound to one molecule of ATP which is hydrolyzed to ADP during polymerization with an intermediate F-actin-ADP-Pi state. ADP-actin is readily depolymerized and this depolymerization is facilitated by severing proteins of e.g. the actin depolymerization factor family (ADF) (Andrianantoandro and Pollard 2006, Wioland et al. 2017). After depolymerization G-actin-ADP dissociates ADP in exchange for ATP replenishing the actin monomer pool. This exchange is facilitated by profilin (Korn et al. 1987, Pollard et al. 2001). Actin filaments are kinetically asymmetric with distinct filament ends named pointed or (-) and barbed or (+) end for their appearance in electron microscopy images (Crevenna et al. 2015). Growth of the filament occurs at the barbed and pointed end *in vitro* with up to an order of magnitude higher elongation rates at the barbed end. This is a result of differences in the critical concentration of actin which is much higher at the pointed end (0.8 μM) (Lodish et al. 2000). In live cells the pointed end will be anchored or tethered by nucleating proteins prohibiting pointed end elongation. The free G-actin concentration in cells is regulated by actin monomer sequestering proteins (profilin, thymosin $\beta 4$), elongation rates or local actin concentrations are regulated by profilins, SBPs and formins and depolymerization factors (Irobi et al. 2004). This allows the cell a high level of control over this important process.

2.6.5.2 Microtubules and microtubule organizing center (MTOC)

Microtubules (MT) are globular proteins that polymerize into hollow tubes. Three tubulin isoforms exist named α , β and γ . α and β subunits form heterodimers which are added to a growing tubule during polymerization. The γ tubulin monomers can be found exclusively in the centrosome or MTOC (Alberts 2002). In T cells MTOC reorientation during IS formation counts as a hallmark of functional IS formation. During migration the intrinsic polarity of activated T cells settles the MTOC behind the nucleus at the uropod (Kupfer and Dennert

1984, Ratner et al. 1997, Alberts 2002, Watanabe and Noritake 2005). LGs are translocated along the microtubules towards the IS allowing for efficient killing of a target cell (Stinchcombe 2006). Yet MTs do neither produce force for migration nor aid in attachment to the extracellular matrix (Watanabe and Noritake 2005). MT dynamics are regulated via RhoGTPase activation by extracellular signals. In migrating cells microtubules are stabilized at their (+) ends which aids in reorienting the MTOC towards the leading edge facilitating a polarized cell (Watanabe and Noritake 2005). Recently it has been shown that the actin dynamics regulator profilin-1 associates with microtubules in a formin-mediated fashion affecting microtubule dynamics (Nejedla et al. 2016) possibly connecting actin and MT dynamics.

2.6.6 Analyzing cell migration

Analyzing migration in 3D matrices that resemble, from simple to a more complex ECM, requires special imaging and analysis methods. Selected plane illumination microscopy or Lightsheet microscopy can overcome the obstacles posed by 4D imaging experiments. The SPIM technique itself was first described in 1903 by Siedentopf and Zsigmondy. The very rudimentary version of a SPIM used sunlight projected through a slit to visualize gold particles in rubin glas (Siedentopf and Zsigmondy 1903). About 23 years ago the Laboratory of Ernst Stelzer developed the confocal theta microscope trying to increase axial resolution (Santi 2011). SPI microscopes have for a long time been self-produced. This resulted in microscopes with different specifications that were given different names. The basic principle is depicted in **Fig. 6** (Santi 2011). SPI microscopes are also commercially available from different microscopy companies (Leica, Zeiss). SPIM uses a μm thick sheet of light to generate optical sections from translucent fluorescent samples like tissue, cells embedded in a matrix and even (cleared) whole organisms (*Drosophila melanogaster*, *Danio rerio*) (Santi 2011, Reynaud et al. 2015). That SPIM requires transparent samples for depth penetration of the illuminating light poses limitations to the sample to be imaged. For cell biology applications, like migration of lymphocytes, a translucent matrix is needed yet collagen does not cause an imaging problem as transparency is given. To be able to analyze migration of highly motile lymphocytes in physiologically environments while avoiding killing animals or using live animals, to include complex spheroids or organoids predestines the use of 3D microscopy techniques and the build-up of 3D matrices of various and increasing complexity and thus physiologic relevance.

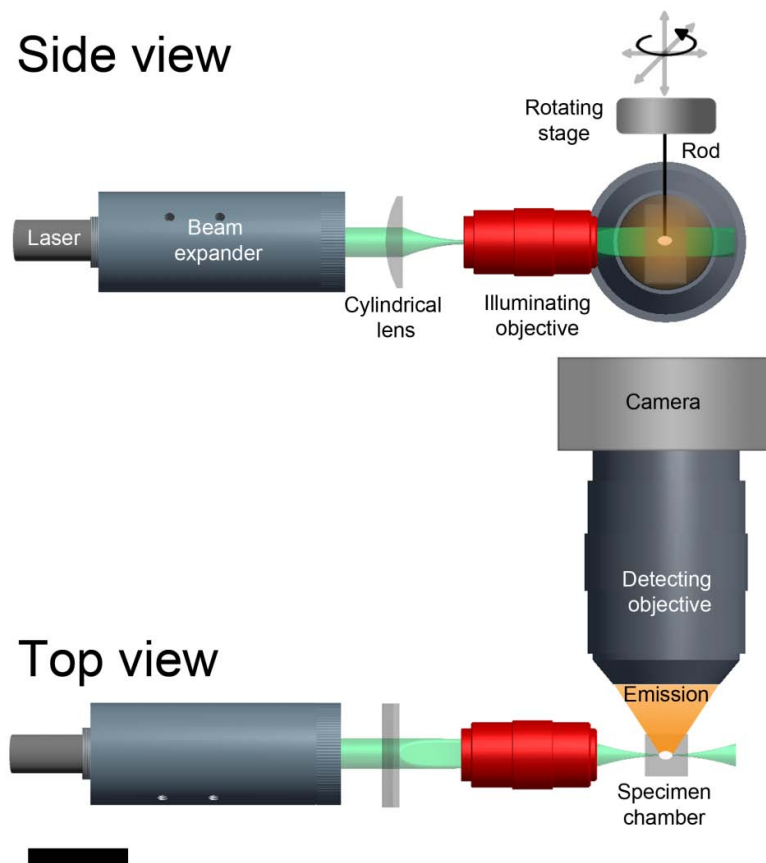


Figure 6 - Schematic of a simple SPIM setup. Shown is a basic SPIM setup. A laser beam is expanded and projected through a cylindrical lens to produce a light sheet which is further projected through an illuminating objective. The specimen chamber can be made of glass or must have optically clear walls and is open at the top. The chamber is filled with medium and the sample (attached to a mounting rod) is inserted into the chamber, where it hangs freely. The sample can be moved and rotated using the rotating sample holder/stage. Emission light is captured by a detection objective in azimuthal orientation. Scale bar = 5 cm (from Santi 2011).

2.5.6.1 Advantages of SPIM for 4D imaging

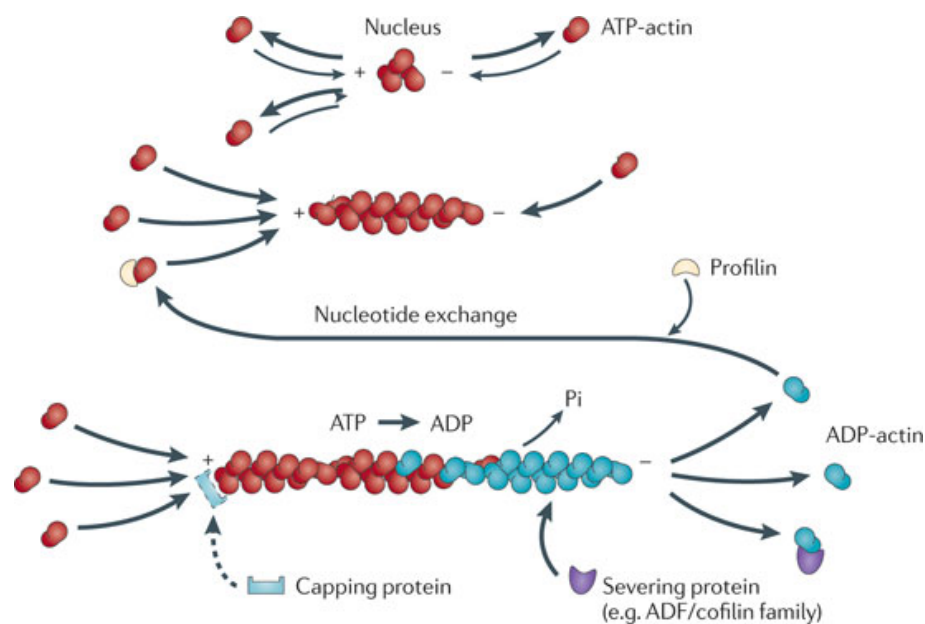
The use of a Lightsheet microscope for immunological research has many advantages yet success depends on overcoming several bottlenecks. SPIM generates ultra-fast (up to 100 fps), high resolution optical sections from tissue explants, organs, organisms and single cell populations. At the same time phototoxicity and bleaching of fluorophores is reduced (Santi 2011, Reynaud et al. 2015). SPIM allows, for the first time, long term imaging of complex 3D samples (multiple channels, large 3D volume and high time resolution). Because of the high frame rates and acquisition speed, large 3D volumes can be sectioned in seconds compared to minutes in epifluorescence or confocal microscopy. The detection objective is directly immersed in the sample chamber liquid, thus lateral resolution is defined by the specifications of the detection objective (Greger et al. 2007). SPIM has improved axial resolution compared to epifluorescence which is comparable to or better than the axial resolution of confocal

microscopes and achieving an isotropic resolution is possible (Greger et al. 2007). The high resolution in SPIM allows catching population movements and dynamic subcellular structures in a single experiment. Imaging fast dynamic processes of highly motile cells in 3D volumes for extended periods of time becomes now feasible. Important for cell dynamics in general is the dynamic control over cellular actin dynamics that can easily be visualized using SPIM.

2.7 Profilin and actin dynamics

Profilins were discovered as a factor that when added to actin solutions *in vitro* would inhibit actin polymerization (Carlsson et al. 1977). It was hence termed profilamentous-actin or profilin and it is from these experiments that the long time accepted function of PFN of sequestering G-actin monomers was coined. Cells control the cytoplasmic G-actin concentration via two proteins: profilin and thymosin $\beta 4$ (Irobi et al. 2004). Both bind G-actin and both are expressed in T cells yet only profilins interact with actin nucleators and polymerization regulators. Thymosin $\beta 4$ (named so for its predominant expression in thymocytes) thus represents the true actin sequestering function initially attributed to profilins (Gómez-Márquez 1989). Profilins are proteins expressed by virtually all animals and plants and cells move by using dynamic processes involving the cells cytoskeleton (Witke 2004). As mentioned before migration is actin polymerization driven process and profilins are the key regulators of actin dynamics we aimed at identifying profilin function in human primary CTL (Krishnan and Moens 2009). Profilins are small (14 - 17kDa (Reinhard et al. 1995, Krishnan and Moens 2009) cytoplasmic proteins that control actin dynamics and changes in profilin expression have been observed for certain neoplasms and it was shown that it can act as a tumor suppressor (Wittenmayer et al. 2004, Yao et al. 2014). All eukaryotes express profilins with the main difference between isoforms being affinity to interactive proteins. The primary sequence is not well conserved yet structural analysis across species showed that PFN structure is highly conserved (Pollard et al. 2001, Witke 2004, Krishnan and Moens 2009). Profilins bind G-actin (globular actin = monomers) blocking an actin:actin interaction site. Profilins also favor the conversion of ADP-actin to ATP-actin which is more readily polymerized. A higher affinity to ATP-actin over ADP-actin favors profilin to present ATP-actin monomers (Korn et al. 1987, Pollard et al. 2001). Actin monomers without presence of controlling proteins like profilin can spontaneously polymerize yet this process is slow. To control the dynamics a cell makes use of a vast number of proteins interacting with profilins to enhance, inhibit, regulate actin polymerization. Free actin monomers in the cell would

spontaneously polymerize in an uncontrolled fashion and initially PFN was thought to be an actin sequestering protein which posed several problems. First the PFN concentration in cells is not high enough to sequester the present G-actin monomers and this function is covered mainly by thymosin $\beta 4$. Also PFN1 overexpression or knock down has diverse effects in different cell types ranging from inhibition of migration to its promotion. The binding of actin might thus not represent a sequestering role of PFN1 but highlight the importance of PFN1-mediated actin delivery to sites of actin polymerization. Although ADP-G-actin can spontaneously switch to ATP-G-actin, binding of ADP-G-actin to profilin increases the rate of this nucleotide exchange by a factor of 1000 (Goldschmidt-Clermont et al. 1992). This quickly replenishes the pool of polymerization available ATP-G-actin (**Fig. 7**). Profilin bound actin (profilactin) can promote growth of actin filaments at the (+) end of the actin filament with the aid of elongation promoting proteins. To fine tune actin dynamics cells use various proteins that interact with profilins via a poly-L-proline interaction site. Both the actin binding region and the poly-L-proline binding domain overlap with the PIP₂ binding site of profilins separating processes mediated via these interactions from occurring simultaneously.



Nature Reviews | Cancer

Figure 7 - Profilin promotes elongation of nucleated actin filaments. Actin polymerization starts from nucleation of an actin multimer which is by itself unstable but can be stabilized by nucleating proteins. Once a filament is initiated by a nucleus, the filament can extend by binding of further actin monomers. Elongation happens at the (+) or barbed end. Profilin enhances ADP to ATP conversion, localizes large amounts of actin:profilin to sites of polymerization and thus increases polymerization rate of the actin filament. Elongation of the filament can be inhibited by e.g. binding of capping protein. “Older” parts of the filament (blue) will spontaneously hydrolyze ATP to ADP resulting in a destabilized filament ultimately resulting in depolymerization. This is further enhanced by proteins of the actin depolymerizing factor family e.g. cofilin (from Nürnberg et al. 2001).

2.7.1 Profilin expression in humans

The human genome encodes for 4 profilin isoforms named PFN1-4 which are products of different genes although alternative splicing can also occur. PFN1 is generally expressed in all eukaryotic cells (except muscle cells), also T cells, while expression of the other isoforms is tissue specific (Witke 2004, Krishnan and Moens 2009, Schoppmeyer et al. 2017). PFN2 is exclusively expressed in the nervous system during development and after differentiation. PFN3 and PFN4 are expressed in testis. PFN1 and PFN3 differ in affinities for interactive proteins yet PFN3 interacts with all common interactors of PFN1. PFN4 does not bind actin nor poly-L-proline ligands but a diverse palette of phospholipids highlighting the role of profilins in phospholipid signaling (Behnen et al. 2009).

2.7.2 Profilin regulation

Profilins have three interactions that define their functions: Binding of G-actin, binding to poly-L-proline ligands and binding to phosphatidylinositol-bisphosphate (PIP₂). Profilins interact with poly-L-proline sites on regulatory proteins from the mEna/VASP family, formin family and WASP/WAVE protein family that elongate or nucleate new filament (Reinhard et al. 1995, Miki et al. 1998, Ding et al. 2009). Poly-L-proline-mediated interaction with actin polymerization regulatory proteins are generally considered important for regulation of actin dynamics by PFN, interestingly overexpression of a mutant deficient of poly-proline binding results in different outcomes for cells either showing an enhancement or inhibition of actin-driven protrusions pinpointing at the differential downstream processes tied to the presence and identity of regulatory proteins (Pollard et al. 2001, Krause et al. 2003). Proteins of the mEna/VASP (*mammalian Enabled/vasodilator stimulated phosphoprotein*) family participate in different actin dependent processes and can bind profilin, F-actin and G-actin. The proteins localize to focal adhesions, lamellipodial and cellular protrusions (Krause et al. 2003). As do formins, mEna/VASP proteins also localize to filopodial tips (Goode and Eck 2007). PFN1 binds to VASP, although with a low affinity, via its poly-proline site (Krause et al. 2003). Next to the poly-L-proline domain mEna/VASP proteins contain two mEna/VASP homology domains (EVH1+2) that are also present in WASP family proteins. Via the EVH domain focal adhesion proteins are bound. Proteins of the mEna/VASP family localize to the barbed end of actin filaments, compete with capping protein for termination of a filament and inhibit formation of Arp2/3 mediated filament branches. *In vitro* mEna/VASP proteins can serve as actin nucleators (Krause et al. 2003, Kwiatkowski et al. 2003). WAVE proteins are downstream signaling targets for RhoGTPase family proteins and activate Arp2/3 complexes resulting in increased actin polymerization. Hematopoietic cells express WASP exclusively of the five genes within this protein family, namely WASP, N-WASP, WAVE1/SCAR1, WAVE2, and WAVE3, yet the other forms are also moderately expressed in hematopoietic cells (Miki et al. 1998, Kurisu and Takenawa 2009). WASP/WAVE proteins localize to the cell membrane by binding to phospholipids where they exert their function of coupling the cell membrane to actin polymerization to coordinate membrane-cytoskeletal dynamics (Kuris and Takenawa 2009). In T cells WASP is important for immunological synapse (IS) stabilization as cells deficient of WASP are able to form an IS yet this synapse collapses and cannot be reestablished. WASP is in this context recruited to the IS after TCR activation via

signaling through the proteins CD3, LAT and SLP76 (Sasahara et al. 2002, Badour et al. 2003, Billadeau et al. 2006). Formins serve in actin nucleation and elongation of unbranched linear actin filaments. After nucleation formins will stay localized to the growing barbed end of the filament they nucleated (Favaro et al. 2003, Goode and Eck 2007, Chalkia et al. 2008). Formins contain three distinct *formin homology domains* FH1+2+3. Profilin is bound via the poly-L-proline rich FH1 while FH2 serves as actin nucleation site and FH3 aids in localizing formins within a cell (Favaro et al. 2003). Next to FH domains formins also possess SH3 (Src-homology domain 3, binds poly-L-proline) and a WW (tryptophan-tryptophan) domain that also binds poly-L-proline rich ligands. Formins are essential regulators of protrusions which are powered by parallel linear actin filament elongation. In T cells formins are essential cytoskeletal regulators and regulate MTOC reorientation towards the IS (Gomez et al. 2007, Andrés-Delgado et al. 2013). Apart from G-actin and poly-L-proline ligands PFN1 binds to membrane bound phosphatidylinositol-biphosphate (PIP₂) and also other phospholipids (Behnen et al. 2009). PIP₂ is a phospholipid found ubiquitously in a cell's membrane and plays a role in calcium signaling and protein kinase C signaling. Extracellular signals activate phospholipase C to cleave PIP₂ to diacylglycerol (DAG) and inositol-triphosphate (IP₃) which participate in a myriad of signaling processes including actin remodeling and vesicle trafficking (Thapa and Anderson 2012). Binding of profilin to PIP₂ is mediated by basic amino acids that interact with the negatively charged head of PIP₂. Binding to PIP₂ inhibits phospholipase C from hydrolyzing PIP₂ to DAG (→ inhibition of protein kinase C) and thus also generation of inositoltriphosphate (IP₃) (binding to InsP₃R(eceptor) on the ER membrane causes calcium release from ER to the cytosol) (Goldschmidt-Clermont 1990, Sohn et al. 1995). This makes PFN1 a negative regulator of phosphoinositide mediated signaling. The interaction of PIP₂ and PFN1 also blocks the actin binding site and partly the poly-proline interaction site of PFN1, inhibiting its function. Next to PIP₂ (PI(4,5)P₂) PFN1 binds with similar affinity to the phosphatidyl-inositol-biphosphates (PtdIns P₂) PI(3,4)P₂, PI(3,5)P₂ and the phosphatidyl-inositol-triphosphate (PtdInsP₃) PI(3,4,5)P₃ indicating a diverse role in PtdIns-mediated signaling pathways (Behnen et al. 2009). Important pathways associated with PIP₃ control the activation of WASP (that itself binds to PIP₂ to be activated) via Cdc42 resulting in Arp2/3 mediated actin polymerization (Johnson and Rodgers 2008). In immune cells PI regulate differential processes by direct interaction with: Ezrin-radixin-moesin (ERM) proteins that control tethering of the actin cytoskeleton to the plasma membrane controlling

cell shape and adhesion, talin (activated by PIP₂) and vinculin connecting focal adhesion dynamics to PI mediated signaling and actin severing proteins like gelsolin are inhibited by PIP₂ binding (Johnson and Rodgers 2008). The binding of PFN1 to PIs is separated from actin modulating functions via overlapping binding sites of actin and poly-L-proline ligands with the PI binding site (Goldschmidt-Clermont 1990, Sohn et al. 1995). Different mutations of PFN1 are known that abolish or drastically reduce binding of PFN1 to actin, PIP₂ and poly-proline rich ligands (Sohn et al. 1995, Wittenmayer et al. 2004, Smith et al. 2015) allowing to test the impact of these interactions in regard to cytoskeletal control. Mutations used include Y59A (no actin binding of PFN1), R88L (no PIP₂ binding), H133S (no poly-proline interaction with regulatory proteins) and C71G (causes cytoplasmic protein aggregates, discovered to cause amyotrophic lateral sclerosis) (Wittenmayer et al. 2004, Smith et al. 2015). Using these mutations the importance of specific interactions can be determined. Profilins have also been implicated with different types of cancer (Wittenmayer et al. 2004 Zou et al. 2007, Bea et al. 2009, Cheng et al. 2013, Yao et al. 2014, Zaidi and Manna 2016). Mammary carcinoma have been found to have a downregulation of PFN1 and this correlates with increased motility/invasiveness of breast cancer cell lines (Bea et al. 2009) also a downregulation of PFN1 compared to surrounding tissue was found in pancreatic adenocarcinoma (Yao et al. 2014). As our collaborator found not only a dysregulation of PFN expression in tumor cells but also in peripheral CTL of pancreatic cancer patients and due to the wide variety of pathological outcomes that arise from dysregulation of PFN expression and its central participation in control over actin dynamics led us to determine PFN function in primary human CTL (Yao et al. 2014).

2.8 Project aims

Aim of this thesis was to develop methods to analyze migration of primary human lymphocytes in 3D matrices, determine the search strategy in different context, the mode of migration applied in an unguided environment and the effect of certain ECM factors on the migration behavior of primary human CTL. Using fluorescent microscopy (Epifluorescence and Lightsheet fluorescence) I wanted to analyze migration by tracking cells in 3D matrices. Using different microscopy technologies the migration parameters of lymphocytes, the effects of stimulation/activation of T cells on these parameters, the effect of matrix modifications by extracellular matrix proteins or glycosaminoglycans were to be analyzed. 3D systems for (primary) culture, immunofluorescence, imaging protocols for matrix based migration and

killing that can easily be adapted to other processes, were to be established for epifluorescence and Selected Plane Illumination microscopy. Together with collaborators in Shanghai (Group of Prof. Dr. Xianjun Yu, Fudan University, PR China) we wanted to analyze the function of the cytoplasmic protein PFN1 in CTL as they could not only find implications of dysregulation of PFN1 expression in tumors but also in CD8⁺ T cells from pancreatic cancer patients. Using primary human CTL and overexpression and knock down approaches we wanted to determine the effects of PFN1 on actin related processes like cell migration and cytotoxicity. Combined this shall partake to answer the question of how T cells can roam the body so efficiently finding and eliminating rare targets and how this is controlled via the cytoskeletal actin-binding protein profilin1 and its interactors.

3. Materials and methods

3.1 Reagents and antibodies

All chemicals that were not specifically mentioned were obtained from Sigma (highest quality grade). The reagents and antibodies used in experiments are listed below.

Table 2 - Material list

Reagent/Material	Supplier	Cat. #
Calcein-AM	Thermo Fisher	C3100MP
Phalloidin Alexa 633	Thermo Fisher	A22284
Hoechst 33342 (H33342)	Sigma Aldrich	H1399
CellMask Orange	Thermo Fisher	C10045
SYTO sampler kit	Thermo Fisher	S7572
Capillary	VWR	613-3373
Piston	VWR	BRND701934
MColorpHast 6.5 - 10	Merck	1.09543.0001
Tween 20	Sigma	P1379-250mL
Triton X100	Eurobio	018774
P3 Primary solution kit	Lonza	V4XP-30XX
Anti-evaporation oil	Ibidi	50051
Fibronectin	ABM	#5050-1MG
Collagen	ABM	#5010-50ML (Nutragen) #5133-20ML (Fibricol)
Interleukin 2	Thermo Fisher	PHC0023
Bovine serum albumin	Sigma	A9418-100G
Penicillin / streptomycin	Thermo Fisher	10378-016
10 x PBS	Thermo Fisher	18912-014

Table 3 - Antibody list

Antibody	Target	Specif.	Source	Cat. #
α -hVin1	Vinculin	human	Sigma	V9131-.2ML
α -PFN1	Profilin1	human	Abcam	ab124904
Goat α -Rabbit 488	IgG (H+L)	rabbit	Life technologies	A-11008
Goat α -Mouse 488	IgG (H+L)	mouse	Life technologies	A-11001
Goat α -Mouse 568	IgG (H+L)	mouse	Life technologies	A-11004
Goat α -Rabbit 568	IgG (H+L)	rabbit	Life technologies	A-11011
Goat α -Mouse 647	IgG (H+L)	mouse	Life technologies	A-21235
Goat α -Rabbit 647	IgG (H+L)	rabbit	Life technologies	A-21244
α -CD3	CD3	human	Serotec	MCA463XZ

Table 4 - Plastic and glass ware

Item	Supplier	Cat. #
μ dish, plastic bottom, high	Ibidi	81156
TC flask for suspension cells	Sarstedt	83.3910.502
6 well plate (culture)	Falcon/Corning	353046
24 well plate (culture)	Falcon/Corning	353047
96 well plate (real time killing)	Falcon/Corning	353219
Capillary	VWR	613-3373
Piston	VWR	BRND701934

3.2 Cell Culture

3.2.1 Continuous cell culture of suspension cell lines

Suspension cell lines (P815, K562, and Raji) were cultured according to the suppliers instructions. In short: continuous cultures were cultured according to **table 5** using the described media. For subculture continuous culture was diluted in fresh medium and culture was continued. Continuous cell culture was performed by Gertrud Schwär, Sandra Janku and Cora Hoxha.

Table 5 - Continuous cell lines and corresponding culture conditions

Cell Line	Split: work days	Split: weekend	Medium	FCS	Pen/Strep
Raji	1:6	1:8	RPMI 1640	10%	1%
P815	1:12	1:18	RPMI 1640	10%	1%
K562	1:4	1:6	RPMI 1640	10%	1%

Table 6 - Continuous cell line sources

Cell line	Source	Origin
P815	ATCC TIB64 (mouse)	Mastocytoma
Raji	ATCC CCL86 (human)	B-cell lymphoblast
K562	ATCC CCL243 (human)	Lymphoblast

3.2.2 Isolation and culture of primary human lymphocytes

Table 7 - Cell culture reagents

Reagent	Origin/Species	Storage	Supplier	Cat. #
AIMV	-	4 °C	Thermo Fisher	12055091
RPMI 1640	-	4 °C	Thermo Fisher	21875-034
FCS	South America	-20 °C	Thermo Fisher	
Penicillin/Streptomycin	-	-20 °C	Thermo Fisher	P4333-100ML
DPBS	-	RT	Thermo Fisher	14190144
Staphylococcal enterotoxin A	<i>Staphylococcus aureus</i>	4 °C	Sigma	S9399-.5mg
HBSS	-	RT	Sigma	H6648-500ML

Table 8 - Primary cell isolation/stimulation kits

Product	Supplier	Cat. #
Dynabeads Untouched Human CD8 T Cells Kit	Thermo Fisher	11348D
Dynabeads CD8 Positive Isolation Kit	Thermo Fisher	11333D
Dynabeads Human T-Activator CD3/CD28	Thermo Fisher	11132D
Dynabeads Untouched Human NK Cells Kit	Thermo Fisher	11349D

3.2.2.1 PBMC isolation

Peripheral blood mononuclear cells (PBMC) were isolated from human blood from healthy donors taken from leukocyte reduction system chambers (LRS chamber) of the TrimaAccel thrombocyte apheresis system provided by the *Klinik für Hämostaseologie und Transfusionsmedizin* of the *Blutspendendienst des Klinikum des Saarlandes*. Leucosep tubes were filled with leukocyte separation medium 1077 (15 mL / 50 mL tube). Blood was flushed from the LRS chamber using Hank's buffered salt solution (HBSS) and carefully mixed shortly. Blood samples were optically checked using a cell culture microscope. This was followed by the gradient centrifugation at 450 g for 30 min at RT. Afterwards the upper yellow layer was aspirated and the leukocyte ring was transferred into a fresh 50 mL conical tube and filled up to 50 mL using HBSS. Cells were pelleted by centrifugation at 250 g for 15

min at RT. Next erythrocytes were lysed using 1 - 3 mL erythrocyte lysis buffer for 60 to 120 s. Afterwards the tube was filled to 50 mL using HBSS followed by a thrombocyte wash at 130 g for 10 min at RT. Supernatant was aspirated and 20 mL cold PBS + 0.5 % BSA were added. Cells were counted and kept on ice until further use. PBMC isolations were routinely performed by Carmen Hässig (Biophysics, Homburg).

3.2.2.2 Staphylococcal enterotoxin A (SEA) stimulation of human PBMC

For SEA stimulation isolated PBMC were centrifuged at 200 g for 8 min and resuspended in pre-warmed AIMV medium at a density of 100×10^6 cells mL^{-1} . SEA was added to the cell suspension at a 1:200 dilution from a 1 mg mL^{-1} stock (5 $\mu\text{g mL}^{-1}$ final SEA concentration). The cells were incubated for 1h at 37 °C and 5 % CO_2 . During this time 50 mL (per 100×10^6 cells) AIMV containing 10 % FCS were incubated along with the cells. Afterwards the cell suspension was added to the 50 mL AIMV +10 % FCS and IL-2 is added to a final concentration of 100 U mL^{-1} . The cells were incubated without medium change for 5 days followed by positive isolation.

3.2.2.3 Positive isolation of CD8^+ from PBMC

PBMC were resuspended in isolation buffer (PBS + 0.5 % BSA) at 10×10^6 mL^{-1} . 25 μL Dynabeads CD8 were added per 10×10^6 cells mL^{-1} cell suspension. The sample was incubated rotating for 20 min at 4°C. A Dynamag magnet (2min) was used to remove the supernatant. The bead solution was resuspended 2 or 3 times using 1 mL isolation buffer and the liquid was removed afterwards using a magnet. Cell:bead suspension was resuspended using culture media containing FCS (100 μL per 10×10^6 cells) and 10 μL per 10×10^6 cells of DETACHaBEAD were added followed by 45 min of incubation at RT. Using a magnet for 2 min the supernatant was transferred into a fresh tube. Repeat resuspension and supernatant transfer 2 or 3 times using 500 μL medium. To remove DETACHaBEAD, volume of suspension was increased to 4 mL per 10×10^6 cells and centrifuged at 400 g for 6 min. Cells were resuspended in AIMV + 10 % FCS.

3.2.2.4 Negative isolation of CD8^+ or NK cells from PBMC

As the NK and CTL untouched isolation kits use the same isolation protocol for both cell types they are combined in this paragraph. Isolation of CTL (untouched) was carried out using the Dynabeads Untouched Human CD8 T Cell Isolation kit (Cat. # 11348D, Thermo Fisher) or Dynabeads Untouched Human NK Cell Isolation kit (Cat. # 11349D, Thermo Fisher).

Isolation MyONE SA Dynabeads were vortexed for 30 s and the needed volume was washed using the same volume or at least 1 mL PBS +0.5 % FCS. The washing solution was removed using a magnet and beads were resuspended in the same volume of isolation buffer as the initial volume of bead solution. PBMC (1×10^8 cells mL⁻¹ isolation buffer) were mixed with FCS (100 μ L per 5×10^7 cells) followed by the corresponding antibody mix (100 μ L per 5×10^7 cells) for the specific cell types followed by incubation at 4°C for 20 min. Afterwards the volume of the cell-antibody suspension was increased several fold and the cells were pelleted at 350 g for 8 min at 4°C. The pellet was resuspended in isolation buffer and washed Dynabeads were added. Samples were incubated for 15 min at RT in a HulaMixer (Cat. # 15920D, Thermo Fisher Scientific) while shaking and rotating. Volume was increased after incubation using isolation buffer and mixed carefully to dissociated clumped beads. The tube was placed in a magnet for 2 min before transferring the supernatant to a new tube. This step was repeated twice and the supernatants combined. To remove bead remnants the final collection tube was placed in a magnet for another 2 min and the cell suspension was transferred into a new tube. Cells were harvested by centrifugation and resuspended in AIMV + 10 % FCS.

3.2.2.5 Cell culture of primary cells

Post isolation, CTL (untouched), CTL (SEA stimulated) or NK cells were cultured in AIMV medium containing 10 % FCS. For specific supplements that were added see **table 9**.

Table 9 - Primary cell culture supplements

Cell type	Supplement	Time of supplementation
CTL (untouched)	IL-2 30 U mL ⁻¹	During bead stimulation/ post transfection
CTL (SEA stim.)	IL-2 10 U mL ⁻¹	Post isolation/"Restimulation" 48h post isolation
NK	IL-2 100 U mL ⁻¹	Restimulation

3.2.2.6 Bead stimulation of untouched isolated CD8⁺ cells using α CD3/CD28 antibody coated beads

Untouched isolated CTL were seeded into 6-well plates at 1.5×10^6 cells mL⁻¹. The necessary volume of beads was calculated as follows. A bead to cell ratio of 0.8 was used instead of 1:1, as recommended by the manufacturer.

$$\frac{\text{Total cell number} * 0.8 \text{ (bead: cell ratio modification)}}{40 \times 10^6 \frac{\text{beads}}{\text{mL}}}$$

$$= \text{Volume of bead solution (mL)}$$

Concentration of bead stock: $40 \times 10^6 \text{ mL}^{-1}$. The bead solution was washed using either the same volume as of bead solution or for volumes below 1 mL of bead solution at least 1 mL of isolation buffer, by mixing. The wash solution was removed using a magnet (Dynamag, Thermo Fisher) and the stimulation beads are resuspended in culture medium before addition to the CTL suspension. Additionally 30 U mL^{-1} of recombinant human interleukin-2 were added and the cells were cultured for 48 h in a cell culture incubator at 37°C with 5 % CO_2 .

3.3 Electroporation (plasmids and siRNA) of primary human CTL

For a single transfection 5×10^6 cells were used per cuvette of the 4D system (Lonza). The “P3 Primary solution kit” (Lonza, Cat. # V4XP-30XX) was used for primary human CTL and 1 μg of plasmid DNA or 20 μM siRNA was used for transfection. The medium was changed the morning after transfection. Prior resuspension of cells in transfection solution the cells were washed twice using PBS. Plasmids used for transfection were of pMAX backbone and prepared by Yan Zhou (Biophysics, Saarland University, Homburg, Germany) PFN1_mCherry and the mutations Y59A, R88L, C71G and H133S were generated as described in Schoppmeyer et al. 2017.

3.3.1 siRNA

The siRNAs against PFN1 were purchased from Qiagen (Flexitube siRNA, **table 10**).

Hs_PFN1_11: 5'-GGCCAGGGCTGGATGGACAGA-3'

Hs_PFN1_10: 5'-CCTCCCGTGTGTGGTTGGAAA-3'

Non-silencing control siRNA (Microsynth): 5'-UUCUCCGAACGUGUCACGUGdTdT-3'

Table 10 - siRNA used in experiments

Name	Source	Modifications	Cat. #	Stock
Hs_PFN_1_10	Quiagen	None	SI04436229	20 μM
Hs_PFN_1_11	Quiagen	None	SI05028240	20 μM
Non silencing	Microsynth	None	1022076 / 1027310	20 μM

3.4 Real-time killing assay (Kummerow et al. 2014)

This Target cells were calcein-AM loaded at 1×10^6 cells mL^{-1} at 500 nM in AIMV + 10 mM HEPES (AIMV°) for 15 min at RT with gentle shaking. Afterwards cells were washed once using AIMV°. Calcein-loaded target cells were resuspended in AIMV° to yield the wanted cell number per 200 μL and this suspension was added to wells of a 96 well plate (black, clear bottom) where cells were allowed to settle during preparation of the killer cells. Killer cells (NK, bead stimulated/SEA-stimulated CTL) were counted and resuspended in 50 μL AIMV° according to the E:T ratio to be used (for 25.000 targets / well and a E:T of 10:1, 250.000 killer cells are prepared in 50 μL $\rightarrow 5 \times 10^6$ killer cells mL^{-1}). The killer cell suspension was carefully added on top of the target cell wells and measurement was started immediately in a TECAN Genius Pro plate reader with incubation control for 4 h at 10 min intervals. The following controls were used:

Live control: Calcein-loaded target cells without killers in 250 μL AIMV°

Medium background control: 250 μL AIMV° medium only (subtracted from Live control and killer samples)

Lysis control: Triton X100 (7.5 %) lysed targets 250 μL AIMV° + 20 μL Triton X100

Lysis background control: 250 μL AIMV° plus 20 μL Triton X100 (subtracted from Lysis control)

The index I for correction of target cell numbers was calculated as follows at $t = 0$:

$$\text{Index} = \frac{\text{Fluorescence}_{\text{experiment}} (\text{at } t=0)}{\text{Fluorescence}_{\text{live control}} (\text{at } t=0)}$$

After subtracting background values target cell killing was calculated as follows:

$$\% \text{ Killing of targets } (t) = \frac{\text{Fluorescence}_{\text{live control}} - \text{Index} * \text{Fluorescence}_{\text{experiment}}}{\text{Fluorescence}_{\text{live control}} - \text{Fluorescence}_{\text{lysis control}}} * 100$$

SEA-pulsed Raji cells (SEA stimulated CTL) or P815 cells using α -CD3 (MCA463XZ, Serotec) antibodies (bead stimulated CTL) were used as target cells. Effector to target (E:T) ratios are indicated in the figures.

3.4.1 Staphylococcal Enterotoxin A pulsing of Raji cells for real time killing

Raji cells were resuspended in AIMV (+10 % FCS) containing 100 $\mu\text{g mL}^{-1}$ SEA. 100 μL per 0.5×10^6 cells were used and cells were incubated for 30 min at 37 °C and 5 % CO_2 . One washing step was applied using AIMV + 10 % FCS. Afterwards cells were labeled using calcein as described in 3.4.

3.5 Live cell imaging

3.5.1 Cell labeling for fluorescence microscopy

Cells were counted and 0.1 to 1×10^6 cells were harvested and collected by centrifugation at 200 g for 8 minutes. Dye stock solutions (see below) were diluted in AIMV (Gibco, Life Technologies) with or without 10 % FCS. Cells were resuspended in the staining solution at a density of 1×10^6 cells mL^{-1} and incubated for the designated times in a cell culture incubator in a well plate. Afterwards the cells were harvested by centrifugation at 200 g for 8 minutes and washed once using AIMV with or without 10 % FCS and harvested by another centrifugation step at 200 g for 8 minutes.

H333342: (1 mg mL^{-1} in H_2O) stock solution was diluted 1:2.000 in AIMV containing 10 % FCS.

Cell Mask Orange: (10 mM in DMSO) was diluted 1:10.000 in AIMV without FCS.

SYTO XX (XX = 10, 13, 16, 21; for all the same) was diluted 1:10.000 in AIMV containing 10% FCS.

Cell Mask DeepRed (10 mM in DMSO) was diluted 1:10.000 in AIMV without FCS.

3.5.2 Preparation of “Nutragen” and “Fibricol” collagen solution

Nutragen ($\sim 6 \text{ mg mL}^{-1}$ stock) or Fibricol ($\sim 10 \text{ mg mL}^{-1}$ stock) (**table 2**, Advanced Biomatrix, USA) was prepared according to the manufacturer's instructions. The pH was checked using MColorpHast non-bleeding pH indicator strips (pH 6.5 - 10, Merck, Cat. # 1.09543.0001) using 0.5 μL of neutralized solution to check for homogeneous neutralization. Once the solution reached a stable pH of ~ 7.4 it was kept on ice until further. Prepared solutions were always used on the same day. A fresh neutralized stock was prepared for every experimental day. All compounds were kept on ice during preparation and until further use.

3.5.5 Epifluorescence Microscopy

Fluorescently labeled samples were analyzed in a *Zeiss Observer Z.1* with a Zeiss Colibri LED illumination system and incubation. The following tables list the components of the microscope.

Table 11 - Colibri LEDs equipped in Cell Observer Z.1

LED	Emission λ
1	365 nm
2	470 nm
3	555 nm
4	625 nm

Table 12 - Objective list of the Cell Observer Z.1

Objective	Mag. / Apert.	Immersion
Fluar	5x/0.25 M27	Air
Fluar	10x/0.5 M27	Air
Fluar	20x/0.75 M27	Air
Plan-Apochromat	63x/1.40 M27 DIC	Oil

Table 13 - Filter sets of the Cell Observer Z.1

Filter Position/Name	Exc. λ (nm)	Optical path	Em. λ (nm)
1 DAPI	359-371	395	397- ∞
2 HE GFP	450-490	495	500-550
3 HE dsRED	538-562	570	570-600
4 HE Cy5 (custom)	620/60	700	700/75

Images were taken using an AxioCamM1 CCD camera using **AxioVision 4.1.8** software.

3.5.7 Fixation of cells in collagen

Cultured cells (on coated coverslips or μ -dishes (Ibidi GmbH) or embedded cells (collagen 0.25 - 0.5 %) were washed with PBS to remove medium remnants and then fixed with 4 % PFA at RT for 10 min (coverslips) or 15 min (collagen matrices). One washing step was applied using PBS. The cells were then covered with PBS and stored at 4 °C for maximally one week before IF staining.

3.5.8 IF staining of CTL in collagen droplets on coverslips / μ dishes

PFA fixed and stored (at 4 °C in PBS) samples were allowed to reach RT followed by 10 min of permeabilization using PBS containing 0.5 % Triton-X100. Without washing steps blocking buffer was applied containing PBS with 1 % BSA for 30 min. This was followed by application of the primary antibody(-ies) diluted in PBS-T (PBS containing 0.05 % Tween-20). Afterwards two washing steps were applied using PBS-T followed by application of the secondary antibody(-ies) for 30 min followed by two further washing steps using PBS-T (when used, phalloidin-alexa_633, DAPI or HOECHST33342 was added to the secondary antibody solution). This was followed by washing steps of 5 min using PBS-T (3 x), PBS (3 x) and ddH₂O (2 x, not for capillaries). The samples were then mounted using Prolong Gold Antifade reagent (Life Technologies) and stored at RT or stored in PBS at 4 °C and imaged directly (capillary).

3.5.9 Height measurement of 2D matrix

The bottom of a μ -dish (35 mm high, plastic bottom, Ibidi) and one side of an 18 mm glass coverslip (strength 1.5: 0.16 - 0.19 mm) were coated using fluorescent microspheres (0.17 μ m, DeepRed, 2 mM) at a 1:10.000 dilution by applying 200 μ L of the diluted fluorescent spheres. The dish and coverslip were allowed to dry at 60 °C in a heating cabinet for 1h. Afterwards 14 μ L of 0.25 % collagen solution was applied as for 2D matrix sample preparation and flattened using the microsphere coated coverslip. The matrix was allowed to polymerize for 1h in an incubator at 37 °C and 5 % CO₂. The sample was then imaged dry (after polymerization before medium addition) and with medium applied. The distance between dish bottom and coverslip was measured using the z-axis positioning system of the Zeiss Cell Observer Z.1 measuring from the focus plane of the microspheres coated onto the dish to the focus plane of the microspheres coated onto the coverslip.

3.6 Single plane illumination microscopy

3.6.1 Sample preparation for SPIM imaging and tracking analysis

In Single plane illumination microscopy (SPIM) CTL were visualized by fluorescent protein transfection or small molecule dyes. Neutralized collagen solution was diluted to a final concentration of 0.5 %, if not otherwise mentioned in the figures, using the media to be used during experimentation. The cell:collagen:medium suspension was polymerized as rods in glass capillaries for imaging in the Lightsheet Z.1 LFSM microscope (Zeiss). SPIM imaging

was performed in RPMI 1640 containing 10 % FCS, 1 % Pen/Strep and 20 mM HEPES. CZI files were converted using Imaris File Converter 8.1.2 and tracking was performed using the spot detection function of Imaris 8.1.2 (Bitplane AG).

3.6.2 Single plane illumination microscopy (SPIM)

Fluorescently labeled samples were imaged in a *Zeiss Lightsheet Z.1* with incubation, solid state laser illumination, dual side illumination and two sCMOS detectors.

The following tables list the components of the microscope.

Table 14 - Solid state laser used in experiments of the Lightsheet Z.1 system

Laser	Emmission λ (nm)	Power [mW]
488-30	488	50
561-20	561	20
638-75	638	60

Table 15 - Detection and illumination objectives of the Lightsheet Z.1

Objective (Detection)	Mag. / Apert.	Immersion	Material Number
W-Plan-Apochromat	20x/1.0 DIC VIS IR	Water	421462-8210-000
Objective (Illumination)	Mag. / Apert.	Immersion	Material Number
(2x) SPIM 10x	10x/0.2	Air	400900-9000-000

Table 16 - Equipped beam splitters of the Lightsheet Z.1

Beam Splitter pos.	Em. Filter 1	Em. Filter 2
0 Mirror	none	none
1 SBS LP 490	BP 420-470	BP 505-545
2 SBS LP 510	BP 420-470	BP 575-615
3 SBS LP 510	BP 460-500	BP 525-565
4 SBS LP 560	BP 505-545	LP 660
5 SBS LP 560	BP 505-530	LP 585

Images were taken using (2x) pco.edge sCMOS camera(s) with the software **Zen black 2014 SP1 Hotfix2 (v9.2.2.54)**.

For long term imaging (several hours) the medium in the sample chamber was overlaid with ~ 1 mL silicone oil (Ibidi, Anti-evaporation oil, *Cat. # 50051*). To image cells in collagen rods the sample was mounted and the rod was pressed out of the capillary a few millimeters.

3.6.3 Fixation of primary CTL in collagen rods

Collagen (0.25 - 0.5 %) embedded cells in capillaries (Brand, *Cat. # 613-3373*) were washed with PBS, by pushing the matrix rod into the liquid to be applied, to remove medium remnants and then fixed with 4 % PFA at RT for 10 min (coverslips) or 15 min (collagen matrices). One washing step was applied using PBS. The cells were then stored immersed in PBS at 4 °C for a few hours before IF staining.

3.6.4 Automated cell detection and tracking of SPIM data using Imaris

The experiment files (.czi, carl zeiss image) were converted into the Imaris file format (.ims) using the Imaris file converter (version 8). The converted files were loaded into Imaris (version 8) and a spot detection was performed (Standard setting for CTL spot detection: Estimated diameter: 7 µm (nuclear) or 10 µm (cytoplasmic)) in the corresponding fluorescence channel. Detected spots were checked for consistent detection over time visually and a suitable quality threshold was set manually. Tracking was performed with a max gap size of 1 and a maximal distance of 20 µm. Single cell specific values and all cell averages values were exported as .xls (excel file format). Data was further analyzed using Graphpad Prism 6. Note that analysis of files in the Terabyte range can take several days up to a week or more.

3.7 2D matrix migration

CTL were counted and harvested by centrifugation at 200 g for 8 min and labeled using Hoechst 33342. Cells were resuspended first in AIMV + 10 % FCS and afterwards neutralized collagen stock solution was added to reach a final concentration of 0.25 % collagen with a cell density of 6×10^6 cells mL⁻¹. 14 µL of this cell/collagen solution were added as a droplet into the center of an Ibidi µ-dish (Ibidi, 35 mm high, plastic bottom) and a sterile coverslip (18mm, round, glass, 1.5, OrsaTech) was carefully added on top of the droplet to flatten the unpolymerized cell/collagen solution. The chamber was closed and incubated for at least 60 min in a standard cell culture incubator. Then 1200 µL of AIMV + 10 % FCS were carefully added to the µ-dish. The cells were then allowed to recover for 60 min in a cell culture incubator before imaging. Imaging was performed using a Cell Observer

(Zeiss, Jena, Germany) with incubation control (37 °C and 5 % CO₂) and a 5 x objective (5x/0.25 M27, Air) that allows to image the cells within one focal plane. Several areas were selected and stored using the positioning system of the AxioVision software (Zeiss, Version 4.8.1.0) and imaged for 30 min at 10 s intervals using the corresponding filter set of the transfected fluorescent protein (GFP/RFP) or H33342 and the corresponding LEDs of the Zeiss Colibri system. Files were auto-saved as .zvi (Zeiss Vision Image) and converted into the Imaris file format (.ims) using the Imaris file converter (7.7.2). The converted files were loaded into Imaris (8.1.2) and a spot detection was performed (Standard setting for CTL spot detection: Estimated diameter: 7 µm (nuclear) or 10 µm (cytoplasmic)) in the corresponding fluorescence channel. Detected spots were checked for consistent detection over time visually and a suitable quality threshold was set manually. Tracking was performed with a max gap size of 1 and a maximal distance of 20 µm. Single cell specific values and all cell averages values were exported as .xls (excel file format). Data was further analyzed using Graphpad Prism 6.

3.8 Data Analysis

Microsoft Excel 2010, Microsoft Office Suite 2010

Fiji ImageJ 1.51A, NIH, using Java 1.6.0_24 64bit, Software available at <https://imagej.net/Fiji/Downloads>

Imaris v7.7.2 or v8.1.2 (Imaris, ImarisTrack, ImarisMeasurementPro, ImarisVantage) Bitplane AG, software available at <http://bitplane.com>

3.9 Statistics and graphing

Legend: $p \leq 0.05 = *$; $p \leq 0.01 = **$; $p \leq 0.001 = ***$; $p \leq 0.0001 = ****$

IgorPro 6.12, Wave Metrics Inc., (Lake Oswego, OR, USA)

Graphpad Prism 6.0.1, for Windows, GraphPad Software (San Diego, CA, USA) software available at www.graphpad.com

3.10 Ethics

This study includes research on human material (leukocyte reduction system (LRS) chambers from human donors after thrombocyte apheresis) and is authorized by the ethic committee (Declaration: 16.4.2015; 84/15; Prof. Dr. Rettig-Stürmer). The profilin1 study was approved

by the Clinical Research Ethic Committee of Shanghai Cancer Center of Fudan University (Shanghai) including written informed consent from each patient.

4. Results

4.1 Development of 3D migration assays

4.1.1 3D Biology

Switching from 2D experiments to 3D experiments is a difficult task. 3D systems increase the physiological relevance of experiments yet also pose a challenge in imaging and analysis of data. Ultimately the 3D system shall be used for analyzing many different aspects of T cell biology including migration, killing, infiltration of tumor spheroids and other processes. To examine these processes there is need to add different cell types (target cells, bystander cells, helper T cells etc.) and to modify the matrix or tune it towards specific properties. Collagen concentrations in tissue are difficult to measure. Matrix rigidity of pure collagen matrices with concentrations of 1 to 4 mg mL⁻¹ lie in the range of 200 to 1600 Pa. These stiffness values represent normal glandular tissue (1 mg mL⁻¹ = ~200 Pa) up to more rigid tumor or the associated stroma (4 mg mL⁻¹ = ~1600 Pa) (Paszek et al. 2005). These values will vary for other types of tissue. We choose to use collagen at a concentration of 2.5 mg mL⁻¹ as a standard to mimic tissue architecture of normal tissue with intermediate density (Wolf et al. 2009). In the beginning the compliance of the collagen matrix (at concentration of 0.25 %) by different cell types (primary human bead stimulated CTL, primary human NK and different cell lines) was qualitatively tested. So far, all cell types and lines tested accept a simple collagen matrix of 0.25 % were viable and showed active migration within the matrix (examples shown in **Fig. 8 A**). Directly after polymerization of the collagen matrix (**Fig. 8 A** - second row) P815 (and Raji, to a lower degree) show different morphologies. After 24 h in the collagen matrix P815 (mastocytoma cells, mast cell derived tumor cells) have spread out and formed a meshwork of cell protrusions not seen in 2D culture systems (**Fig. 8 A** - lower right panel). Raji (B cells) do not generate protrusions and stay round. The morphology of bead stimulated CTL in 2D and 3D was very similar, yet in 3D systems cells are more motile and the cells do not get stuck at the uropod as commonly seen in 2D migration experiments which could be attributed to the much higher stiffness exerted by glass or plastic surfaces. CTL begin to move within the matrix already shortly after polymerization of the collagen and most CTL are viable and cells still move after 24 h (**Fig. 8 A** - right row).

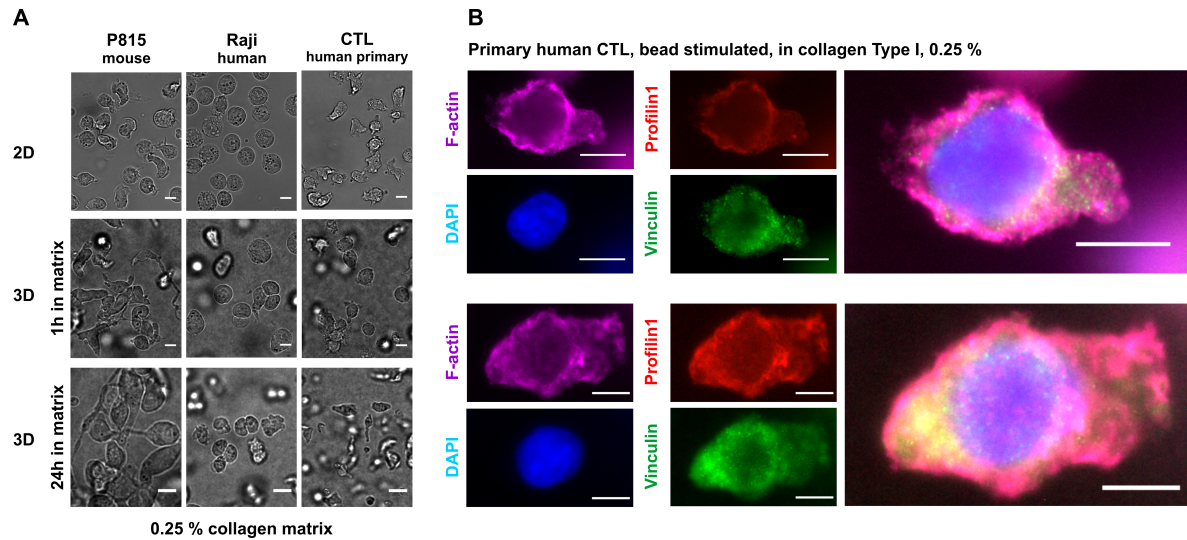


Figure 8 - Cell morphology in 3D collagen. (A) Two commonly used cell lines (P815 = target cells for CTL killing experiments and Raji = targets for NK in ADCC killing experiments) or bead stimulated human CTL were either seeded on μ -dish (plastic bottom, no coating) or mixed with collagen (Fibricol) and applied onto a μ dish in droplets. The upper image line shows the morphology of these cells in 2D on plastic. (Scale bars = 10 μ m). (B) Bead stimulated CTL were embedded in collagen (0.25 % (Fibricol)) and cast as droplets onto μ dishes. Cells were labeled using α -PFN1 (Abcam, ab124904), α -Vinculin (hVin1, Sigma, V9131), 4',6-diamidino-2-phenylindole (DAPI) and phalloidin-Alexa_633 (Thermo Fisher, A22284) (secondary Abs: G α R-Alexa_568, G α M-Alexa_488, Thermo Fisher). PFN1 localizes to sites of high F-actin content. Vinculin marks focal adhesions (FA) and is localized in small clusters around the cell membrane. (Scale bars = 5 μ m).

As especially in 3D matrices contact or attachment to the matrix can affect migration behavior, bead stimulated CTL embedded in collagen matrices (0.25 % as for 2D matrix) were stained for vinculin, a focal adhesion marker and profilin1 a cytoplasmic protein that regulates actin dynamics. In (Fig. 8 B) two example cells are shown. Vinculin is distributed in small clusters around the cell membrane marking focal adhesions. CTL do not adhere to collagen thus it is also used as negative control in adhesion assays. The presence of small vinculin clusters implies the formation of small focal adhesions that due to reluctant adhesion of CTL to collagen appear unexpectedly. Profilin-1 a cytoplasmic protein central to actin dynamics was also tested and found to localize in bead stimulated CTL in 3D to sites of high F-actin content (Fig. 8 B).

4.1.2 Automated cell tracking and analysis

It was necessary to quantify cell migration for this project. After image acquisition cell migration can be quantified using automated tracking software. Analysis of migration (especially 3D and SPIM) requires powerful and high performance automated tracking software that is also able to handle large data sets (several 100 Gigabyte up to Terabytes from SPIM). To determine migration parameters cells can be tracked manually or automatically.

For manual tracking, imaged cells are recorded and manually marked with a mouse-click at each time point. These marks are later automatically analyzed yet the manual “detection” is highly time consuming and prone to analysis bias. In addition, it is not feasible to manually analyze experiments in 3D with larger cell numbers over long time periods. For example, a standard 2D matrix experiment of around 200 cells per frame recorded for 181 time points would (ideally) require 36,200 individual mouse-clicks. Modern software integrates detection, tracking and analysis of imaging data. We used Imaris (versions 7 and 8, Bitplane AG, Switzerland) as it can perform all the needed tasks for tracking and analysis and also handle large data formats e.g. terabyte sized experimental files from SPIM. The 2D matrix method allows combining the advantages of single plane (and thus very fast) imaging and usage of a low magnification objective (5x/0.25 M27 Air) with the advantage of allowing interactions of cells with a “physiological” external matrix. The 3D matrix system on the other hand mimics a more physiological environment, yet despite high acquisition speed the need to record large volumes over a single plane in 2D matrix results in a lesser time resolution for imaging of cell populations or large tumor spheroids or organoids. Additionally the analysis of SPIM data is more difficult and highly time consuming. For the analysis of the data shown in this thesis Imaris in versions 7 and 8 were used for analysis of 2D matrix and 3D imaging data. For cell tracking the modules ImarisTrack and ImarisMeasurementPro were employed, and the data analysis and plotting module ImarisVantage was used for large experimental files and statistical analysis.

4.1.2.1 Parameters for quantification of migration

Fig. 9 illustrates the derivation of two important migration parameters. Migration can be quantified using different parameters including average velocity, persistence and MSD (**Fig. 9 A+B**). Average velocity, referred to in this thesis as track speed mean (in $\mu\text{m per s}$) depends on actin polymerization rate. Persistence (**Fig. 9 B**) is a measure of straightness in movement and is calculated as the Euclidean distance (start to end) divided by the track length or the actual path taken by the cell. Persistence is a factor of polarity or the maintenance of polarity and increases for example if a cell encounters chemo-, hapto- or durotactic cues. MSD of migrating cells can be used as an indicator for the mode of migration (**Fig. 9 A**) which can be grouped as confined (exponential declining MSD), random (linear) or directed movement (exponential increase).

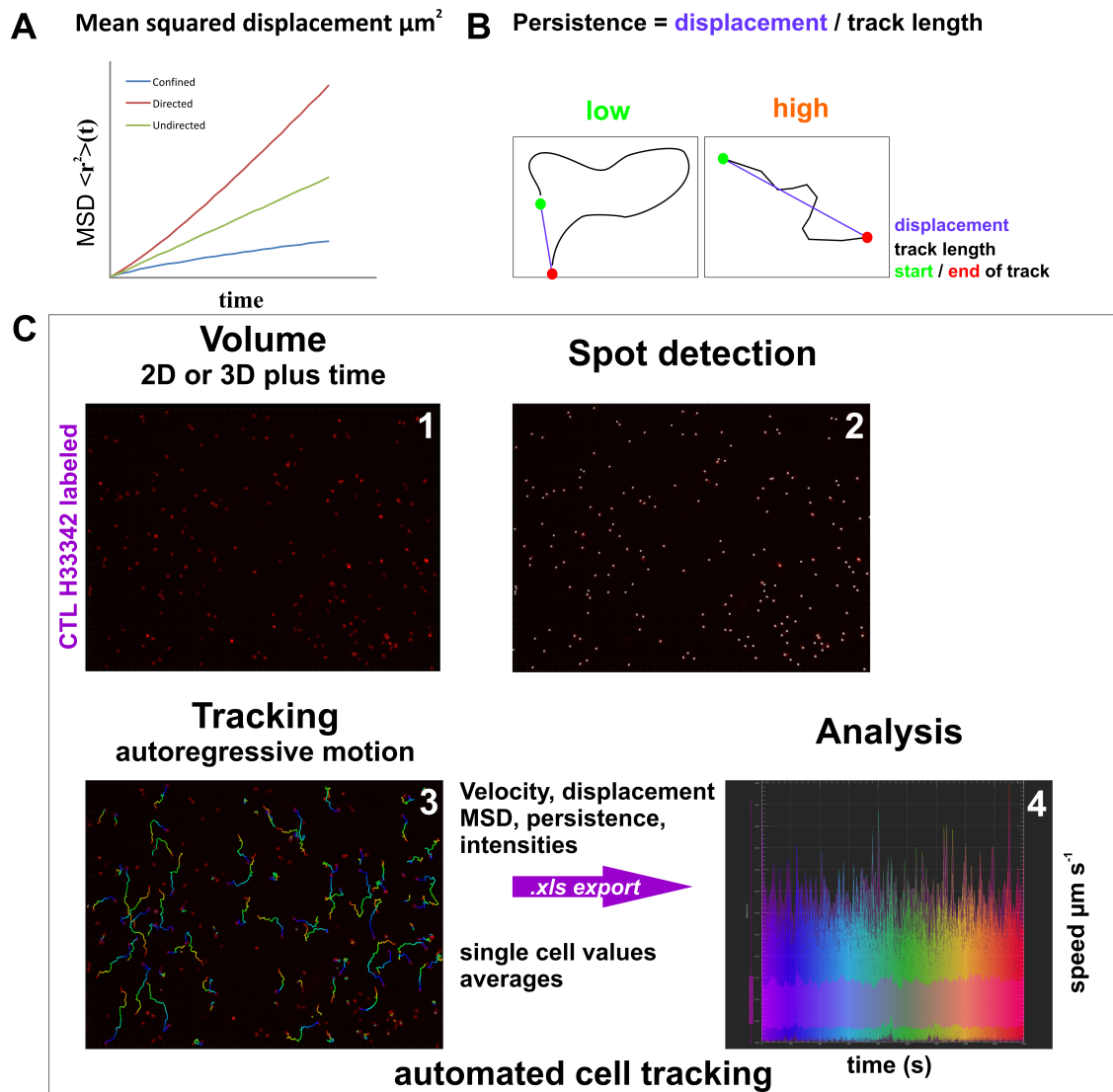


Figure 9 - Migration analysis using automated tracking software (Imaris, Bitplane AG). (A) Mean square displacement (stylistic) is shown and the corresponding interpretation of the resulting curve, were exponential increase (red) indicates directed movement, a linear progression (blue) indicates a random movement and exponential decay (green) indicates confined movement. (B) The derivation of cell persistence as factor of displacement over full track length serving as an indicator of directional movement is shown. (C) Example of the analysis of a 2D matrix experiment of human CTL in 0.25 % collagen. Each nuclear signal is detected at each time point via its fluorescent signal and detected spots are connected via an autoregressive motion algorithm. For each cell a track represented by the colored lines in the third image is overlaid (color code heat map: blue = start; red = end of track). (C) Image numbers follow tracking workflow: **1:** Raw Data of H33342 labeled primary human CTL in 0.25 % collagen (pseudo-colored red). **2:** Result of the spot detection feature of Imaris showing one time point and the detected nuclei are marked with white spheres. **3:** Result of automated autoregressive motion tracking with overlaid tracks. **4:** Average speed of all cells at a given time point was plotted using Imaris Vantage (graph is color-coded for time (blue = start of experiment, red = end of experiment)).

4.1.3 Choosing a fluorescent dye for automated tracking analysis

As tracking by algorithms is dependent on fluorescent images for detection I tested different fluorescent dyes as markers for tracking. Fluorescent probes exist for almost every organelle and can stain more or less specifically most structures within a cell. As algorithms of tracking software most effectively detect spot-like features, the nucleus, usually rounded in morphology, appeared as a suitable target for fluorescent labeling for cell tracking.

4.1.3.1 Testing fluorescent small molecule dyes for cell tracking

Many small molecule fluorescent probes exist yet no other suitable option could be found. Tested were: Syto (10, 13, 16 and 21), CellMask Orange, CellMask DeepRed and CellTracker DeepRed and CellTracker BMQC. The staining using these dyes was dim (or absent) or affected cell behavior in that cells became immotile (**Fig. 10**). CellMask Orange resulted in a good staining with motile cells yet the membrane label caused difficulties during detection in analysis requiring manual editing (see **Fig. 10 B**) but was used as non-transfection label for SPIM as H33342 cannot be visualized with available 405 nm laser. CellTracker BMQC was also successfully used to stain CTL and NK for SPIM imaging yet for long term imaging at low intervals even with reduced phototoxicity from SPIM the 405 nm excitation can potentially damage the cells. **Fig 10** shows staining patterns obtained using the designated small molecule dyes. Initial test were performed using SEA stimulated CTL as precedent projects were performed in this cell system. The rather low motility of SEA stimulated CTL compared to bead stimulated CTL led us to change the system towards bead stimulated CTL. At that time Hoechst 33342 has already proven superior to other dye options in SEA stimulated CTL and the staining method was transferred to bead stimulated CTL without problems and possible effects of Hoechst 33342 on migration were quantified in bead stimulated CTL using manual tracking (**Fig. 11**).

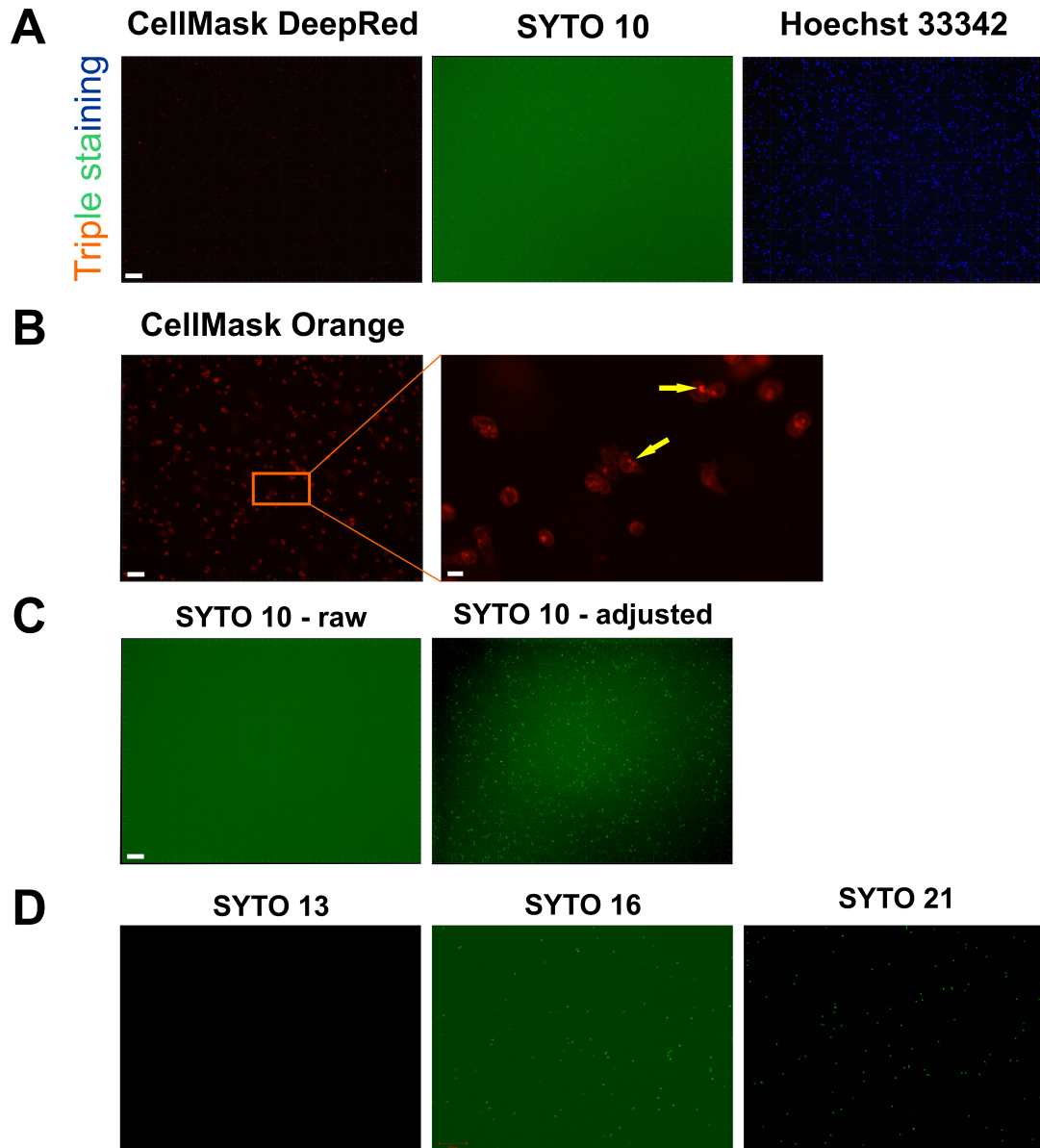


Figure 10 - A fluorescent label for analysis of migration. SEA stimulated primary human CTL were labeled using the designated small molecule and cast into a 2D matrix. **(A)** Triple staining of a single population of SEA CTL using CellMask orange (1:10.000), Syto 10 (1:10.000) and H33342 (1:2.000). CellMask DeepRed and Syto 10 resulted in signal intensities hardly above background. H33342 resulted in a bright nuclear staining and the resulting signal, even at low illumination settings, was sufficiently above background intensity. **(B)** SEA stimulated primary human CTL were labeled using CellMask orange and cast into a 2D matrix. The label intensity is sufficiently above background yet high intensity spot-like structures (yellow arrows) that probably represent vesicles pose a challenge for the detection algorithms. Scale bars: left image: 50 μ m; right image: 10 μ m. **(C)** SEA stimulated primary human CTL were Syto 10 labeled and cast in a 2D matrix. The left image shows raw imaging data of the best achievable quality. Adjusting the image settings (background excluded) already resulted in strong image artifacts as visible in the corners of the image left in **(C)**. Scale bar 100 μ m (for images in **C** and **D**). **(D)** Syto nuclear dyes (13, 16 and 21) were used to label primary human NK at 1:10.000 dilution in AIMV medium with 10 % FCS for 30 min and cast in 2D matrix samples. Afterwards cells were imaged using a Zeiss Cell Observer Z.1 with a 5x/0.25 M27, air objective using the 488 nm LED and the HE GFP (450-490) filter. Signal quality increases from Syto 13 to 21 yet in all cases cells did not migrate.

4.1.3.2 H33342 nuclear labeling does not affect primary human lymphocyte migration

Hoechst 33342 (Ex: 355 nm (bound to DNA) Em: 465 nm) is a bisbenzimidazole small molecule that is cell permeable, thus can be used to stain living cells, does not detectably interfere with cellular functions, shows low cytotoxicity and is stable for long term analysis (Purschke et al. 2010). A disadvantage is the excitation wavelength of 355 - 365 nm located in the UV range. As CTL migrate fast, a low interval time of in the range of seconds is needed. Depending on the total experimental time (30 min to several hours) the exposure of CTL to UV light can damage the cells. H33342 used with bead stimulated CTL and NK results in a bright and stable nuclear staining. It was shown before that potential toxicity from H33342 depends on two factors namely dye concentration and frequency of exposure to the excitation wavelength of ~ 365 nm (Purschke et al. 2010). I observed a collective drop in speed of CTL migrating in collagen labeled with H33342 and imaged under standard illumination settings (**Fig. 11 E+F**). To assess possible toxic effects of UV excitation or the dye H33342 itself, CTL, with and without H33342 label, were analyzed for 30 min at 10 s intervals with brightfield illumination with or without UV excitation. Standard illumination settings of the UV LED led to a drastic global drop in migration of CTL which could easily be accounted for by lowering the illumination intensity (**Fig. 11 F**). As signals close to background (2 - 3 x background intensity) proved sufficient for tracking despite poor image quality it was possible to turn down illumination intensity to levels that did not cause this effect (**Fig. 11 E**). To test how H33342 labeling or UV illumination or both combined affect CTL migration, CTL were labeled using H33342 or left unlabeled. Imaging was performed in 2D matrix either with or without UV illumination. As unlabeled cells cannot be easily tracked automatically, cells in this experiment were manually tracked using Imaris. The results show that H33342 itself does not affect CTL average velocity or persistence (**Fig. 11 C+D**). This confirmed that for analyzing migration of CTL H33342 is a suitable marker and thus we used it in the upcoming experiments to determine migration parameters of CTL within the 2D matrix system using collagen as a matrix.

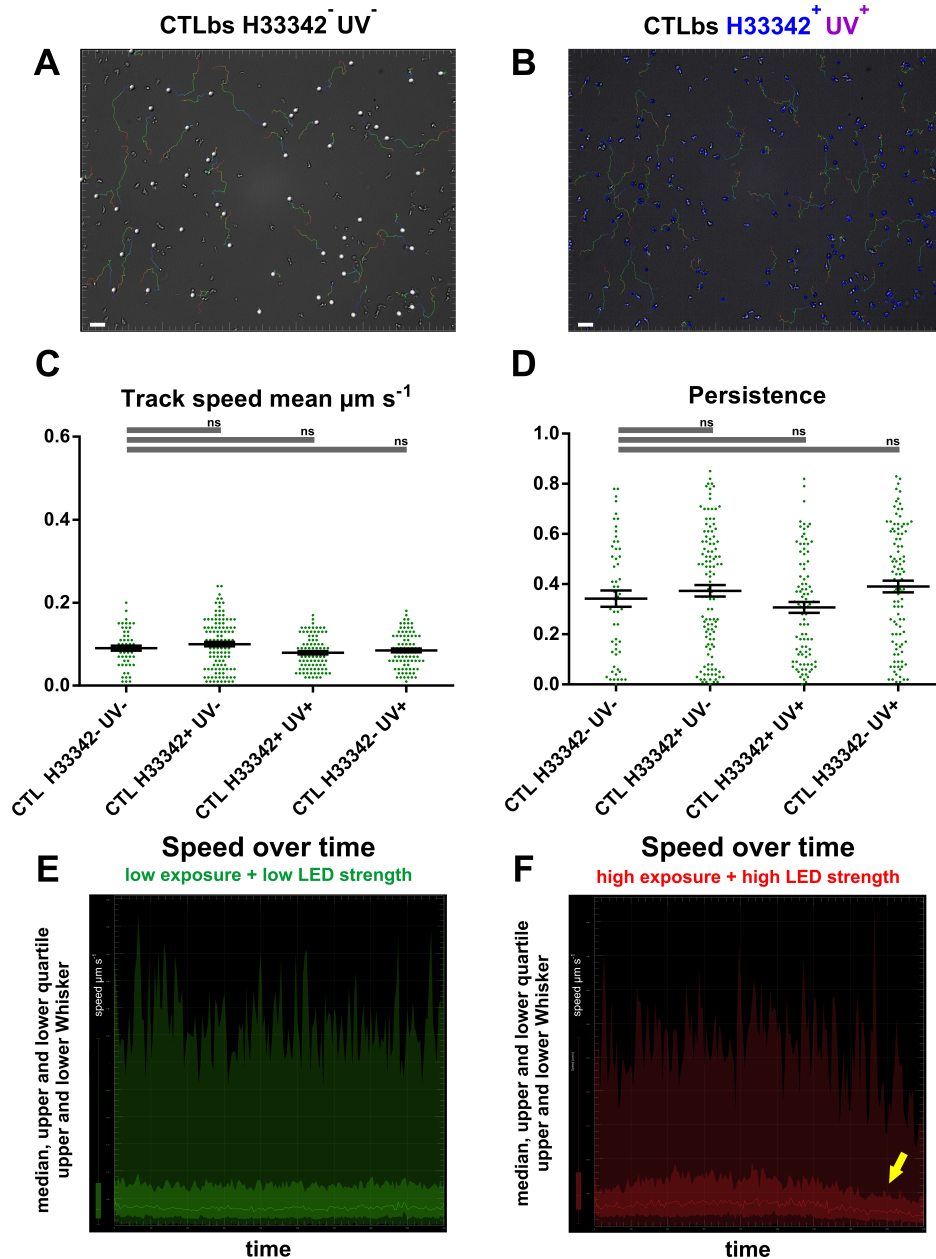


Figure 11 - H33342 does not alter migration parameters of primary human bead stimulated CTL in collagen. (A + B) Example of a 30 min experiment using CTLbs. Left = unlabeled + no UV exposure; right H33342 labeled + UV exposed. Tracks were manually generated using Imaris 8.1.2. (C + D) Bead stimulated primary human CTL were either loaded with H33342 or mock stained and then imaged using BF illumination only or a combination of BF and UV illumination (@ 10 % LED). Cells were manually tracked using Imaris 8.1.2 and statistics were exported as .xls. Data is given as Mean \pm SEM from two donors (with one individual experiment per donor) and was plotted using Graphpad Prism 6. CTLbs = bead stimulated CTL. (E+F) Bead stimulated CTL were H33342 labeled and analyzed in the 2D matrix system. The sample in (E) was exposed to 10 % LED strength and the lowest exposure setting that would yield a signal (Colibri system, Zeiss) whereas the sample in (F) was imaged under “standard conditions” at 25 % LED strength and exposure adapted to result in best image quality. The yellow arrow marks the “collective” cease in migration not observed under imaging settings with reduced intensity. Statistics: unpaired t-test: $p < 0.0001 = ****$; $p < 0.001 = ***$; $p < 0.01 = **$; $p < 0.05 = *$; $p > 0.05 = \text{ns}$.

4.1.4 The 2D matrix migration system

Aiming to analyze migration behavior of lymphocytes in 3D matrices requires reliable methods and a matrix system that is ideally modifiable and simple at the same time. The trouble of cells moving out of focus when recording single planes, terminating tracking attempts, can be tackled by using a flattened collagen matrix. A system using a flattened collagen matrix was developed to allow 3D matrix interactions while performing 2D recordings, which allow fast imaging of a single focal plane. Post-polymerization matrix thickness was ~ 10 to 15 μm (diameter was determined using fluorescent microspheres coated cover slips and dish bottom, **Fig. 12 D**). The system is simple, fast, economic and reliable for analyzing migration in matrix-based systems. **Fig. 12** shows the scheme of the 2D matrix method. The 2D matrix method allowed reliable analysis of migration and actin dynamics by allowing high frame rates in a 2D matrix (3D) environment using epifluorescence microscopy that is necessary to observe the high motility of lymphocytes.

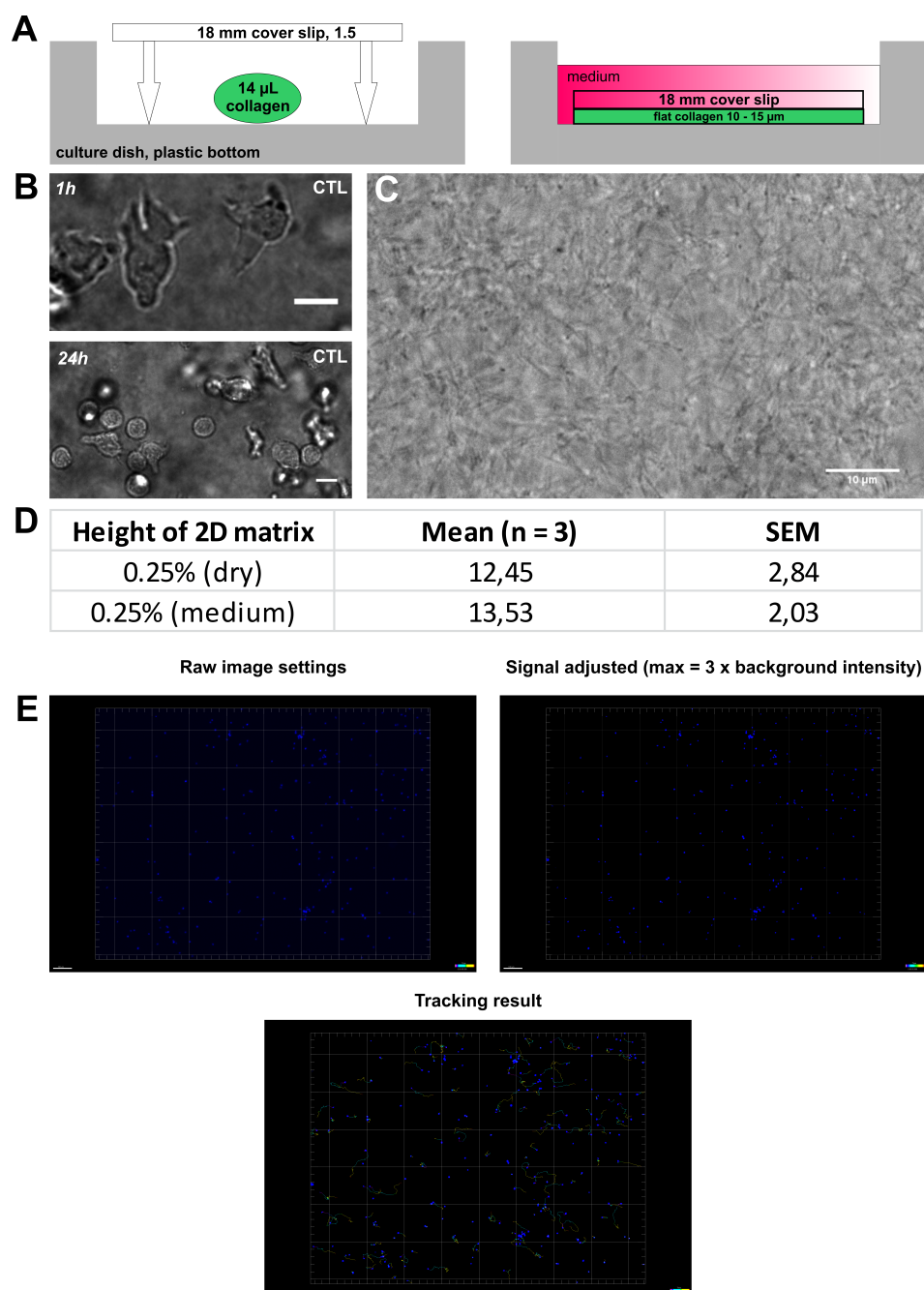


Figure 12 - The 2D matrix system generates a thin matrix that allows cells embedded in a matrix to be imaged within a single imaging plane. To combine the advantages of 3D matrix interactions with the epifluorescence imaging the 2D matrix system was developed. In general: CD8⁺ T cells isolated from PBMC were bead stimulated, fluorescently labeled and mixed with collagen solution after resuspension in medium and the resulting liquid is applied dropwise (14 µL for a 18 mm cover glass) into a microscope culture dish and a cover slip (18 mm, round) is added on top of the droplet (**A**) and the matrix was left to polymerize for 1 h before medium was added. In (**B**) bead stimulated CTL in 0.25 % collagen are shown in the 2D matrix system showing the common morphology of migrating lymphocytes (Brightfield, 200 x magnification). (**C**) Shows a brightfield image of collagen type I matrix (0.25 %) after polymerization (630 x magnification). (**D**) Height (in µm) of the 2D matrix was measured by coating the dish bottom and coverslip used to flatten the matrix with fluorescent beads (0.17 µm fluorescent microspheres) from the focal point at the dish to the focal point at the glass surface. Three individually prepared matrices were measured at 3 positions each. (**E**) Example of a 2D matrix experiment with H33342 labeled CTLBs in 0.25 % collagen. Shown are a raw data image and the adjusted image (min intensity 150, max intensity 450). Despite low image quality tracking is performed without problems or detection errors. Scale bar **B+C** = 10 µm; **E** = 100 µm.

4.1.5 3D matrix migration system - Single plane illumination microscopy (SPIM)

4.1.5.1 Imaging primary lymphocytes in 3D matrices using SPIM

The “2D approach in a matrix” is certainly more physiological than experiments performed on protein coated plastic or glass surfaces as it allows cell matrix interaction. Approaching 3D systems is thus obviously desirable. The standard microscopes used for cell analysis (confocal, epifluorescence) have an enormous disadvantages when considering 3D experiments (depending of course on the system to be used). These disadvantages include low volume sectioning speed, prominent bleaching (especially confocal microscopy). As imaging interval times are highly limiting when performing 3D imaging of large volumes in conventional microscopes we set up *single plane illumination microscopy* (SPIM or Lightsheet microscopy). Using SPIM interval times can be reduced drastically as the camera captures the light from the complete focal plane and not from each pixel separately (as in laser scanning confocal microscopy) much higher frame rates are possible as compared to e.g. confocal microscopy. Additionally SPIM reduces off-plane exposure of cells by single plane illumination which reduces bleaching and phototoxicity during imaging, making SPIM the favored technique for complex long-term imaging experiments. Access to SPIM was available after starting the project. In the beginning it proved very difficult to simply transfer 2D to 3D: especially handling and preparation of stable matrices in a controlled environment (temperature, gas exchange, pH) proved to be a challenge. SPIM measurements were optimized during my thesis and finally, all problems were satisfactorily solved during my thesis. However, since optimal 3D conditions were not readily available, many experiments were conducted using the 2D matrix. The 2D matrix experiments were performed using 0.25 % of collagen, yet 3D SPIM experiments had to be performed using 0.5 % or higher collagen concentrations, because matrices of concentrations below 0.5 % were unstable during imaging in the Zeiss Lightsheet Z.1. This means that, if during image acquisition the sample is moved through the focal plane the matrix itself started to move in an uncontrolled way and often the focus was lost, rendering the experiment useless. Comparing migration parameters of bead stimulated CTL in 2D matrix versus 3D SPIM experiments, it was found that persistence is slightly reduced yet cell velocity is significantly lower (**Fig. 13 C**). In **Fig. 13 C** persistence and average velocities of individual cells are plotted (one dot represents one cell) and **Fig. 13 D** shows the frequency distribution of the values in (**C**). In higher concentrated collagen frequency of lower persistence values is increased (**Fig. 13 C**). Average velocities are shifted

towards lower values (**Fig. 13 C**). The range of parameters is broad as TSM values range from 0.01 (non-motile) to $\sim 0.2 \mu\text{m s}^{-1}$ in 0.5 % collagen and persistence values range from 0.01 to ~ 0.8 . Maximal possible velocity is reduced in higher concentrated collagen. Thus higher concentrated collagen effectively reduces CTL velocity, probably by posing a stronger resistance through higher stiffness of the matrix. Considering that stiffness differs substantially in different tissues of the human body and especially tumor tissue show high stiffness (Paszek et al. 2005), it is meaningful to analyze CTL migration in collagen matrices.

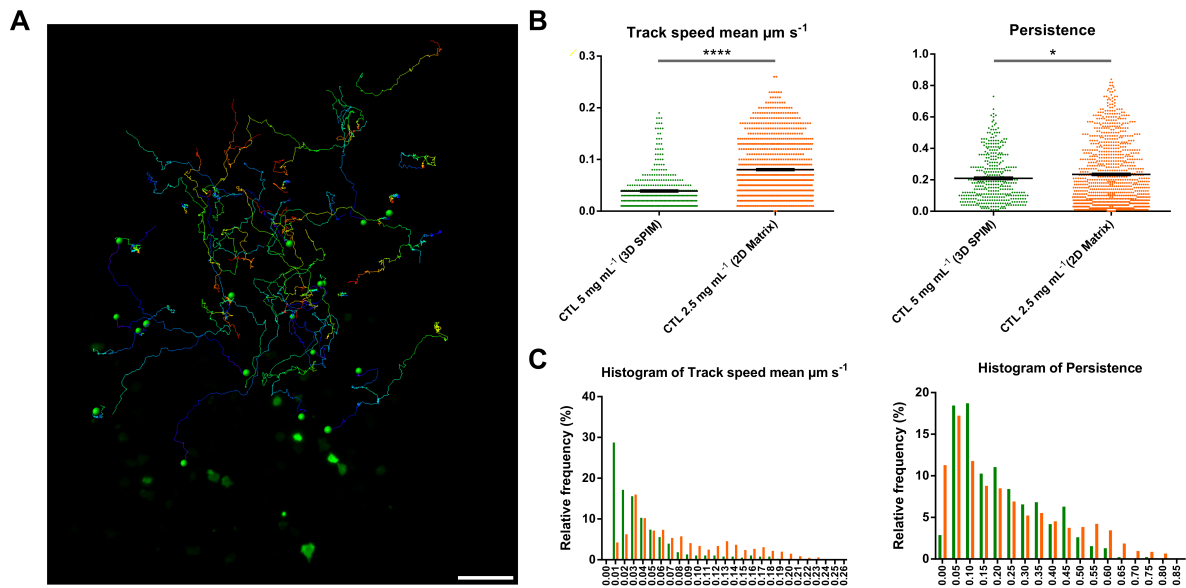


Figure 13 – SPIM and 2D Matrix allow versatile analysis of CTL migration in short and long term. Primary human CTL were isolated from PBMC and bead stimulated. Bead stimulated CTL were transfected with pMax_LifeAct_mEGFP or labeled using CellMask Orange and one day post transfection or after labeling cells were embedded in 0.5 % collagen type I (Fibricol). Cells were imaged for 6 h at 37 °C 5 % CO₂ in a Zeiss Lightsheet Z.1. (**A**) Result of automated Imaris tracking of a (~1TB) experimental file. Tracks shown are full length tracks automatically detected by the software. (200 x mag., scale bar = 50 μm; Color code: blue start; red = end of track) (**B + C**) LifeAct_mEGFP expressing or CellMaskOrange loaded CTL were imaged over 6h in SPIM (3D LFSM) or H33342 loaded CTL were imaged for 30 min in 2D matrix (2.5D Epi). Single cell values for velocity and persistence were exported and analyzed and plotted using Graphpad Prism 6. In (**C**) the frequency distribution of data shown in (**B**) is shown. Data in (**B + C**) from 4 donors each; shown as Mean \pm SEM. (Imaging settings SPIM: 40s, 539 z-planes, 440 x 440 x 538 μm volume, 6h total) (Imaging settings Epi 10s, 1 z-plane, 30 min total). Statistics: unpaired t-test: $p < 0.0001 = ****$; $p < 0.001 = ***$; $p < 0.01 = **$; $p < 0.05 = *$; $p > 0.05 = \text{ns}$.

4.1.5.2 Collagen concentrations and CTL migration in 3D and 2D matrix systems (data courtesy of Dr. Renping Zhao, University of Saarland, Biophysics, Homburg, Germany)

2D matrix experiments in this thesis were mainly performed using 0.25 % collagen matrices and 3D SPIM experiments using 0.5 % collagen (**Fig. 13 B**). The results from these experiments suggest that collagen concentration, resulting in altered stiffness of the matrix, predominantly affects cell velocity. My colleague Dr. Renping Zhao, who is also working on 3D migration of T cells, has analyzed bead stimulated CTL using the 2D matrix and 3D SPIM system under different collagen concentrations. The results shown in figure XX are from Dr. R. Zhao and represent experiments performed on primary human CTL in different collagen concentrations in 2D matrix and 3D SPIM. Comparing 2D matrix experiments performed by me (2.5 mg mL⁻¹ collagen, Fig. 6 B) with 3D SPIM experiments performed by Dr. R. Zhao (2 mg mL⁻¹ collagen) averages velocity is highly similar as is the range of parameters. The results obtained in 3D SPIM by myself (**Fig. 13 B**) also fit to those obtained by Dr. Zhao (**Fig. 14 3D SPIM 5 mg mL**) and from his data a consistent decrease of average velocity with increasing collagen concentration can be observed. The same effect is visible in Dr. Zhao's 2D matrix data where CTL migrating in 2 mg mL⁻¹ collagen are close to the results obtained in 2D matrix by myself at 2.5 mg mL⁻¹. Also in this system increasing collagen concentration decreases average velocity.

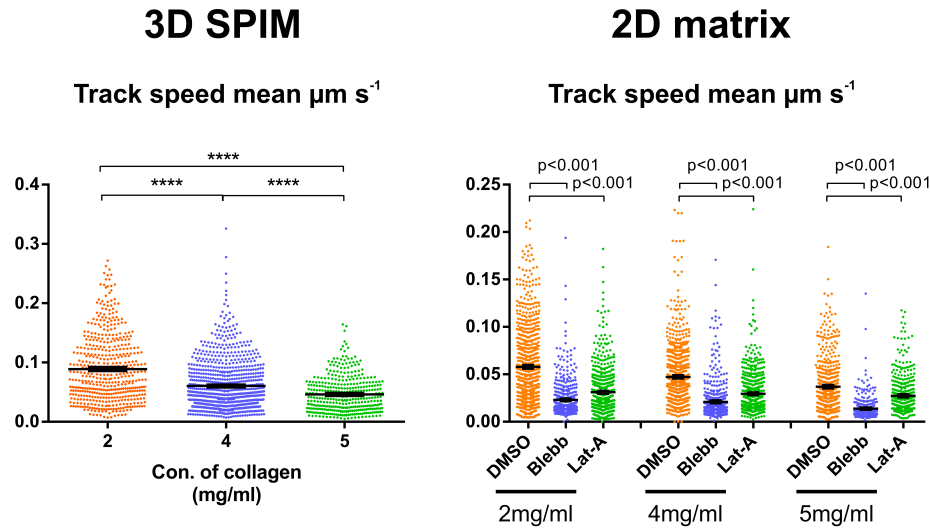


Figure 14 - Increasing collagen concentration effectively reduces average velocity and maximal velocity in 3D SPIM and 2D matrix - 3D SPIM: Bead stimulated CTL were histone 2B (H2B_GFP) transfected, mixed with collagen to the final designated concentration and polymerized in capillaries as rods. After polymerization and recovery samples were imaged using a Zeiss Lightsheet Z.1. **2D matrix:** Bead stimulated primary human CTL were H33342 labeled and cast into 2D matrix collagen samples at the designated concentrations. Control cells were treated during imaging with DMSO (0.1%), blebbistatin (\pm , 50 μM) or latrunculin-A (50 nM) and recorded in a Zeiss Cell Observer Z.1. (Data courtesy of Dr. Renping Zhao, University of Saarland, Biophysics, Homburg, Germany).

4.1.6 Migration parameters of primary human lymphocytes in collagen type I

4.1.6.1 Bead stimulated CTL migrate with higher persistence than unstimulated CTL or NK in collagen

Migration of bead stimulated CTL from primary healthy human donors was analyzed in the 2D matrix system. **Fig. 15** shows the results of 2D matrix experiments from primary human CTL ($\alpha\text{CD3/CD28}$ bead stimulated and unstimulated after isolation) as well as primary human NK. The migration parameters most meaningful for interpretation are mean velocity and persistence (straightness of the track). The velocity of primary NK and CTL, unstimulated (CTLus) or bead stimulated (CTLbs), show only marginal differences, yet persistence increases significantly after bead stimulation in CTL (**Fig. 15 A+B**). The frequency distribution of velocity and persistence of the three cell types analyzed are shown in **Fig. 15 C+D**. The linear increase of the MSD of CTL and NK is defined as undirected, random movement (**table 17** and **Fig. 15 E**). All cell types and conditions analyzed showed an undirected migration behavior. CTL move on average with $4.80 \pm 0.12 \mu\text{m min}^{-1}$ (bead stim.) $4.38 \pm 0.12 \mu\text{m min}^{-1}$ (unstimulated) and NK at $4.68 \pm 0.06 \mu\text{m min}^{-1}$ in 0.25 % collagen (see **table 17**). The range of velocities is the same for all cell types (from 0.01 (immotile) to 0.3

$\mu\text{m s}^{-1}$) (**Fig. 15 A+B**). Persistence values range is broad and in the range from 0.01 to ~ 0.8 (**Fig. 15 B**). Migration parameters of CTL (stimulated and unstimulated) or NK thus show similar broad ranges with regard to velocity (30 fold range) and persistence (80 fold range). The most significant difference is the change in persistence in bead stimulated CTL (**Fig. 15 B**) that show a higher frequency of intermediate velocities (**Fig. 15 C**) as well as a higher frequency in higher persistence values (**Fig. 15 D**). Bead stimulated CTL in collagen show speed fluctuations (**Fig. 15 F**) as observed *in vivo* when migrating in a collagen only matrix (Krummel et al. 2016).

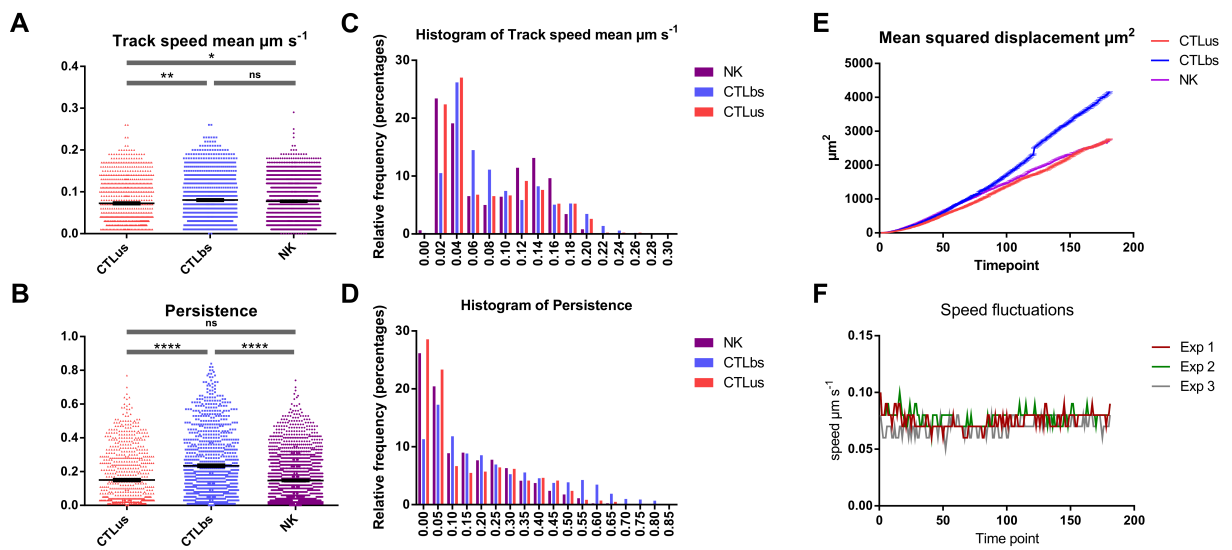


Figure 15 - Bead stimulated CTL migrate with higher persistence than unstimulated CTL. Human NK, bead stimulated and unstimulated CTL were cultured for 24h post isolation and loaded with HOECHST 33342. (**A - D**) Cells were imaged for 30 min with 10 second intervals in 0.25 % collagen (Nutragen) and tracked using Imaris 8.1.2. Calculated parameters were exported as .xls and plotted using Graphpad Prism 6. (**C + D**) Relative frequencies of TSM and persistence values (Bin size TSM: 0.02; Persistence: 0.05) for NK, CTLbs and CTLus. (**E**) Mean squared displacement of cells analyzed in **A + B**. (**F**) Example of the average speed over time from 3 independent experiments of CTLbs showing the speed fluctuations that can also be observed *in vivo* (Krummel et al. 2016). Data shown are pooled from different donors (see **table 17**) as mean \pm SEM. TSM = track speed mean in $\mu\text{m s}^{-1}$. Statistics: unpaired t-test: $p < 0.0001 = ****$; $p < 0.001 = ***$; $p < 0.01 = **$; $p < 0.05 = *$; $p > 0.05 = \text{ns}$.

Table 17 - Migration parameters determined for primary human lymphocytes. Complementary data to **Fig. 15 (A+B+E)**.

<i>Cell Type</i>	<i>TSM ($\mu\text{m s}^{-1}$)</i>	<i>SEM</i>	<i>Persistence</i>	<i>SEM</i>	<i>n =</i>	<i>R² MSD</i>
NK (9 donors)	0.078	± 0.001	0.148	± 0.004	1714	0.9949
CTLbs (4 donors)	0.080	± 0.002	0.235	± 0.006	840	0.9796
CTLus (7 donors)	0.073	± 0.002	0.150	± 0.006	1080	0.9949

4.1.6.2 Matrix modifications using ECM components to modulate CTL and NK migration

4.1.6.2.1 Non-crosslinked modification of a collagen matrix

After determination of basic migration parameters of CTL and NK cells I wanted to test modifications of the basic collagen matrix by adding certain extracellular matrix components as are present under physiological conditions. Modifications of the matrix can affect matrix stiffness, cell health and attachment, and they may provide information on the inflammatory state of the local tissue or provide survival signals and would allow us to create a controlled, defined matrix with specific physical properties and specific cellular attachment or signaling targets. Also specific cell types (helper T cells, regulatory T cells, target cells and bystander cells) can depend on certain ECM factors for survival or proper functionality.

4.1.6.2.1.1 Fibronectin modulates migration of bead stimulated CTL by altering persistence and velocity

The 2D matrix system based on collagen Type I can be modified using different substances and without the need for crosslinking. Fibronectin modulates migration via integrin interactions ($\alpha 4\beta 1$ and $\alpha 5\beta 1$). Fibronectin isolated from human plasma (dimerized form) was added to the matrix in two different concentrations located below the average plasma concentration of FN (4 % and 8 % w/w of collagen). CTL that encounter fibronectin in a collagen matrix show modulated migration. Prominent is the drastic increase in maximal velocity for bead stimulated CTL at 4 % w/w fibronectin and a strong increase in average persistence can be observed for 8 % w/w fibronectin in bead stimulated CTL (**Fig. 16 A+B**). In the case of fibronectin an increase in average velocity involves a decrease in persistence and vice versa. 8% w/w FN shifts CTL towards intermediate velocities and high persistence while 4% w/w FN shift CTL towards low persistence and high velocities (**Fig. 16 C+D**).

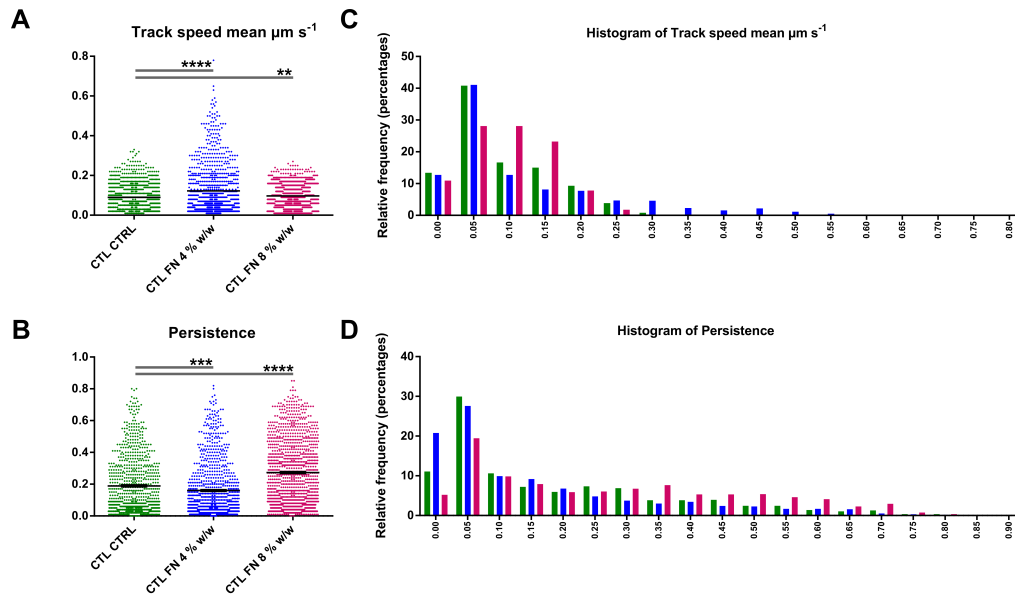


Figure 16 - Fibronectin modulates velocity and persistence of bead stimulated CTL in 3D. Human bead stimulated CTL were loaded with Hoechst 33342. Cells were resuspended in 0.25 % collagen (Fibricol) solution containing 4 % or 8 % w/w of collagen of human fibronectin. Cells were tracked in the DAPI fluorescence channel (H33342) using Imaris 8.1.2. In (C + D) the frequency distribution of TSM (A) and persistence (B) values is shown as histogram (TSM bin size 0.05; persistence bin size 0.05). Data shown = mean \pm SEM from 3 donors each. (High MW = 300 - 500 kDa; Low MW = 8 - 15 kDa). Statistics: unpaired t-test: $p < 0.0001$ = ****; $p < 0.001$ = ***; $p < 0.01$ = **; $p < 0.05$ = *; $p > 0.05$ = ns. Data are given as mean \pm SEM.

4.1.6.2.1.2 Hyaluronic acid modulates persistence of bead stimulated CTL

In addition to fibronectin, glycosaminoglycans like hyaluronic acid or heparan are important factors of the ECM. Upon inflammation or injury hyaluronic acid is degraded into smaller fragments that have been shown to cause pro-inflammatory signals whereas high MW hyaluronic acid molecules signal a healthy state of the environment (Cyphert et al. 2015). It is not unreasonable to assume that different molecular weights of HA fragments may (differently) affect the migration behavior of CTL at a site of inflammation. HA of different molecular weight (low MW = 8 - 15 kDa; high MW = $1.5 - 3.0 \times 10^5$ kDa) were added to the collagen matrix prior to polymerization. Bead stimulated CTL (Fig. 17, lower panel) average velocity is not affected by the presence of either low or high molecular weight hyaluronic acid (Fig. 17 A), yet persistence decreases significantly for both conditions (low and high MW) (Fig. 17 C). Presence of low MW HA fragments induces migration of CTL as visible in the frequency of distribution where low MW HA exposed CTL show only few cells of low average velocity which represent immotile cells.

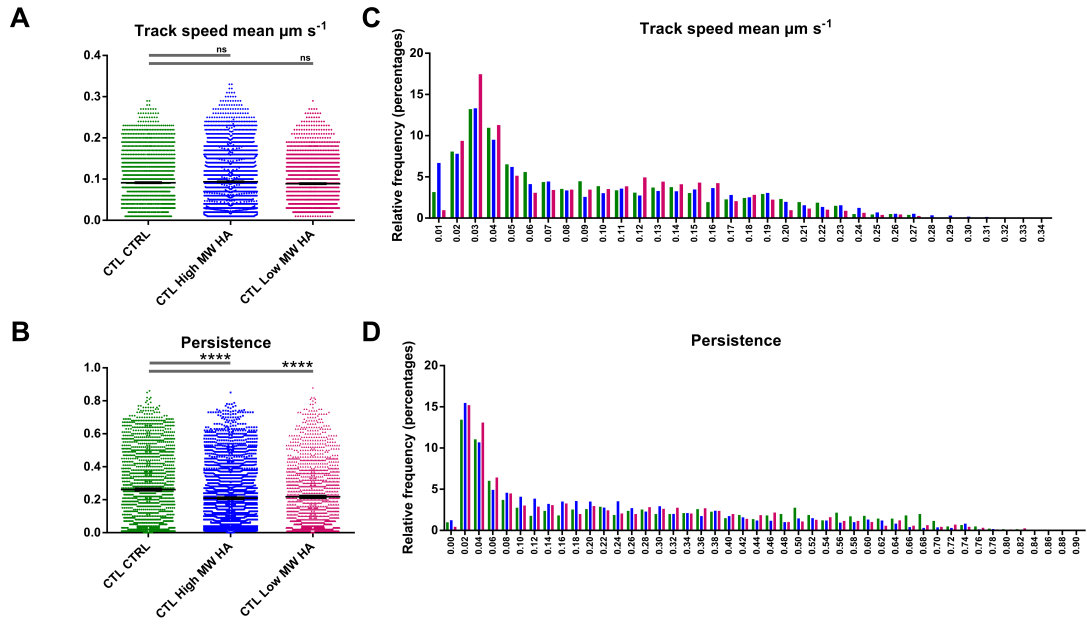


Figure 17 - Hyaluronic acid modulates persistence of CTL in 3D. Human bead stimulated CTL were cultured for 24h and loaded with HOECHST 33342. Cells were resuspended in 0.25 % collagen (Fibricol) solution containing 1.25 % w/w of collagen hyaluronic acid at different molecular weights. Cells were tracked using the DAPI fluorescence channel (H33342) with Imaris 8.1.2. (**A + B**) Automated tracking analysis of H33342 labeled CTLBs in 0.25 % collagen containing the designated HA fragments. In (**C + D**) the frequency distribution of TSM (**A**) and persistence (**B**) values is shown as histogram (TSM bin size 0.02; persistence bin size 0.02). Data shown = mean \pm SEM from 3 donors each. (High MW = 300 - 500 kDa; Low MW = 8 - 15 kDa). Statistics: unpaired t-test: $p < 0.0001 = ****$; $p < 0.001 = ***$; $p < 0.01 = **$; $p < 0.05 = *$; $p > 0.05 = \text{ns}$. Data are given as mean \pm SEM.

4.2 Profilin-1, pancreatic cancer and CTL

In collaboration with the Shanghai group (Prof. Dr. Xianjun Yu, Fudan University, Shanghai, P.R. China) CD8⁺ T cells from pancreatic patients and healthy individuals were tested for PFN1 expression, as the collaborating group has reported changes of PFN1 levels in tumors and adjacent tissues (Wittenmayer et al. 2004, Cheng et al. 2013, Yao et al. 2014, Zaidi and Manna 2016). Our collaborators in Shanghai were able to analyze the profilin-1 levels in CTL of patients bearing malignant pancreatic cancer. Compared to healthy individuals (with no former history of cancer), these patients show a significant downregulation of profilin-1 levels in peripheral CD8⁺ using flow cytometry analysis (**Figure 18 A**). Additional Western blot analysis of samples from 9 patients and 5 healthy individuals confirmed the flow cytometry results as we could show that PFN1 protein levels are significantly reduced in CD8⁺ cells isolated from PBMC from the tested individuals (**Fig. 18 B**). In seven out of nine (77.78 %) patients with pancreatic cancer, a decrease in profilin1 expression in their CTL was detected. In six samples a drastic decrease (No. 2 - 7) and in one patient (No. 1) a moderate decrease was observed whereas no change was observed in patients No. 8 and 9 compared to healthy controls (**Fig. 18 C**). Western blot data are averaged in the densitometry plot in **Fig. 18 D**.

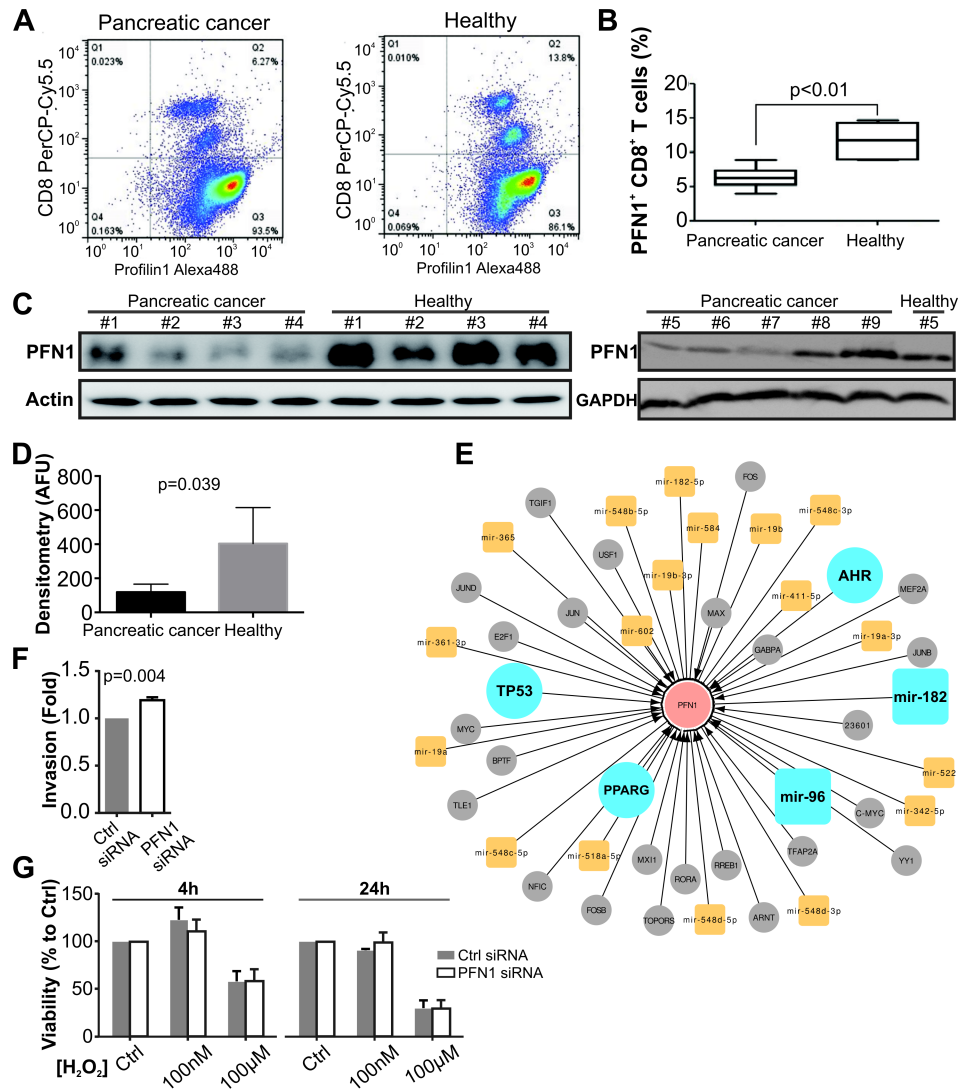


Figure 18 Expression of PFN1 is decreased in peripheral CD8⁺ T cells from patients with pancreatic cancer. CD8⁺ T cells were isolated from PBMC of patients and healthy individuals and directly used for experiments. The expression of PFN1 in CD8⁺ T cells was determined by flow cytometry (**A**, **B**, n = 7) or using Western Blot (**C**, **D**, n = 2 with 9 randomly chosen patients with pancreatic cancer and 5 healthy individuals). (**F**) Invasion of CTL is enhanced by PFN1 down-regulation. Trans-well migration assay (Matrigel) was performed to examine the invasion. CTL transfected with siRNA were used 24 hours after transfection. CXCL12 (100 μg/ml) was applied in lower wells (n = 3). (**G**) Viability of CTL with elevated environmental H₂O₂ was not compromised by PFN1 down-regulation. SEA specific CTL transfected with control or PFN1 siRNA were used 36 hours after transfection. H₂O₂ was added into the wells and incubated for 4 hours and 24 hours prior to CellTiter-Blue viability assay (n=3). (**E**) Transcription factors (circles) and miRNAs (boxes) that regulate PFN1 mRNA levels according to the HMDD and DisGeNET databases. Marked in blue are 3 transcription factors and 2 miRNAs that have been associated with pancreatic cancer. Experiments in **F**+**G** were performed by Dr. Renping Zhao (Biophysics, University of Saarland, Homburg, Germany). Experiments shown in **A**-**D** were performed by our Chinese collaborators in the group of Prof. Dr. Xianjun Yu (Fudan University, Shanghai, P.R. China). *Figure is taken from Schoppmeyer et al., Human profilin 1 is a negative regulator of CTL mediated cell-killing and migration, Eur J Immunol, 2017 Jul 8, PMID: 28688208*

4.2.1 PFN1 dysregulation can result in CTL dysfunctionality and induce cancer

To test a potential function of PFN1 downregulation in cancer we mimicked a tumor-related scenario using matrigel as a 3D matrix and observed the invasiveness of CTL with downregulated PFN1. PFN1 down-regulation increased the number of invasive CTL through matrigel *in vitro* (**Fig. 18 F**). Additionally, the resistance of CTL with PFN1 downregulation to reactive oxygen species was also tested as in pancreatic cancer microenvironments ROS levels are increased (Vaquero et al. 2004, Liou and Storz 2010). To mimic this scenario CTL were incubated for 4 h and 24 h with 100 nM or 100 μ M of H₂O₂. PFN1 downregulation did not affect the viability of CTL in presence of low or high amounts of hydrogen peroxide (**Fig. 18 G**). **Fig. 18 E** shows established molecular regulatory interactions that target PFN1. This interaction scheme was generated using the TFmiR network (TFmiR, *disease-specific miRNA/transcription factor co-regulatory networks v1.2*, <http://service.bioinformatik.uni-saarland.de/tfmir>). Interactions determined using TFmiR include 20 miRNAs and 27 transcription factors (**Fig. 18 E**). From these regulators we determined associations with pancreatic cancer using HMDD (Human microRNA Disease Database, <http://www.cuilab.cn/hmdd>) (Lu et al. 2008) and DisGeNET (<http://www.disgenet.org>) (Piñero et al. 2016). This analysis gave three hits for transcription factors (TP53, PPARG and AHR **Fig. 18 E**) and two miRNAs (*hsa-mir-182* and *hsa-mir-96*) being associated with pancreatic cancer (Koliopanos et al. 2002, Kristiansen et al. 2006, Maitra and Hruban 2008, Yu et al. 2010, Yu et al. 2012). Development of pancreatic cancer and the observed downregulation of PFN1 in CTL of pancreatic cancer patients might thus be a consequence of dysfunctional transcription control. That CTL with downregulated PFN1 show increased invasion *in vitro* and show no reduced viability in a hydrogen peroxide rich (tumor mimicking) environment could imply an increased functionality of these CTL as a side effect of the transcriptional dysregulation that drives pancreatic cancer in these patients. We thus further characterized the effects of the PFN1 downregulation in bead stimulated CTL with regard to migration and cytotoxicity. Localizing and killing the target cell includes functional migration, IS formation, cell polarization and release of LGs which are all actin dependent processes and thus PFN1 was expected to participate in these mechanisms.

4.2.2 Profilin-1 expression in primary human CTL

We characterized PFN family member expression in primary human CTL before and after bead or SEA stimulation. qRT-PCR revealed, that of the human isoforms PFN1-4, analyzed

by total mRNA that was isolated from unstimulated and stimulated (SEA stimulation or bead stimulation) CTL from the same donors, only PFN1 is expressed in all primary human CTL samples tested (**Fig. 19 A**). The mRNA levels of staphylococcal enterotoxin A (SEA) stimulated CTL show a slightly higher amount of PFN1-mRNA compared to unstimulated and bead stimulated cells. Western blot showed no significant differences in PFN1 protein expression in SEA stimulated cells compared to bead stimulated or unstimulated CTL (**Fig. 19 B+C**). Using overexpression systems with mCherry fusion proteins or siRNA mediated knockdown of PFN1 we aimed to determine how this affects migration and killing of CTL.

4.2.3 Profilin-1 is a negative regulator of CTL cytotoxicity

Overexpression studies were performed using cloned human PFN1 (or its mutants) which were all N-terminally fused to mCherry (PFN1_mCherry and the mutants were prepared by Yan Zhou, Biophysics, Homburg, Germany). Downregulation of PFN1 was achieved using a pool of two siRNAs. The effect of increased or reduced profilin1 levels on the killing capacity was determined *in vitro* applying a real time killing assay. Bead stimulated CTL overexpressing PFN1 showed a decrease in killing when compared to control CTL from the same donor as is evident from time resolved data (**Fig. 19 D**) and statistics (**Fig. 19 E**). When PFN1 levels were downregulated using siRNA the inverse behavior could be observed as CTLs killing capacity was increased compared to control CTL from the same donor (**Fig. 19 F+G**). This indicates a role of PFN1 in (at least part) of the mechanisms that are essential for effective target acquisition and execution of the pathologic target. In conclusion: PFN1 is a negative regulator in cell mediated killing by CTL.

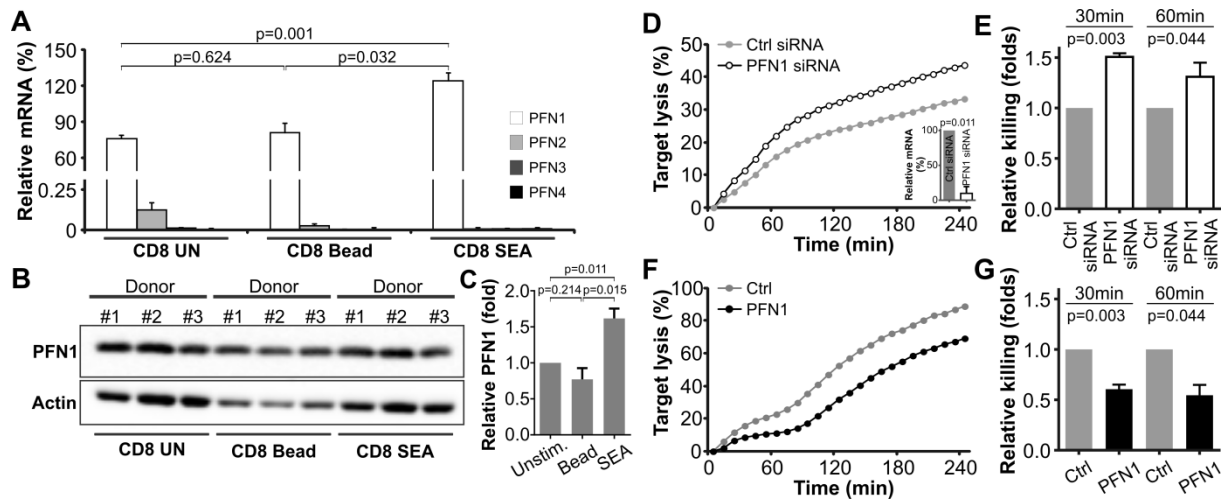


Figure 19 - PFN1 is a negative regulator for CTL-mediated cytotoxicity. Expression of PFN isoforms in CD8⁺ T cells at mRNA (A) and protein levels (B, C). Unstimulated primary human CD8⁺ T cells (CD8 UN), anti-CD3/anti-CD28 antibody-coated bead-stimulated CD8⁺ T cells (CD8 Bead) and SEA activated CD8⁺ T cells (CD8 SEA) from the same donor were collected. The level of mRNA was determined by qRT-PCR in A, where TBP (TATA box binding protein) was used as the internal control (n=3). The relative change of PFN1 at protein level from B is shown in C (n=3). (D-G) The real-time killing assay was carried out to determine the killing kinetics of CTL. Down-regulation and overexpression of PFN1 was carried out in SEA- and bead-stimulated CTL, respectively. The efficiency of PFN1 down-regulation is shown in the inset (n=2) in D. Analyses in E and G are from three donors. qRT-PCR (A + D inset) and Western blot (B) were performed by Gertrud Schwär (Biophysics, Homburg, Germany). **Figure is taken from Schoppmeyer et al., Human profilin 1 is a negative regulator of CTL mediated cell-killing and migration, Eur J Immunol, 2017 Jul 8, PMID: 28688208**

4.2.4 Profilin-1 in cell migration

A possible explanation for the effect of profilin-1 on CTL cytotoxicity, are changes in cell migration and thus search parameters. A putative role of profilin-1 was tested on CTL migration by using the established 2D matrix system.

4.2.4.1 CTL migration in 3D depends on PFN1 binding to poly-L-proline ligands and PIP₂

Using the 2D matrix system we analyzed migration of CTL using PFN1 overexpressing cells. To test the role of profilin-1 in migration, the following mutations were included: Y59A to abolish actin binding, R88L to ablate of PIP₂ binding, H133S to abolish binding of control proteins via poly-L-proline rich regions and C71G a mutations that causes amyotrophic lateral sclerosis (ALS). C71G possesses all functional interaction sites yet is unstable and inserts into the plasma membrane. To test effects of PFN1 downregulation siRNA targeting PFN1 was used (Fig. 20). Overexpression of PFN1 resulted in a significant increase of cell velocity, which was even higher for the Y59A mutant. Consistently CTL with downregulated PFN1

showed an increase in velocity (**Fig. 20 A**). With regard to average speed, overexpression of the mutants H133S and R88L resulted in drastically decreased average velocity. The ALS causing mutation C71G resulted in increased cell velocity in a similar degree as did the Y59A mutant. Comparing persistence we found that overexpression of PFN1_Y59A changed cell persistence significantly. In CTL with downregulated PFN1 no effect on persistence could be observed (**Fig. 20 B**). The mutations C71G, R88L and H133S all had a drastic effect on cell persistence during migration (**Fig. 20 A**). All MSDs of CTL overexpressing PFN1 constructs or siRNA transfected CTL show high linearity ($R^2 > 0.95$ for all) showing that migration can be categorized as diffusive or random, unguided migration (**Fig. 20 C, table 18**). I conclude that profilin-1 modulates migration and that this modulation is independent of the available PFN1:G-actin pool that likely changes during overexpression (PFN1-mCherry) or downregulation (siRNA). Reducing (PFN1 siRNA KD) or increasing (PFN1_mcherry) the available PFN1 pool has only slight effects on migration parameters **Fig. 20 A+ B**. The PFN1 knockdown shows significant reduction of velocity (but not persistence) and considering the effective reduction of PFN1 mRNA levels to ~ 10 % using two pooled siRNAs the knock down was expected to affect cell velocity by altering the actin polymerization rate as PFN1 actin shuttling becomes scarcer. PFN1 modulation of migration, considering the drastic drop in migration parameters for R88L and H133S mutations, appears highly dependent on functional interactions with regulatory proteins and phospholipids interactions.

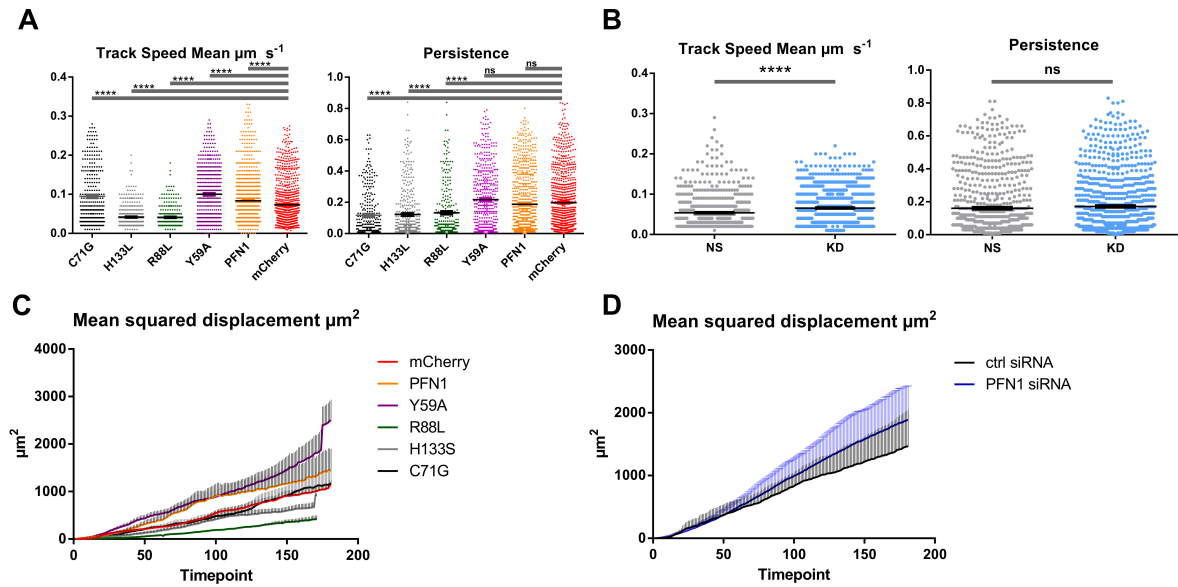


Figure 20 - PFN1 regulates CTL persistence and velocity via phospholipid and poly-L-proline interactions. CTL were isolated from PBMC, bead stimulated and transfected using a pMax vector with the corresponding mCherry fusion protein or using siRNA. Afterwards cells were mixed with collagen to reach a final concentration of 0.25 % (Nutragen) and prepared for 2D matrix analysis. Cells were recorded for 30 min at 10 s intervals in the RFP channel (overexpression) or DAPI channel (siRNA transfected CTL were H33342 labeled) and tracking was performed afterwards using Imaris 8.1.2 (**A + B**). (**A**) Automated tracking analysis of CTLbs expressing the stated mCherry fusion constructs. Cells were tracked using the mCherry channel. In (**C**) the average MSD of all cells in (**A**) is shown. (**B + D**) Automated tracking analysis of H33342 labeled SEA stimulated CTL transfected with control (NS) or PFN1 siRNA (KD) in 0.25 % collagen. In (**D**) the MSD of the cells analyzed in (**B**) is shown (10 s per time point). Data in (**A + C**) is from 11 (mCherry), 15 (PFN1), 11 (Y59A), 3 (R88L), 8 (C71G) and 6 (H133S) independent experiments and pooled from several donors. Data in (**B + D**) is from 4 independent experiments with one donor per experiment. Tracking was performed using Imaris 8.1.2. Statistics: unpaired t-test: $p < 0.0001 = ****$; $p < 0.001 = ***$; $p < 0.01 = **$; $p < 0.05 = *$; $p > 0.05 = \text{ns}$. Data are given as mean \pm SEM.

Table 18 - Coefficients of correlation from the average MSDs (Fig. 20) and the correlating mode of migration. The coefficient of correlation was calculated in Excel. MSD of all conditions analyzed indicate random movement of cells.

Condition	MSD R^2	Mode of migration
mCherry	0.988	random
PFN1	0.985	random
Y59A	0.951	random
R88L	0.971	random
H133S	0.974	random
C71G	0.974	random
Non-silencing siRNA	0.997	random
PFN1 siRNA	0.998	random

5. Discussion

5.1 Migration of lymphocytes

Determination of cellular and extracellular factors influencing and controlling migration of lymphocytes is essential to understand how T cells can perform so efficiently to roam the body's tissues and detect and eliminate pathologic cells. Of high interest concerning lymphocyte migration is the search strategy of CTL under different immunological contexts. What is the applied search strategy? How is this strategy regulated? Are T cells depending on environmental signals to define their mode of migration or induce migration itself? T cells clear tumor cells and to do this effectively finding the target after activation is one crucial step. But tumors can evade the immune system in different ways by targeting regulatory T cells, interfering with antigen presentation, shifting the immune response towards tolerance, interfere with chemotactic gradients or remodel the local ECM (Krummel and Macara 2006, Dass et al. 2015). These immune evading tumors can be senescent and become active again later in life. Especially the function of CTL, the tumor cell killers, can be suppressed by tumors through the release of cytokines with immune suppressive effects by tumor cells or cells of the tumor microenvironment (Dass et al. 2015). Additionally solid tumors tend to have a higher rigidity than normal tissue and CTL migration is reduced in high rigidity matrices (Paszek et al. 2005). The tumor microenvironment, its heterogeneity, ECM composition of the tumor and surrounding tissue and the general immune response are for themselves complex and have the potential to manipulate T cell behavior. Understanding the function and effects of the compounds and cells that make up this complexity requires us to reduce complexity and build up 3D matrices part by part to determine the context specific effects in CTL migration and tumor clearance. To achieve this 2D systems are not feasible and a switch to 3D is the next crucial step to improve physiological relevance of *in vitro* scientific experiments. In the past migration studies were conducted on 2D surfaces (with or without protein coatings) and mainly with cells from continuous cell lines like fibroblasts (Friedl et al. 1998, Ridley et al. 2003, Wei et al. 2009, Ridley 2015). Fibroblasts are large (Fibroblast: 30 - 60 μm , T cell: 5 - 15 μm), show mainly chemotactic induced persistent migration at speeds around 0.1 - 0.5 $\mu\text{m min}^{-1}$ while T cells can migrate at higher maximal velocity (\sim 5 - 15 $\mu\text{m min}^{-1}$ range depends on the matrix or substrate and if it is a 2D or 3D or *in vivo* environment) in 3D applying a persistent random walk (Friedl et al. 1998, Cahalan et al. 2003). The first level of approaching physiological experimental systems is to provide

cells a 3D matrix, a structural base, as they would encounter in the human body and the first obstacle in 3D experiments is imaging of matrix based systems.

5.1.1 Imaging 3D volumes

Microscopes commonly used for live cell imaging (confocal, epifluorescence) have an enormous disadvantages when considering 3D experiments. These include slow volume sectioning, prominent bleaching and phototoxicity through constant excitation of out-of-focus cells. The 3D imaging technology Lightsheet fluorescence microscopy (or single plane illumination microscopy, SPIM) allows to rapidly image 3D matrix based samples for extended periods of time with reduced phototoxicity and bleaching by using selected or single plane illumination (Santi 2011). A few micrometer thick sheet of light is used to optically section a sample, which must be translucent (Reynaud et al. 2015). As SPIM is still under development for cell biology experiments and access to this technology was not possible at start of the project a second economic and simple system that can be used in an epifluorescence microscope was developed. Reducing the thickness of a collagen matrix to roughly a T cell's diameter allows single plane imaging of cells in 3D matrices. This offers benefits from 3D systems (matrix interaction, microdomains) and allows observation of cells in 3D by recording a single focal plane at the while using a more broadly available epifluorescence microscope. This allows making use of the high frame rates of modern microscope cameras (30 - 100 fps) in a 3D context without need for volume sectioning, a time limiting step in image recording.

5.1.2 3D Migration

This work concerns primary human cytotoxic T lymphocytes (CTL) or CD8⁺ T cells. Once activated by antigen they will home to their target tissue. Here their task is to migrate within the interstitial matrix and clear all malignant cells while leaving healthy cells unharmed. Despite growing knowledge of the immune system, cellular subtypes and participating networks, the strategy that killer cells apply to search an area of tissue effectively and how and by what signals migration is tuned is hardly understood. This is for a large part due to the complexity *in vivo* that cannot be reproduced *in vitro* so far. The starting point for 3D experiments is the choice of a matrix system. Choosing a simple matrix system, that generates homogeneous matrices, allows analysis of the unguided migration of CTL, meaning without presence of chemotactic signals.

5.1.2.1 Choosing a matrix system

A suitable matrix should fulfill several requirements. The compound should be of natural origin, non-toxic, ideally provide native signals to cells, allow modifications of the substrate, addition of soluble factors and once polymerized must be stable for extended periods of time. Ideally the matrix can also be remodeled by cells. For tissue engineering purposes different natural and synthetic compounds have been studied for their ability to produce 3D matrices with different physical properties ranging from pore size to stiffness (Ma et al. 2008). To rebuild a physiological environment for immunological experiments that allows modifications in various ways (ECM factors, cytokines, cell types, matrix structure and stiffness) favors the use of a natural matrix system. Collagens are the most abundant protein of the ECM, are biologically active, can be modified through simple addition or chemical crosslinking, provide haptokinetic cues and are stable after polymerization. Another option are basement membrane-like matrices (BMLM, e.g. Matrigel) a complex mixture of ECM proteins and growth factors secreted by Engelbreth-Holm-Swarm sarcoma cells. This substrate is well accepted by many cell types due to its complexity, also by primary cells. The partly undefined content especially of cytokines, which elicit strong effects on many different cell types, can affect cell behavior and ultimately migration (Hughes et al. 2010, Zhou et al. 2017). Collagen can form sponge-like matrices by polymerization *in vitro* forming rather homogenous fibrillary networks with nearly equal-sized pores (Wolf et al. 2009). Tissues that are roamed by CTL are complex environments consisting of a vast variety of compounds including proteins, glycosylated proteins, proteinated glycans, glycosaminoglycans and also cells like fibroblasts. The use of collagen as a basic matrix component allows the controlled build-up of a matrix with specific properties. Adding ECM components like fibronectin or hyaluronic acid to the collagen matrix allows testing for specific effects that these factors can pose on cells. To date collagen reagents from different sources (rat, bovine) mainly consisting of collagen type I, the most abundant type found in animals, representing a fibrillary collagen, are available. Natural collagen Type I fibrils have telopeptides attached to the N- and C-terminus that facilitate fiber alignment and serve as cross-linking sites (Eyre et al. 1984). Depending on the extraction method (acid extraction, pepsin extraction) the collagen fibrils will either have telopeptides (acid extraction) or telopeptides were removed (pepsin extraction). Presence of telopeptides can affect cell behavior (Packard et al. 2009, Sabeh et al. 2009) as e.g. pepsinized collagen formulations will form larger pores compared to non-

pepsinized (Wolf et al. 2009). We choose to use a pepsin-extracted mainly collagen Type I (~3% of total collagen are of Type III) containing matrix system of bovine origin. This system suits best to study and determine the random migration behavior of primary human CTL and later further modify the system using other ECM components to determine their specific effects on CTL migration, as these compounds might tune migration behavior, through interaction with cellular receptors (Uijtdewilligen et al. 2016, Artym and Matsumoto 2011). The matrices generated by pepsinized atelocollagen show generally an intermediate density located between high and low density dermis *in vivo* making them a suitable environment for most cell types (small leukocytes and larger cells like fibroblasts, myoblasts) (Wolf et al. 2009). This is important if at later stages next to lymphocytes also other cell types shall be included into the experimental system (Wolf et al. 2009). Collagen matrices can also be chemically modified (e.g. crosslinking of collagen fibers) changing physical properties. Additionally collagen matrices are stable under physiological conditions once polymerized. Normal tissue is rather soft depending on the specific constituents while tumors are often more rigid (Paszek et al. 2005). Collagen-only matrices can range in rigidity between tumors and tissues, with the specific elastic modulus being dependent on the concentration of collagen. Matrices with collagen concentration around 2 mg mL⁻¹ show an elastic modulus similar to normal tissue (several hundred Pa) at 4 mg mL⁻¹ already an elastic modulus of ~1500 Pa is reached which corresponds to more solid tumor-like tissue (Paszek et al. 2005). We choose to use 2.5 mg mL⁻¹ as a standard concentration for migration analysis to stay in the range of normal tissue stiffness. My colleague Dr. Renping Zhao, who has been working side by side on the SPIM system also during development and who has been using the 2D matrix system extensively, could show that CTL migrate at reduced average speed, in the 2D matrix as well as 3D SPIM based system, with increasing collagen concentrations. Having defined a fundamental matrix system the next bottleneck in analyzing migration is the analysis of imaging data.

5.1.2.2 Methods for analysis of lymphocyte migration

Two methods that use different imaging technologies were established to analyze migration in 3D environments. Both methods avoid partly the weak points that made it so difficult so far to transfer methods from 2D to 3D environments: phototoxicity, bleaching, frame rate in 3D volumes and volume sectioning speed, stable incubation and data handling. Using the 2D matrix methods most disadvantages can easily be avoided. Recording a flattened matrix

containing cells reduces the high phototoxicity resulting from continuous UV illumination in an epifluorescence microscope when recording 3D volumes as imaging one z plane will always illuminate all of the specimen or sample that is located in the path of the light. The slow volume sectioning can be avoided by imaging a single plane where all cells are located in and where cells cannot walk out of. Recording a single focal plane instead of a 3D volume also effectively reduces experimental file size (30 min, 2D matrix, 1 channel = 500 MB) boosting analysis speed drastically.

5.1.2.2.1 2D matrix

Using the 2D matrix system covers a problem of 3D imaging. Cells embedded in a 3D matrix can move out of the focal plane within the matrix and this is not possible in 2D (glass, plastic) systems. To record the full information about a cells trajectory 3D imaging requires the recording of a z-stack or several z-planes per time point creating a 3D volume (xyz). This is step is time limiting. In the 2D matrix system cell containing collagen suspension is flattened using a microscopy coverslip resulting in a matrix with a height of about the average size of a T cell (10 - 15 μm). The cells can be imaged within a single focal plane while still providing interaction with the matrix. While SPIM solves the volume sectioning speed problem of epifluorescence or confocal microscopes (see next paragraph) 2D matrix solves a speed problem in 3D imaging. This problem occurs as 3D samples in SPIM could in principal be imaged in a single focal plane yet the cells in the 3D sample cannot be limited to a single focal plane, although by using SPIM very high frame rates are possible (30 - 100 fps for the Zeiss Lightsheet microscope sCMOS cameras). Removing the need to section a volume allows for 2D matrix samples to reduce this time-limiting step to the frame rate limitation of the CCD camera of the microscope, which is usually fast (up to 30 fps). The 2D matrix system is simple with minimal preparation and material cost is low (glass coverslip; imaging dish; collagen; H33342). 2D matrix also represents a method for testing 3D compliance of cells, analyze migration in short term in combination with other processes (killing) and of course allows to make use of the benefits of the presence of a 3D matrix in a more commonly available epifluorescence microscope compared to the expensive SPIM systems.

5.1.2.2.2 3D SPIM

The 2D matrix system already offers a simple and economic method to analyze cell behavior in 3D matrices. To ultimately remodel *in vivo* tissues or tumors and analyze complex

immunological dynamics in 3D one cannot avoid the use of SPIM. High frame rates and fast volume sectioning to capture fast events of highly mobile and dynamic T cells with reduced bleaching for stable long term imaging and most important low phototoxicity through reduced off plane illumination are the benefits of SPIM. Long term low interval imaging will also benefit strongly from reduced phototoxicity and bleaching achieved in SPIM through single plane illumination. For technical reasons the concentration of collagen used for 2D matrix experiments (0.25 %) could not be used reliably for LSF experiments. A concentration of collagen of 0.4 - 0.5 % or above was essential for stability of the matrix during imaging as the sample is moved and low concentrated collagen is not stable during this movement. Comparing migration parameters from 0.25 % (2D matrix) and 0.5 % (3D SPIM) a slight change in persistence compared to short term experiments could be determined and velocity is reduced highly significantly in 0.5 % compared to 0.25 %. Higher concentrated collagen causes an increase of matrix rigidity. This generally results in reduced average cell velocity as cells need to produce more force to protrude through the matrix (Lo et al. 2000, Wolf et al. 2013) as is evident in 2D matrix and 3D SPIM experiments for CTL in higher concentrated collagen.

5.1.4 Tracking cells in 3D

Analyzing migration has long been a difficult task yet automated tracking software has made great advances in the past years as well as microscopy techniques and computing power. Efficient tracking objects over time in 3D volumes poses certain requirements. Data size increases with increasing 3D volume size and time scale (Experimental files in SPIM are 100 GBs to several TBs) posing a storage and analysis problem. Automated detection and processing of objects in large image files and the ability to handle Terabyte sized data sets has emerged rather recently in that technological advancements (mainly computer processing power) allow analysis of Terabyte sized files in reasonable time frames (can still be days to weeks). We used proprietarily available software from Bitplane: Imaris. This software bundle allows detection of fluorescent objects, tracking objects over time, analysis of statistical parameters and TB sized files can be handled. All tracking data in this work was generated using Imaris in version 7.7.2 or 8.1.2.

5.1.5 A fluorescent label for migrating cells

To automatically track cells a fluorescent signal is needed as tracking software works most effectively with fluorescent spot-like features by applying a Gaussian detection algorithm. The algorithms for detection are much more effective for spot-like objects over irregular shapes. For this the nucleus appeared as perfect target for labeling CTL for migration and tracking. Hoechst 33342 (H33342, 2'-(4-Ethoxyphenyl)-5-(4-methyl-1-piperazinyl)-2,5'-bi-1H-benzimidazole) has been used before to study migration of different cell types including lymphocytes (Parish et al. 1999, Paszek et al. 2005). H33342 resulted in a simple, economic and reproducible staining of NK as well as CTL and was stable over several days. It was reported before that potential toxicity from H33342 is a product of dye concentration and intensity of excitation (Purschke et al. 2010) and experiments showed a collective cease in migration of primary lymphoid cells during imaging in method development. To test the source of the toxic effect CTL labeled with or without H33342 were exposed to UV light or not during imaging. These data show that the negative effects on migration of CTL observed result from UV excitation and not from the dye H33342 itself. UV exposure at 365 nm can induce ROS generation and cause DNA damage (McMillan et al. 2008, Ge et al. 2013). 2D matrix experiments were limited to 30 minutes. Within this time frame no cease of migration could be observed after optimization of imaging setting. Having set up the experimental systems we analyzed migration behavior of primary human CTL and NK in 0.25 % collagen matrices to determine the range of migration parameters and the mode of migration applied by CTL and NK in this system. For long term imaging (several hours) using SPIM a different option was needed as H33342 could not be visualized in the SPIM system. CellMask Orange produced a reproducible staining yet the staining pattern of the plasma membrane caused difficulties in detection during image analysis. Most reliable results for tracking with regard to photostability and cell viability were achieved using transfected fusion proteins. Tracking can be performed using cytoplasmic fluorescent proteins or nuclear fluorescent proteins.

5.1.6 Migration of lymphocytes in a collagen matrix

The migration behavior determined using the 2D matrix system will represent the basic mode of migration of CTL in a homogenous collagen matrix. Experiments were performed in pepsinized bovine atelocollagen that usually shows a pore size in the lower μm range after polymerization. Because of the physical properties of the used matrix, migration of CTL will be dependent on protrusion and contraction. Primary NK and CTL (unstimulated and bead

stimulated) have nearly identical average velocities yet persistence substantially increases upon bead stimulation of CTL compared to unstimulated or NK cells. Comparing the range of parameters (velocity and persistence) to lymphocyte migration studies in 2D systems show that in 3D matrix systems cells tend to be slower which can be attributed to the resistance of the matrix fibers the cells experience in 3D (Lo et al. 2000, Zhou et al. 2017). For CTL average velocities in 2D were reported in the ranges of 5 - 10 $\mu\text{m min}^{-1}$ (Friedl et al. 1998, Ding et al. 2012) and during *in vivo* interstitial migration of mouse T cells average velocities of 4 to over 10 $\mu\text{m min}^{-1}$ have been reported depending on tissue context and cell type (Cahalan et al. 2003, Lämmermann et al. 2008). We determined the average velocity of primary human CTL and NK cells in 3D 0.25 % collagen to be between 4 - 5 $\mu\text{m min}^{-1}$. The average speed depends on various factors and *in vivo* migration differs from migration in collagen matrices as cytokines, chemokines, microenvironments defined by local cells, ECM fibers and compounds can all modulate migration of lymphocytes. The range of parameters observed *in vivo* and 3D matrix systems is very similar. The increase of persistence for CTLs correlates with an increase in MSD. The frequency distribution of persistence for CTLs shows, that CTL after bead stimulation shift to higher persistence values. This can be explained by high effector and effector memory numbers generated during bead stimulation which are highly mobile and tend to switch from a persistent random walk strategy to a Lévy walk (higher persistence length) upon activation (Sallusto et al. 1999, Geginat et al. 2003). This leads to a straighter movement behavior usually applied by effector cells to locate their rare targets effectively compared to the random more sub-diffusive migration applied by e.g. naïve cells when searching for cognate antigen among densely packed APCs in lymphoid tissue. Persistence of migration or straightness of movement is a factor of cell polarity. Upon bead stimulation many different genes are up or downregulated that can influence cell polarity or its maintenance. Possible targets influencing persistence are mechanically or ligand activated ion channels, cytokine/chemokine receptors, Rho family GTPases and PLC pathway-associated proteins, the latter two being important in maintaining polarity (Palena et al. 2003). The mode of migration applied by CTL or NK can be deduced from mean squared displacement (MSD). The linearity of the MSD indicates if a cell population moves in a confined fashion, applies a random walk or shows directed or guided movement. For primary human CTL (unstimulated and stimulated) and NK the mode of migration within the collagen based system used is a random walk. MSDs of all cell types show high linearity implying

random migration. As reported *in vivo* CTL in collagen show speed fluctuations which alter search efficiency and have been linked e.g. to integrins interactions with other immune cells (Krummel et al. 2016). Comparing the data in this work to data generated by Dr. Renping Zhao (University of Saarland, Biophysics, Homburg, Germany) shows that the collagen concentration has a large impact on the migration of bead stimulated CTL. The range of average velocities (up to $0.3 \mu\text{m s}^{-1}$) and persistence (up to 0.8) in collagen is highly similar in experiments that use the collagen concentration used as a standard (= 0.25 %). Increasing collagen concentrations decrease average velocity and maximal velocities but have only a marginal effect on persistence even if comparing long (6h, 3D SPIM) and short time frames (30 min, 2D matrix). This implies that increased collagen concentrations that are accompanied by increased stiffness of the resulting matrix effectively reduces CTL velocity at least in part owed to the higher resistance posed by the stiffer matrix. In conclusion primary human CTL and NK cells apply a random walk strategy in a collagen-based matrix. Bead stimulation increases CTL persistence significantly owing to the enriched effector and effector memory subpopulations that apply a different strategy for hunting their prey than naïve cells that scan APCs for antigen. Next we modified the basic matrix using ECM components that can provide signals to T cells: fibronectin and hyaluronic acid.

5.2 Migration tuning by extracellular matrix components

The extracellular matrix is not made up of collagen alone. Connective tissue is complex containing many different proteins, carbohydrate complexes, soluble factors and cells. Controlled addition of ECM factors to a matrix can be used to determine the specific effects of that compound on the migration of CTL. Adding a substance to a matrix is simplest when a substance is added to the collagen solution prior to polymerization. This will result in a more even distribution of the added component inside the matrix when compared to application after polymerization of the collagen. Modifications after polymerization are possible yet depend on the molecular size and diffusion of a substance into a polymerized matrix. And, as addition of proteins or glycosaminoglycans does not inhibit polymerization (up to a certain concentration e.g. for hyaluronic acid), addition prior to polymerization is favored. Our approach also does not include crosslinking, although this method can be applied for modification the collagen backbone and its stability or to covalently attach specific factors to the matrix.

5.2.1 Fibronectin and CTL migration

ECM proteins like fibronectin (FN) and collagen serve as binding sites for integrins and can initiate intracellular signaling. Fibronectin binds to integrin pairs found on primary human T lymphocytes, namely $\alpha 4\beta 1$ and $\alpha 5\beta 1$ (Hautzenberger et al. 1994, Greger et al. 2007). The matrix-based imaging systems offer the possibility to determine the effects of specific ECM factors on the random migration behavior of CTL. Fibronectin exists in two general forms: soluble plasma fibronectin and insoluble matrix fibronectin that is bound to complex ECM molecules (Mosher 2006). The former aids coagulation and wound healing, is a disulfide-bonded dimer and attracts leukocytes to aid tissue regeneration (Mosher 2006). Human plasma FN was added non-crosslinked at concentrations of 4 % w/w of collagen and 8 % w/w of collagen and migration parameters were determined for primary human CTL. The used concentrations are below the average plasma concentration of $300 \mu\text{g mL}^{-1}$, namely $100 \mu\text{g mL}^{-1}$ (4 % w/w) and $200 \mu\text{g mL}^{-1}$ (8 % w/w) (Mosher 2006). Presence of plasma fibronectin thus mimics influx of plasma into the interstitial space as occurs upon vasodilation during acute inflammation. Addition of human fibronectin to collagen in the 2D matrix system modulates CTL migration and in CTL this is mediated via two distinct FN-binding integrins. It was shown that neutrophil migration is optimal at an intermediate stiffness of the substrate yet fibronectin concentration defines the stiffness of optimal migration as low concentrations of FN increase the optimal stiffness and high concentrations decrease the optimal stiffness (Stroka and Aranda-Espinoza 2009). In the 2D matrix system stiffness is defined by the collagen formulation and its concentration yet fibronectin concentrations differ by 2-fold. This can result in a switch of the optimal stiffness and thus differently affect CTL migration at differing concentrations of FN. By adapting to substrate stiffness and integrin ligand density CTL can via a simple feedback mechanism of mechano-sensing and signaling intensity adapt to varying environments as they can occur in inflammation and infection or neoplastic changes.

5.2.2 Hyaluronic acid and CTL migration

Another important group of ECM compounds are GAGs, large carbohydrate polymers. Addition of hyaluronic acid to collagen scaffolds has been successfully shown before (Uijtdewilligen et al. 2016) up to a concentration of 0.05 % w/v or 6.25 % w/w (of collagen) of hyaluronic acid (HA). HA can signal anti- or pro-inflammatory states to surrounding cells dependent on the size of the HA fragments where higher MW HA is associated with a healthy

state (Cyphert et al. 2015, Lee-Sayer 2015). By adding high (300 - 500 kDa) and low (8 - 15 kDa) molecular weight HA at a concentration of 1.25 % HA w/w of collagen the effect of HA on T cell migration was studied. In mice reactivated T cells undergo rapid activation induced cell death (AICD) when encountering HA with high MW fragments being most potent death inducers and this could be a security mechanism to induce cell death in T cells re-activated in healthy non-inflamed tissue (Ruffell and Johnson 2008). Using large ($>10^6$ Da) MW fragments of HA could thus have a detrimental effect on bead stimulated effector cell enriched populations as used within this work. HA is already considered fragmented when MW fragments below 500 kDa are present (Lee-Sayer 2015). This makes both conditions (high and low MW HA) to inflammatory conditions and with decreasing MW mimics more severe inflammation. The chosen high MW fragments are the largest fragments that could be used experimentally without disturbances in collagen polymerization, yet the differentially sized fragments used in experiments already elicit different effects. The receptor for HA (CD44) regulates cell motility in interstitial tissue matrices where it aids in maintaining cell polarization (Baaten et al. 2010), its expression is upregulated upon T cell activation (Maeshima 2011) and it serves as a homing receptor to target tissues (Baaten et al. 2010). A study in mice using CD44^{-/-} CD8⁺ T cells showed defective migration effectively reducing T cell mediated tumor clearance (Mrass et al. 2008) and there is evidence that highly proliferative memory T cells bind strongly to HA (Lee-Sayer 2015, Maeshima 2011). CD44 affecting cell polarization complements the result that HA affects significantly persistence but not cell velocity of CTL in a collagen matrix. Persistence is influenced mainly by processes modulating cell polarization or its maintenance and persistence is reduced for CTL (low and high MW). It was reported that migration within a tumor of adoptively transferred tumor-specific CTL is regulated by CTL CD44 interactions in mice. This interaction stabilizes CTL polarity and induces migration potentially leading to more effective tumor clearance (Mrass et al. 2008). In the 2D matrix system hyaluronic acid decreases the persistence of CTL. This could enrich CTL in an area of acute inflammation or lesion, where HA fragments are generated. In conclusion hyaluronic acid modulates CTL persistence in a collagen based matrix by affecting cell polarity and reducing average persistence. Low MW fragments of HA can induce migration effectively in CTL without alterations of average velocity as evident in the histogram showing less cells of low motility (low average velocity) in the presence of low

MW HA fragments which can be attributed to induction and maintenance of polarization of usually non-motile cells.

5.2.3 Matrix modifications and experimental design

The simple mixing of collagen and other ECM components offers a fast technique to alter a matrix biological activity. Fibronectin affects both velocity and persistence of CTL and NK with e.g. a drastic boost on average and maximal velocity of CTL at 4% w/w. This is unusual as the range of parameters (velocity $0.01 - 0.3 \mu\text{m s}^{-1}$ and persistence $0.01 - 0.8$) is generally the same despite if altering cellular (overexpression) or matrix properties (ECM components). Using the effects these substances elicit on cells (higher speed, stronger persistence) matrices that favor an experimentally wanted behavior can be used to amplify more subtle effects especially as primary T cell cultures are highly heterogeneous populations.

5.2.4 Mechano-sensing by CTL

Although attachment to collagen appears not essential for CTL migration in collagen, binding to collagen, even at low affinity, can serve as mechano-sensor and initiator of focal adhesions for this purpose. Mechano-sensing of the collagen matrix can aid CTL in sensing environmental structures. Apart from the TRMP mechano-sensing another mechanism could be used by CTL to sense the fibrous surrounding. Focal adhesions are used by cells for mechano-sensing the environment as determined in fibroblasts and this mechanism is mediated via focal adhesion kinase FAK (Wang et al. 2001). Primary human CTL, when placed in collagen matrices, form small but numerous clusters distributed around the whole cell body. Contact to the surrounding collagen fibers reveals CTL important haptotactic and haptokinetic information. The presence of small vinculin-containing cluster in the cell membrane on one hand and the integrin-independence of migration on the other hand indicate a possible sensory role of focal adhesions for CTL.

5.3 Conclusion on lymphocyte 3D migration

In conclusion collagen-based migration systems offer a versatile system to study migration of motile cells on short and long term, allows modifications of the collagen system by different substances (proteins, glycans), can be used with epifluorescence microscopes and SPIM and for nearly all cell types as collagen is the fundamental building block of all the body's matrices. ECM components can be easily added to the collagen solution before polymerization. This allows not only to determine the specific effects of these components on

CTL migration but allows addition of compounds in combination to favor a general increase in survival (long term experiments) or boost persistence or average speed for specific applications. Lymphocytes migration behavior is tuned by protein and glycan ECM components and depends on the activation state of the migrating T cell. Stimulated T cells show a different migration behavior than unstimulated in that their persistence increases favoring effective search for a rare target. When migrating unguided in collagen matrices, CTL employ a diffusive random walk strategy that can be observed for primary human CTL and NK and which is modulated by ECM factors like fibronectin and hyaluronic acid. Migration behavior of CTL is depending on activation state, matrix composition and physical matrix properties. I developed two methods for 4D imaging and 3D culture systems that allow use of the benefits of 3D matrices, despite the increasing biological complexity that arises from the advantages of 3D matrix based systems. Using collagen as fundamental building block allows constructing a tissue matrix of wanted complexity and composition to determine the effects of specific extracellular factors on cell behavior. The most physiological experiments are performed *in vivo*, as this of course represents reality best. In an animal, although physiologically fully functional, complexity of observed responses especially in an immunobiology context is immense. Reverse engineering tissues gives the experimenter the full control over the experimental environment. Ultimately this could lead to stepping away from many animal experiments boosting ethical progression as well as scientific.

5.5 Profilin and CTL

Migration, as well as killing and its accompanying mechanisms make use of the cytoskeletal system of a cell to induce polarization, migration and formation of an immunological synapse. A prominent mechanism is the ability of cells to use polymerization of actin filaments as driving force for migration and aid in stabilization of cellular structures. Actin dynamics underlie a complex control system by many proteins including nucleation and elongation promoting factors, G-actin monomer providing proteins, proteins linked to integrins, extracellular signaling cascades and second messenger activated proteins (e.g. Ca^{2+} dependent proteins). At the heart of actin dynamics lay profilins as they represent the link between signaling pathways and actin polymerization regulation. The function of profilins in human CTL was unknown. Tumor and adjacent tissues had been screened for PFN1 expression and PFN1 was found to be differentially expressed (Cheng et al. 2013, Wittenmayer et al. 2004, Zaidi and Manna 2016, Yao et al. 2014). Our collaborator identified a downregulation of

PFN1 in neoplastic cells to be a possible tumor driver in pancreatic cancer, and that decreased PFN1 levels correlated with lower survival of the patients (Yao et al. 2014). In our recently published work a downregulation of PFN1 in CD8⁺ T cells from peripheral blood of malignant pancreatic cancer patients is described (Schoppmeyer et al. 2017). The effects of PFN1 have thus been analyzed in regard to cytotoxicity and migration to assess possible effects on tumor infiltration and detection as well as killing of tumor cells by CTL.

5.5.1 Profilin1, CTL and cancer

In regard to tumor immunology PFN1 has been shown to be a tumor suppressor in different kinds of tumors (breast cancer, pancreatic cancer). Also tumor and adjacent tissues have been screened for PFN1 expression and PFN1 was found to be differentially expressed (Cheng et al. 2013, Wittenmayer et al. 2004, Zaidi and Manna 2016, Yao et al. 2014). Our collaborator found not only a downregulation of PFN1 in neoplastic cells being a possible tumor driver in pancreatic cancer, they also found that decreased profilin1 levels correlated with lower survival of the patients (Yao et al. 2014) and that CTL isolated from peripheral blood of end stage pancreatic cancer patients showed (in 7 out of 9 cases) a lower PFN1 level (mRNA and protein level). To determine which mechanisms could explain the downregulation of PFN1 in pancreatic cancer patients a search for transcriptional regulators (transcription factors, micro RNAs) using the HMDD (Human microRNA Disease Database, <http://www.cuilab.cn/hmdd>) and DisGeNET (www.disgenet.org) databases was done. The microRNAs hsa-mir-96 and hsa-mir-182 and the transcription factors PPARG (peroxisome proliferator-activated receptor gamma), TP53 (p53) and AHR (aryl hydrocarbon receptor) control PFN1 transcriptionally and/or post-transcriptionally and are known to be either mutated or dysregulated in pancreatic cancer (Yu et al. 2012, Yu et al. 2010, Maitra and Hruban 2008, Kristiansen et al. 2006, Koliopanos et al. 2002). The changes in transcriptional control associated with pancreatic cancer can thus also affect the immune system directly through changes in expression of functionally important proteins. Changes in CTL PFN1 levels can thus be a result of dysfunctional transcription control affecting pancreatic cells (towards neoplasm) and CTL in their functionality.

5.5.2 Profilin characterization in human CTL

To determine which isoforms of PFN are expressed in primary human CTL total RNA and protein lysates were gathered from unstimulated (negatively isolated) and bead stimulated and

SEA stimulated CTL from the same donors. The qRT-PCR analysis of this samples showed that only PFN1 mRNA is expressed of the four isoforms in primary human CTL and this was in agreement with Western blot analysis of protein lysates from primary human CTL, although CTL after SEA stimulation showed a slight effect on PFN1 protein levels while bead stimulated CTL show no significant differences. The other isoforms PFN2/3/4 show reported tissue specific non-hematopoietic expression (PFN2 = neurons; PFN3/4 = testis) (Behnen et al. 2009) and are not expressed in primary human CTL. The question on the function of PFN1 in primary human CTL was to be answered. Because of limitations in efficiencies of transfection (either plasmids or siRNA) we used bead stimulated CTL for overexpression studies and SEA stimulated CTL for siRNA experiments. PFN1 and its mutants were overexpressed as mCherry fusion proteins (*N*-mCherry_PFN1-C).

5.5.3 Profilin1 function in primary human CTL

5.5.3.1 Profilin1 and CTL cytotoxicity

A diverse variety of cellular processes relies on proper actin dynamics, to which PFN1 plays a central role and many of these processes participate in successful target search and effective killing of the target. Downregulation of PFN1 via siRNA, mimicking the situation observed in the pancreatic cancer patients, increased the killing capacity of CTL and overexpression of PFN1 on the other hand reduced the killing capacity consistently in CTL from different donors. PFN1 thus has a negative regulatory effect on the killing capacity of primary human CTL *in vitro*. The killing capacity of CTL was determined using an *in vitro* kinetic killing assay (Kummerow et al. 2014). In this assay effector cells (CTL) are present in excess (10 effectors per target cell) and migration is, at least in the initial phases of the assay only of minor importance, but gains importance in later stages when target cells become scarcer. Apart from migration, IS formation and LG exocytosis are necessary for target cell killing and we analyzed these processes with regard to profilin function (Schoppmeyer et al. 2017). Using a degranulation assay we could show that PFN1 is a negative regulator of LG exocytosis and modulates actin structures at the IS offering a possible explanation for impaired LG exocytosis (Schoppmeyer et al. 2017). Analysis of CTL migration was performed in a 3D collagen-matrix using overexpression of PFN1 or its mutants and siRNA KD to pinpoint if the cause of the negative regulatory role of PFN1 in the cytotoxicity primary human CTL could also be migration related.

5.5.3.2 Profilin1 and CTL migration

Profilin function in migration is highly variable. A study of breast cancer cells revealed that metastasis correlated with lower PFN1 expression levels (Ding et al. 2014), in endothelial cell cord morphogenesis PFN1 downregulation inhibited migration as well as proliferation (Ding et al. 2006) and in breast cancer cells (MDA-MB-231) invasiveness correlated with decreased PFN levels (Zou et al. 2007) resulting from increased persistence (Bea et al. 2009). Profilins are described as requisite for cell migration but the effects observed elicited in different cell types by PFN up or downregulation are manifold and its function in CTL migration remained unknown. In the 2D matrix system effects on migration through either modulation of actin polymerization rates or maintenance of cell polarity define the migration behavior of CTL. In the 2D matrix system migration is random and depends on the inherent polarity of activated CTL (Codling et al. 2008, Wei et al. 2009). Using siRNA or PFN1 overexpression either reduces endogenous PFN1 (siRNA) or increases the PFN1 concentration in cells (overexpression). This can affect the actin polymerization rate thus affecting cell velocity. It has been reported that the effect PFN1 elicits on actin polymerization depends on the relative concentrations of PFN1, G-actin and free barbed ends of F-actin filaments (Ding et al. 2012). Without free barbed ends, e.g. being blocked by capping proteins, PFN1 will serve as actin sequestering protein yet if barbed ends are free PFN1 can elongate filaments given a sufficient pool of ATP:G-actin is present (Ding et al. 2012). PFN1 overexpression as well as downregulation via siRNA show relatively low but significant effects on average velocity yet not persistence. This is in compliance with the fact that PFN1 can affect actin polymerization rates via modulating actin monomer provision. In these conditions the effect on the relative concentration of PFN1, G-actin and free barbed ends is strongly affected yet the effect on migration of CTL is minor. This implies that actin monomer shuttling for polymerization depends only minor on the amount of PFN1:G-actin present in a cell at a certain time point. To assess if other functions than actin monomer shuttling by PFN are important for proper CTL migration we mutated its interaction sites to inhibit binding of interaction partners. Mutants that ablate functional interactions of PFN1 were analyzed for their effect on cell migration. Y59A (Wittenmayer et al. 2004) (abolished actin binding) will not provide G-actin thus negatively influencing promotion of actin polymerization via PFN1. By binding to PIP₂ Y59A can modulate cell polarization which can explain the increase in persistence. Endogenous profilin can still deliver sufficient actin monomers to growing filaments thus

partly countering the abolished actin provision to sites of polymerization. Overexpression of the mutants lacking either PIP₂ (R88L) (Sohn et al. 1995) or poly-L-proline (H133S) (Ding et al. 2009) binding drastically reduced the motility of CTL in 3D. The R88L mutant can still bind monomeric actin yet membrane localization (PIP₂ binding) is disturbed. This indicates the importance of PIP₂ binding (R88L) to regulate migration by affecting cell polarization pathways apart from directly regulating actin polymerization. Knock down via siRNA and PFN1 overexpression imply actin polymerization can function properly over a broad range of PFN1 levels within cells. In the cases of R88L overexpression actin is bound but phospholipid binding is abolished (R88L) resulting in strong effects on CTL motility. In case of the R88L mutant it was shown that actin interaction is hindered in this mutant form (Ding et al. 2012). This kind of competitive interaction between PIP₂ and actin also exist for PIP₂ and poly-L-proline ligands (Ding et al. 2012). Apart from this binding to PIP₂ by PFN1 results in rapid dissociation of actin from profilactin (Ding et al. 2012). This can inhibit PIP₂ signaling pathways via PFN1 at the cell front causing a disturbance of the cellular Ca²⁺ gradient resulting in impaired polarization. The PFN1-H133S bound G-actin can no longer recruit regulatory proteins to promote actin polymerization thus effectively reducing the available free G-actin concentration. This inhibits polymerization, the driving force for cellular locomotion. It has been shown before that actin polymerization dependent cell motility relies on functional poly-L-proline interactions and PFN1 needs interacting proteins to be able to shuttle actin to growing filaments (Ding et al. 2012). Poly-L-proline interaction partners are numerous and associated with many different cellular function. For migration cytoskeletal regulators are important which include WASP/WAVE and mENA/VASP. The mENA/VASP proteins are capping protein competitors freeing barbed ends for PFN1 mediated elongation and if not recruited by PFN1 actin polymerization can be inhibited resulting in inhibited migration. WASP/WAVE proteins are initiators of Arp2/3 mediated actin polymerization and are activated by binding to phospholipids like PIP₂ (Kurusu and Takenawa 2009). Favored binding of H133S to PIP₂ could thus also inhibit WAVE/Wasp mediated actin polymerization. The C71G mutant was discovered to cause amyotrophic lateral sclerosis through formation of cytoplasmic aggregates and disruption of cytoskeletal structures (Wu et al. 2012, Yang et al. 2016). In CTL the C71G mutant causes a substantial decrease in persistence similar to that observed for the mutants R88L and H133S yet velocity increases to an extend comparable to the Y59A mutant. Due the ability of C71G to interact normally with

interaction proteins, phospholipids and actin velocity is not reduced. C71G expressing cells migrate with increased speed compared to control indicating an increase of actin polymerization rate. Recently C71G has been shown to be thermodynamically destabilized into an unfolded state that interacts strongly with membranes transforming the disordered unfolded protein into a non-native helical structure (Lim et al. 2017). This insertion into the membrane can interfere with normal cellular signaling functions affecting polarization and thus persistence. Classically termed actin sequestering protein, PFN1 has unveiled a vast complexity in its functionality. Apart from shuttling actin monomers to growing F-actin strands PFN1, via its PIP₂ and poly-L-proline interaction domains, PFN1 cross-talks with lipid pathways and cytoskeletal regulators, which are highly complex processes. We found that during migration in 3D collagen PFN1 function is highly dependent on functional PIP₂ and poly-L-proline interactions. The diverse effects of PFN1 observed in cells of different origin depend strongly on the cellular background (Ding et al. 2006, Ding et al. 2014). Activity and presence of elongation promoting factors like mENA/VASP, phospholipids turnover, generation or binding competition affect the stoichiometry of PFN1 and PFN1:PI (PI = phospholipid) and either promote (PFN1 free) or inhibit (PFN1:PI) migration (Ding et al. 2012).

5.5.4 Conclusion on PFN1 function in CTL

Profilins lay at the heart of actin dynamics which mediate a broad spectrum of cellular functions. In a paper published this year our group and collaborators analyzed the function of PFN1 in primary human CTL (Schoppmeyer et al. 2017). In primary human CTL, PFN1, the only expressed isoform, regulates cytotoxicity via modulation of LG release and migration. LG release is negatively regulated by PFN1 which represents one part of the negative regulatory role of PFN1 on CTL cytotoxicity (Schoppmeyer et al. 2017). During migration PFN1 modulates the protrusion pattern and regulates cell mainly velocity (Schoppmeyer et al. 2017). Although increased velocity can increase the searched area in a given time frame, this can also result in lower contact times with target cells, effectively reducing search efficiency experimentally as observed for PFN1 overexpressing cells. Using mutants of PFN1 that can no longer bind actin, poly-L-proline ligands or PIP₂, the functional domains of PFN1 we found PIP₂ binding and poly-L-proline interactions to be essential for proper CTL migration. Downregulation and overexpression of PFN1 had almost no effect on migration which showed that actin polymerization driven migration of CTL in 3D does not depend on the

relative concentrations of PFN1, actin and actin nuclei. Interestingly we could show using bioinformatics that changes in transcriptional control of PFN1 have been associated with changes observed in pancreatic cancer patients (Schoppmeyer et al. 2017). Genetic changes that drive cancer progression can also affect immune cells, this way modulating a possible immune response for better or worse. *In vitro* data of CTL with downregulated PFN1 shows increased cytotoxicity in a kinetic killing assay. In the pancreatic patients microenvironments, cytokines profiles, immunosuppressive mechanisms of cancer cells and other factors come into play that are not covered *in vitro*. Although CTL with downregulated PFN1 show increased cytotoxicity and invasiveness *in vitro* this must not pose a benefit for CTL cytotoxicity *in vivo*. It remains to debate if increases in *in vitro* killing are generally an improvement, physiologically, as more is not always better.

6. References

- Abram CL and Lowell CA, **The Ins and Outs of Leukocyte Integrin Signaling**, *Ann Rev Immunol*, **2009**, 27, 339 - 362
- Alarcón B et al., **The immunological synapse: a cause or consequence of T-cell receptor triggering?**, *Immunol*, **2011**, 133(4), 420 - 425
- Alberts B et al., **Molecular Biology of the Cell**, New York, Garland Science, **2002**
- Andrés-Delgado L et al., **Centrosome Polarization in T Cells: A Task for Formins**, *Front Immunol*, **2013**, 4, 191
- Andrianantoandro E and Pollard TD, **Mechanism of Actin Filament Turnover by Severing and Nucleation at Different Concentrations of ADF/Cofilin**, *Mol Cell*, 24(1), **2006**, 13 - 23
- Angus KL and Griffiths GM, **Cell polarisation and the immunological synapse**, *Curr Op Cell Biol*, **2013**, 25(1), 85 - 91
- Arstila TP et al., **A Direct Estimate of the Human $\alpha\beta$ T Cell Receptor Diversity**, *Science*, **1999**, 286(5441), 958 - 961
- Artym V and Matsumoto K, **Imaging Cells in Three-Dimensional Collagen Matrix**, *Curr Protoc Cell Biol*, **2010**, 10.1820
- Baaten BJG, et al., **Multifaceted regulation of T cells by CD44**, *Comm Integr Biol*, **2010**, 3(6), 508 - 512
- Badour K et al., **The Wiskott-Aldrich syndrome protein acts downstream of CD2 and the CD2AP and PSTPIP1 adaptors to promote formation of the immunological synapse**, *Immunity*, **2003**, 18, 141 - 154
- Bea YH et al., **Loss of profilin-1 expression enhances breast cancer cell motility by Ena/VASP proteins**, *J Cell Physiol*, **2009**, 219(2), 354 - 364
- Behnen M et al., **Testis-expressed profilins 3 and 4 show distinct functional characteristics and localize in the acroplaxome-manchette complex in spermatids**, *BMC Cell Biol*, **2009**, 10(34)
- Bertrand F et al., **An initial and rapid step of LG secretion precedes microtubule organizing center polarization at the cytotoxic T lymphocyte/target cell synapse**, *PNAS*, **2013**, 110(15), 6073 - 6078
- Bijian K et al., **Collagen-mediated survival signaling is modulated by CD45 in Jurkat T cells**, *Mol Immunol*, **2007**, 44(15), 3682 - 3690
- Billadeau DD et al., **Regulation of cytoskeletal dynamics at the immune synapse: new stars join the actin troupe**, *Traffic*, **2006**, 7, 1451 - 1460
- Bosch FX et al., **The causal relation between human papillomavirus and cervical cancer**, *J Clin Pathol*, **2002**, 55(4), 244 - 265
- Bovellan M et al., **Cellular Control of Cortical Actin Nucleation**, *Curr Biol*, **2014**, 24(14), 1628 - 1635
- Brown AC et al., **Remodelling of cortical actin where LGs dock at natural killer cell immune synapses revealed by super-resolution microscopy**, *PLoS Biology*, **2011**, e1001152
- Brownlie RJ and Zamoyska R, **T cell receptor signalling networks: branched, diversified and bounded**, *Nat Rev Immunol*, **2013**, 13, 257 - 269
- Cahalan MD et al., **Real-time imaging of lymphocytes *in vivo***, *Curr Op Immunol*, **2003**, 15(4), 372 - 377

- Campbell JJ and Butcher EC, **Chemokines in tissue-specific and microenvironment-specific lymphocyte homing**, *Curr Op Immunol*, 12, 3, **2000**, 336-341
- Carlsson L et al., **Actin polymerizability is influenced by profilin, a low molecular weight protein in non-muscle cells**, *J Mol Biol*, 115(3), **1977**, 465 - 483
- Carrega P and Ferlazzo G, **Natural killer cell distribution and trafficking in human tissues**, *Front Immunol*, **2012**, 3, 347
- Chalkia D et al., **Origins and Evolution of the Formin Multigene Family That Is Involved in the Formation of Actin Filaments**, *Mol Biol Evol*, **2008**, 25(12), 2717 - 2733
- Chattopadhyay S and Raines RT, **Collagen-Based Biomaterials for Wound Healing**, *Biopolymers*, 101(8), **2014**, 101(8), 821 - 833
- Chen J et al., **Integrins and Their Extracellular Matrix Ligands in Lymphangiogenesis and Lymph Node Metastasis**, *Int J Cell Biol*, **2012**
- Cheng H et al., **Profilin1 sensitizes pancreatic cancer cells to irradiation by inducing apoptosis and reducing autophagy**, *Curr Mol Med*, **2013**,13, 1368 - 1375
- Chung AW et al., **Activation of NK cells by ADCC antibodies and HIV disease progression**, *J Acquir Immune Defic Syndr*, **1999/2011**, 58(2), 127 - 131
- Codling EA et al., **Random walk models in biology**, *J Roy Soc Interf*, 5(25), **2008**, 813-834
- Cole TS and Cant AJ, **Clinical experience in T cell deficient patients**, *Aller Asth Clin Immunol*, **2010**, 6(1), 9
- Crevenna AH et al., **Side-binding proteins modulate actin filament dynamics**, Hyman AA, ed. *eLife*, **2015**, 4, e04599
- Cyphert JM and Trempus CS et al., **Size Matters: Molecular Weight Specificity of Hyaluronan Effects in Cell Biology**, *Int J Cell Biol*, **2015**, 8
- Dass S et al., **Immune evasion in cancer: Mechanistic basis and therapeutic strategies**, *Sem Cancer Biol*, 35, **2015**, S185 - S198
- de la Roche M and Asano Y et al., **Origins of the cytolytic synapse**, *Nat Rev Immunol*, **2016**, 16, 421 - 432
- Decaestecker C et al., **Can anti-migratory drugs be screened in vitro? A review of 2D and 3D assays for the quantitative analysis of cell migration**, *Med Res Rev*, **2007**, 27(2), 149 - 176
- DeGrendele HC, et al., **Functional activation of lymphocyte CD44 in peripheral blood is a marker of autoimmune disease activity**, *J Clin Invest*, **1998**, 102(6),1173 - 1182
- Ding Z et al., **Both actin and polyproline interactions of profilin-1 are required for migration, invasion and capillary morphogenesis of vascular endothelial cells**, *Exp Cell Res*, 315 (17), **2009**, 2963 - 2973
- Ding Z et al., **Molecular insights on context-specific role of profilin-1 in cell migration**, *Cell Adhe Migr*, **2012**, 6(5), 442 - 449
- Ding Z et al., **Profilin-1 downregulation has contrasting effects on early vs late steps of breast cancer metastasis**, *Oncogene*, **2014**,33(16), 2065 - 2074
- Ding Z et al., **Silencing profilin-1 inhibits endothelial cell proliferation, migration and cord morphogenesis**, *J Cell Sci*, **2006**,119(Pt 19), 4127 - 4137
- Dominguez R and Holmes KC, **Actin structure and function**, *Annu Rev Biophys*, **2011**, 40, 169–186

- Dosch HM et al., **Severe combined immunodeficiency disease: a model of T-cell dysfunction**, *Clin Exp Immunol*, **1978**, 34(2), 260 - 267
- Duarte RF et al., **Functional impairment of human T-lymphocytes following PHA-induced expansion and retroviral transduction: implications for gene therapy**, *Gene Therapy*, **2002**, 9, 1359 - 1368
- Dustin ML, **The immunological synapse**, *Can Immunol Res*, **2014**, 2(11), 1023 - 1033
- Ebert PJR et al., **Functional Development of the T Cell Receptor for Antigen**, *Prog Mol Biol Transl Sci*, **2010**, 92, 65 - 100
- Eyre DR et al., **Cross-linking in collagen and elastin**, *Annu Rev Biochem*, **1984**, 53, 717 - 48
- Favaro PM et al., **Human leukocyte formin: a novel protein expressed in lymphoid malignancies and associated with Akt**, *Biochem Biophys Res Comm*, **2003**, 311 (2), 365 – 371
- Ferber MJ et al., **Integrations of the hepatitis B virus (HBV) and human papillomavirus (HPV) into the human telomerase reverse transcriptase (hTERT) gene in liver and cervical cancers**, *Oncogene*, **2003**, 22(24), 3813 - 3820
- Feske S et al., **Ion channels and transporters in lymphocyte function and immunity**, *Nat Rev Immunol*, **2012**, 12(7), 532 - 547
- Fletcher DA and Mullins RD, **Cell mechanics and the cytoskeleton**, *Nature*, **2010**, 463(7280), 485-92
- Friedl P et al., **Cell Migration Strategies in 3-D Extracellular Matrix: Differences in Morphology**, *Micros Res Tech*, **1998**, 43(5), 369 - 378
- Gandhi NS et al., **The Structure of Glycosaminoglycans and their Interactions with Proteins**, *Chem Biol Drug Des*, **2008**, 72, 455 - 482
- Ge J et al., **Standard Fluorescent Imaging of Live Cells is Highly Genotoxic**, *J Int Soc Anal Cytol*, **2013**, 83(6), 552 - 560
- Geginat J et al., **Proliferation and differentiation potential of human CD8⁺ memory T-cell subsets in response to antigen or homeostatic cytokines**, *Blood*, **2003**, 101, 4260 - 4266
- Gelse K et al., **Collagens—structure, function, and biosynthesis**, *Advanced Drug Delivery Reviews*, 55 (12), **2003**, 1531 - 1546
- Gérard A et al., **Detection of rare antigen-presenting cells through T cell-intrinsic meandering motility, mediated by Myo1g**, *Cell*, **2014**, 158(3), 492 - 505
- Goldschmidt-Clermont PJ et al., **The Actin-Binding Protein Profilin Binds to PIP₂ and Inhibits Its Hydrolysis by Phospholipase C**, *New Series*, **1990**, 247, 4950, 1575 - 1578
- Goldschmidt-Clermont PJ et al., **The control of actin nucleotide exchange by thymosin beta 4 and profilin. A potential regulatory mechanism for actin polymerization in cells**, *Mol Biol Cell*, **1992**, 3(9), 1015 - 1024
- Gomez TS et al., **Formins regulate the Arp2/3-independent polarization of the MTOC to the Immunological Synapse**, *Immunity*, **2007**, 26(2), 177 - 190
- Gómez-Márquez J, **Thymosin-beta 4 gene. Preliminary characterization and expression in tissues, thymic cells, and lymphocytes**, *J Immunol*, **1989**, 143(8)
- Goode BL and Eck MJ, **Mechanism and function of formins in the control of actin assembly**, *Annu Rev Biochem*, **2007**, 76, 593 - 627
- Gorski A and Kupiec-Weglinski JW, **Extracellular Matrix Proteins, Regulators of T-Cell Functions in Healthy and Diseased Individuals**, *Clin Diag Lab Immunol*, **1995**, 2(6), 646 - 651

- Gough NR et al., **Moving in 2D Versus 3D**, *Science Signal*, **2010**, 3(138), ec274
- Govaerts A, **Cellular antibodies in kidney homotransplantation**, *J Immunol*, **1960**, 85, 516 - 522
- Greger K et al., **Basic building units and properties of a fluorescence single plane illumination microscope**, *Rev Sci Instrum*, **2007**, 78(2), 023705
- Grégoire C et al., **The trafficking of natural killer cells**, *Immunol Rev*, **2007**, 220(1), 169 - 182
- Harris ES et al., **The Leukocyte Integrins**, *J Biol Chem*, **2000**, 275(31), 23409 - 23412
- Harris TH et al., **Generalized Lévy walks and the role of chemokines in migration of effector CD8⁺ T cells**, *Nature*, **2012**, 486, 545 - 548
- Hautzenberger D et al, **Functional specialization of fibronectin-binding beta 1-integrins in T lymphocyte migration**. *J Immunol*, **1994**, 153(3), 960 - 971
- Heasman SJ and Ridley AJ, **Mammalian Rho GTPases: new insights into their functions from in vivo studies**, *Nat Rev Mol Cell Biol*, **2008**, 9, 690 - 701
- Hughes CS et al., **Matrigel: a complex protein mixture required for optimal growth of cell culture**, *Proteomics*, **2010**, 10(9), 1886 - 1890
- Humphries J, **Integrin ligands at a Glance**, *J Cell Sci*, **2006** 119, 3901 - 3903
- Hynes RO, **The Extracellular Matrix: Not Just Pretty Fibrils**, *Science*, **2009**, 27, 1216 - 1219
- Hyun YM et al., **Leukocyte integrins and their ligand interactions**, *Immunol Res*, **2009**
- Imamura Y et al., **Comparison of 2D- and 3D-culture models as drug-testing platforms in breast cancer**, *Oncol Rep*, **2015**, 33(4), 1837-1843
- Irobi E et al., **Structural basis of actin sequestration by thymosin- β 4: implications for WH2 proteins**, *The EMBO J*, **2004**, 23(18), 3599 - 3608
- Jameson SC and Bevan MJ, **T-cell selection**, *Curr Op Immunol*, **1998**, 10(2), 214 - 219
- Janeway Jr., CA and Medzhitov R, **Innate Immune Recognition**, *Ann Rev Immunol*, **2002**, 20(1), 197 - 216
- Johnson CM and Rodgers W, **Spatial Segregation of Phosphatidylinositol 4,5-Bisphosphate (PIP₂) Signaling in Immune Cell Functions**, *Immunol Endo Metab Agents Med Chem*, **2008**, 8(4), 349 - 357
- Jung J et al., **A cell-repellent sulfonated PEG comb-like polymer for highly resolved cell micropatterns**, *J Biomater Sci Polym*, **2008**, 19(2), 161 - 173
- Kagi D et al., **Cytotoxicity mediated by T cells and natural killer cells is greatly impaired in perforin-deficient mice**, *Nature*, **1994**, 369, 31 - 37
- Kim CH, **Crawling of effector T cells on extracellular matrix: role of integrins in interstitial migration in inflamed tissues**, *Cell Mol Immunol*, **2014**, 11, 1 - 4
- Kleinmann HK and Martin GR, **Matrigel: basement membrane matrix with biological activity**, *Semin Cancer Biol*, **2005**, 15(5), 378 - 386
- Kogan G et al., **Hyaluronic acid: a natural biopolymer with a broad range of biomedical and industrial applications**, *Biotech Let*, **2007**, 29(1), 17 - 25
- Koliopanos A et al., **Increased arylhydrocarbon receptor expression offers a potential therapeutic target for pancreatic cancer**, *Oncogene*, **2002**, 21, 6059-6070
- Korn ED et al., **Actin Polymerization and ATP Hydrolysis**, *Science*, **1987**, 238(4827), 638 - 644

- Krause M et al., **ENA/VASP Proteins: Regulators of the Actin Cytoskeleton and Cell Migration**, *Annu Rev Cell Dev Biol*, **2003**, 19, 541–64
- Krishnan K and Moens PDJ, **Structure and function of profilins**, *Biophys Rev*, **2009**, 1, 71 – 81
- Kristiansen G et al., **Peroxisome proliferator-activated receptor gamma is highly expressed in pancreatic cancer and is associated with shorter overall survival times**, *Clin Cancer Res*, **2006**, 12, 6444-6451
- Krummel MF and Macara I, **Maintenance and modulation of T cell polarity**, *Nat Immunol*, **2006**, 7(11), 1143 - 1149
- Krummel MF et al., **T cell migration, search strategies and mechanisms**, *Nat Rev Immunol*, **2016**, 16, 193 - 201
- Kumar H et al. **Pathogen recognition by the innate immune system**, *Int Rev Immunol*, **2011**, 30(1), 16 - 34
- Kummerow C et al., **A simple, economic, time-resolved killing assay**. *Eur J Immu*, **2014**
- Kupfer A and Dennert G, **Reorientation of the microtubule-organizing center and the Golgi apparatus in cloned cytotoxic lymphocytes triggered by binding to lysable target cells**, *J Immunol*, **1984**, 133(5), 2762 - 2766
- Kurusu S and Takenawa T, **The WASP and WAVE family proteins**, *Gen Biol*, **2009**, 10(6), 226
- Kwiatkowski AV et al., **Function and regulation of Ena/VASP proteins**, *Trends Cell Biol*, **2003**, 13(7), 386 - 92
- Lämmermann T and Sixt M, **Mechanical modes of ‘amoeboid’ cell migration**, *Cur Op Cell Biol*, 21(5), **2009**, 636 - 644
- Lämmermann T et al., **Rapid leukocyte migration by integrin-independent flowing and squeezing**, *Nature*, **2008**, 51 - 55
- Le Clairche C and Carlier MF, **Regulation of Actin Assembly Associated With Protrusion and Adhesion in Cell Migration**, *Physiol Rev*, **2008**, 88(2), 489 - 513
- Lee SH and Dominguez R, **Regulation of actin cytoskeleton dynamics in cells**, *Mol Cells*, **2010**, 29(4), 311-25
- Lee-Sayer SS, **The Where, When, How, and Why of Hyaluronan Binding by Immune Cells**, *Front Immunol*, **2015**, 6(150)
- Li Y and Kurlander RJ, **Comparison of anti-CD3 and anti-CD28-coated beads with soluble anti-CD3 for expanding human T cells: Differing impact on CD8 T cell phenotype and responsiveness to restimulation**, *J Transl Med*, **2010**, 8, 104
- Lim L et al., **ALS-causing profilin-1-mutant forms a non-native helical structure in membrane environments**, *BBA - Biomembranes*, **2017**, 1859(11), 2161 - 2170
- Liou GY and Storz P, **Reactive oxygen species in cancer**, *Free Radic Res*, **2010**, 44, 479 - 496
- Lo CM et al., **Cell Movement Is Guided by the Rigidity of the Substrate**, *Biophys J*, **2000**, 79(1), 144-152
- Lodish H et al., **Molecular Cell Biology**, 4th edition, New York: W. H. Freeman, **2000**
- Lu M et al., **An analysis of human microRNA and disease associations**, *PLoS One*, **2008**, 3(10), e3420
- Luca AC et al., **Impact of the 3D microenvironment on phenotype, gene expression, and EGFR inhibition of colorectal cancer cell lines**, *PloS one*, **2003**, 8(3), e59689
- Ma PX, **Biomimetic materials for tissue engineering**, *Adv Drug Del Rev*, **2008**, 60(2), 184 - 198

- Maeshima N et al. **Hyaluronan binding identifies the most proliferative activated and memory T cells**, *Eur J Immunol*, **2011**, 41(4), 1108 - 1119
- Maitra A and Hruban RH, **Pancreatic cancer**, *Annu Rev Pathol*, **2008**, 3, 157-188
- Makkouk A and Weiner GJ, **Cancer immunotherapy and breaking immune tolerance: new approaches to an old challenge**, *Cancer Res*, **2015**, 75(1), 5 - 10
- Martín-Cófreces NB and Robles-Valero J et al., **MTOC translocation modulates IS formation and controls sustained T cell signaling**, *J Cell Biol*, **2008**, 182(5), 951 - 62
- Masopust D, **The integration of T cell migration, differentiation and function**, *Nat Rev Immunol*, 13, **2013**, 309
- McCarthy JB and Furcht LT, **Laminin and fibronectin promote the haptotaxis of B 16 melanoma cells in vitro**, *J Cell Biol*, **1984**, 98(1474)
- McDonald HR, Nabholz M, **T cell activation**, *Ann Rev Cell Biol*, **1986**, 2, 231 - 53
- McEver RP and Zhu C, **Rolling cell adhesion**, *Annu Rev Cell Dev Biol*, **2010**, 26, 363 -396
- Mcmillan TJ et al., **Cellular effects of long wavelength UV light (UVA) in mammalian cells**, *J Pharm Pharmacol*, **2008**, 60(8), 969 - 76
- Miki H et al., **WAVE, a novel WASP-family protein involved in actin reorganization induced by Rac**, *EMBO J*, **1998**, 17, 23, 6932 - 6941
- Mogilner A and Oster G, **Cell motility driven by actin polymerization**, *Biophys J*, 71, **1996**, 3030 - 3045
- Mora JR and von Andrian UH, **T-cell homing specificity and plasticity: new concepts and future challenges**, *Trends Immunol*, **2006**, 27(5), 235 - 243
- Mosher DF, **Plasma fibronectin concentration: a risk factor for arterial thrombosis?** *Arterioscler Thromb Vasc Biol*, **2006**, 26(6), 1193 - 1195
- Mouw JK et al., **Extracellular matrix assembly: a multiscale deconstruction**, *Nat Rev Mol Cell Biol*, **2014**, 15(12), 771 - 785
- Mrass P et al., **CD44 mediates successful interstitial navigation by killer T cells and enables efficient antitumor immunity**, *Immunity*, **2008**, 29(6), 971 - 985
- Mrass P et al., **Successful interstitial navigation by killer T cells enables efficient anti-tumor immunity**, *Immunity*, **2008**, 29(6), 971 - 985
- Munoz MA et al., **T cell migration in intact lymph nodes in vivo**, *Curr Opin Cell Biol*, **2014**, 30, 17 - 24
- Murphy K et al., **Janeway's immunobiology**, 7th Edition, **2008**, New York: Garland Science
- Myungjin JL et al., **A three-dimensional microenvironment alters protein expression and chemosensitivity of epithelial ovarian cancer cells in vitro**, *Laborat Invest*, **2013**, 93(5), 528 - 542
- Nejedla M et al., **Profilin connects actin assembly with microtubule dynamics**, Blanchoin L, ed. *Mol Biol Cell*, **2016**, 27(15), 2381 - 2393
- Nürnberg A et al., **Nucleating actin for invasion**, *Nat Rev Cancer*, **2011**, 11, 177 - 187
- Obino D et al., **Actin nucleation at the centrosome controls lymphocyte polarity**, *Nat Comm*, **2016**, 7, 10969
- Packard BZ et al., **Direct visualization of protease activity on cells migrating in three-dimensions**, *Matrix Biol*, **2009**, 28(1), 3 - 10

- Palena C et al., **Differential Gene Expression Profiles in a Human T-cell Line Stimulated with a Tumor-associated Self-peptide versus an Enhancer Agonist Peptide**, *Clin Cancer Res*, **2003**, 9(5), 1616 - 1627
- Parish CR, **Fluorescent dyes for lymphocyte migration and proliferation studies**, *Immunol Cell Biol*, **1999**, 77, 499 - 508
- Parkin J and Cohen B, **An overview of the immune system**, *The Lancet*, 357(9270), **2001**, 1777 - 1789
- Paszek MJ et al., **Tensional homeostasis and the malignant phenotype**, *Cancer Cell*, **2005**, 8(3), 241 - 254
- Paul AS and Pollard TD, **Review of the mechanism of processive actin filament elongation by formins**, *Cell Motil Cytoskel*, **2009**, 66, 606–617
- Pegram HJ et al., **Activating and inhibitory receptors of natural killer cells**, *Immunol Cell Biol*, **2011**, 89, 216 - 224
- Petrie RJ and Yamada KM, **At the leading edge of three-dimensional cell migration**, *J Cell Sci*, **2012**, 125(24), 5917 - 5926
- Petrie RJ and Yamada KM, **Multiple mechanisms of 3D migration: the origins of plasticity**, *Curr Opin Cell Biol*, **2016**, 42, 7 - 12
- Petrie RJ et al., **Random versus directionally persistent cell migration**, *Nat Rev Mol Cell Biol*, **2009**, 10(8), 538 - 549
- Piñero J et al., **DisGeNET: a comprehensive platform integrating information on human disease-associated genes and variants**, *Nucl Acids Res*, **2016**
- Pinner SE and Sahai E, **Integrin-independent movement of immune cells**, *F1000 Biology Reports*, **2009**, 1(67)
- Plotnikov SV et al., **Force Fluctuations within Focal Adhesions Mediate ECM-Rigidity Sensing to Guide Directed Cell Migration**, *Cell*, **2012**, 151(7), 1513 - 1527
- Pollard TD et al., **Actin dynamics**, *J Cell Sci*, **2001**, 114(3)
- Prockop DJ et al., **COLLAGENS: Molecular Biology, Diseases, and Potentials for Therapy**, *Annu Rev Biochem*, **1995**, 64, 403 - 434
- Purschke M et al., **Phototoxicity of Hoechst 33342 in time-lapse fluorescence microscopy**, *Photochem Photobiol Sci*, **2010**, 9, 1634
- Quintana A et al., **T cell activation requires mitochondrial translocation to the immunological synapse**, *Proc Natl Acad Sci USA*, **2007**, 104(36), 14418 - 14423
- Ratner S et al., **Microtubule retraction into the uropod and its role in T cell polarization and motility**, *J Immunol*, **1997**, 159(3), 1063 - 1067
- Reinhard M et al., **The proline-rich focal adhesion and microfilament protein VASP is a ligand for profilins**, *EMBO J*, **1995**, 14(8), 1583 - 1589
- Reynaud EG et al., **Guide to light-sheet microscopy for adventurous biologists**, *Nat Methods*, **2015**, 12(1), 30 - 34
- Ricard-Blum S, **The Collagen Family**, *Cold Spring Harb Perspect Biol*, **2011**, 3(1), a004978
- Ridley AJ et al., **Cell Migration: Integrating Signals from Front to Back**, *Science*, **2003**, 302(5651), 1704 - 1709
- Ridley AJ, **Rho GTPase signalling in cell migration**, *Cur Op Cell Biol*, **2015**, 36, 103 - 112

- Rougerie P and Delon J, **Rho GTPases: masters of T lymphocyte migration and activation**, *Immunol Lett*, **2012**, 142, 1 - 13
- Ruffell B and Johnson P, **Hyaluronan induces cell death in activated T cells through CD44**, *J Immunol*, **2008**, 181(10), 7044 - 7054
- Runnels LW et al., **The TRPM7 channel is inactivated by PIP2 hydrolysis**, *Nat Cell Biol*, **2002**, 4, 329 - 336
- Russell JH and Ley TJ, **Lymphocyte-Mediated Cytotoxicity**, *Ann Rev Immunol*, **2002**, 20, 323 - 370
- Sabeh F et al., **Protease-dependent versus -independent cancer cell invasion programs: three-dimensional amoeboid movement revisited**, *J Cell Biol*, **2009**, 185(1), 11 - 19
- Sallusto F et al., **Two subsets of memory T lymphocytes with distinct homing potentials and effector functions**, *Nature*, **1999**, 401(6754), 708 - 712
- Sánchez-Madrid F and delPozo MA, **Leukocyte polarization in cell migration and immune interactions**, *The EMBO J*, **1999**, 18, 501 - 511
- Santi PA, **Light sheet fluorescence microscopy: a review**, *J Histochem Cytochem*, **2011**, 59(2), 129 - 138
- Saoudi A et al., **Rho-GTPases as key regulators of T-lymphocyte biology**, *Small GTPases*, **2014**, 5, e28208-1
- Sasahara Y et al., **Mechanism of recruitment of WASP to the immunological synapse and of its activation following TCR ligation**, *Mol Cell*, **2002**, 10, 1269 - 1281
- Saunders AE and Johnson P, **Modulation of immune cell signalling by the leukocyte common tyrosine phosphatase, CD45**, *Cell Signal*, 22(3), **2010**, 339 - 348
- Schoppmeyer R et al., **Human profilin 1 is a negative regulator of CTL mediated cell-killing and migration**, *Eur J Immunol*, **2017**, 47(9), 1562 - 1572
- Schulz G et al., **Extracellular matrix: review of its roles in acute and chronic wounds**, WorldWideWounds, **2005** (last visited 10.07.2017 <http://www.worldwidewounds.com/2005/august/Schultz/Test-ECM.html>)
- Sebzda E et al., **Selection of the T cell repertoire**, *Annu Rev Immunol*, **1999**, 17, 829 - 874
- Shanker A, et al., **Innate-Adaptive Immune Crosstalk**, *J Immunol Res*, **2015**, 2015(982465)
- Siedentopf H and Zsigmondy R, **Über Sichtbarmachung und Größenbestimmung ultramikroskopischer Teilchen, mit besonderer Anwendung auf Goldrubingläser**, *Ann Phys*, **1903**, 4(10)
- Smith BN et al., **Novel mutations support a role for Profilin 1 in the pathogenesis of ALS**,
- Smith-Garvin JE, **T cell activation**, *Annu Rev Immunol*, **2009**, 27, 591 - 619
- Sohn RH et al., **Localization of a Binding Site for Phosphatidylinositol 4,5-Bisphosphate on Human Profilin**, *J Biol Chem*, **1995**, 270, 36, 21114 - 21120
- Somersalo K and Saksela E, **Fibronectin facilitates the migration of human natural killer cells**, *Eur J Immunol*, **1991**, 21 - 35
- Soriano SF et al., **In vivo analysis of uropod function during physiological T cell trafficking**, *J Immunol*, **2011**, 187(5), 2356 - 2364
- Sorokin L, **The impact of the extracellular matrix on inflammation**, *Nat Rev Immunol*, 10, **2010**, 712 - 723
- Stinchcombe JC and Griffiths GM, **The role of the secretory immunological synapse in killing by CD8⁺ CTL**, *In Sem Immunol*, 15(6), **2003**, 301 - 305

- Stinchcombe JC et al., **The immunological synapse of CTL contains a secretory domain and membrane bridges**, *Immunity*, **2001**, 15, 751 - 61
- Stinchcombe JC, **Centrosome polarization delivers secretory granules to the immunological synapse**, *Nature*, **2006**, 443, 462 - 465
- Stroka KM and Aranda-espinoza H, **Neutrophils display biphasic relationship between migration and substrate stiffness**, *Cell Motil Cytoskeleton*, **2009**, 66(6), 328 - 341
- Tanizaki H et al., **Rho-mDia1 pathway is required for adhesion, migration, and T-cell stimulation in dendritic cells**, *Blood*, **2010**, 116 (26), 5875 - 5884
- Teschner D et al., **In Vitro Stimulation and Expansion of Human Tumour-Reactive CD8+ Cytotoxic T Lymphocytes by Anti-CD3/CD28/CD137 Magnetic Beads**, *Scand J Immunol*, **2011**, 74, 155 - 164
- Thapa N and Anderson RA, **PIP2 signaling, an integrator of cell polarity and vesicle trafficking in directionally migrating cells**, *Cell Adhes Migrat*, **2012**, 6(5), 409 – 412
- Topham NJ and Hewitt EW, **Natural killer cell cytotoxicity: how do they pull the trigger?**, *Immunol*, **2009**, 128(1), 7 - 15
- Tybulewicz VL and Henderson RB, **Rho family GTPases and their regulators in**
- Uijtdewilligen PJ et al., **Towards embryonic-like scaffolds for skin tissue engineering: identification of effector molecules and construction of scaffolds**, *J Tissue Eng Regen Med*, **2016**, 10(1), E34 - 44
- Uribe R and Jay D, **A review of actin binding proteins: new perspectives**, *Mol Biol Rep*, **2009**, 36, 121
- Vaquero EC et al., **Reactive oxygen species produced by NAD(P)H oxidase inhibit apoptosis in pancreatic cancer cells**, *J Biol Chem*, **2004**, 279, 34643 - 34654
- Vestweber D, **How leukocytes cross the vascular endothelium**, *Nat Rev Immunol*, **2015**, 15
- Wang HB et al., **Focal adhesion kinase is involved in mechanosensing during fibroblast migration**, *PNAS USA*, **2001**, 98(20), 11295 - 11300
- Wang W et al., **NK Cell-Mediated Antibody-Dependent Cellular Cytotoxicity in Cancer Immunotherapy**, *Front Immunol*, **2015**, 6, 368
- Waring P and Müllbacher A, **Cell death induced by the Fas/Fas ligand pathway and its role in pathology**, *Immunol Cell Biol*, **1999**, 77(4), 312 - 317
- Watanabe T and Noritake J et al., **Regulation of microtubules in cell migration**, *Trends Cell Biol*, **2005**, 15(2), 76 - 83
- Wei C et al., **Calcium flickers steer cell migration**, *Nature*, **2009**, 457, 901 - 905
- Wioland H et al., **ADF/Cofilin Accelerates Actin Dynamics by Severing Filaments and Promoting Their Depolymerization at Both Ends**, *Curr Biol*, **2017**, 27(13), 1956 -1967
- Witke W, **The role of profilin complexes in cell motility and other cellular processes**,
- Wittenmayer N et al., **Tumor Suppressor Activity of Profilin Requires a Functional Actin Binding Site**, Pollard T, Ed. *Mol Biol Cell*, **2004**,15(4), 1600 - 1608
- Wolf K et al., **Collagen-based cell migration models *in vitro* and *in vivo***, *Sem Cell Dev Biol*, 20(8), **2009**, 931 - 941
- Wolf K et al., **Physical limits of cell migration: Control by ECM space and nuclear deformation and tuning by proteolysis and traction force**, *J Cell Biol*, **2013**, 20(7), 1069 - 1084

- Wozniak MA et al., **Focal adhesion regulation of cell behavior**, *BBA - Mol Cell Res*, **2004**, 1692(2), 103 - 119
- Wu CH et al. **Mutations in the Profilin 1 Gene Cause Familial Amyotrophic Lateral Sclerosis**, *Nature*, **2012**, 488(7412), 499 - 503
- Yao W et al., **Profilin-1 suppresses tumorigenicity in pancreatic cancer through regulation of the SIRT3-HIF1 α axis**, *Mol Cancer*, **2014**, 13, 187
- Yu J et al., **MicroRNA alterations of pancreatic intraepithelial neoplasias**, *Clin Cancer Res*, **2012**, 18, 981-992
- Yu S et al., **miRNA 96 suppresses KRAS and functions as a tumor suppressor gene in pancreatic cancer**, *Cancer Res*, **2010**, 70, 6015-6025
- Zaidi AH and Manna SK, **Profilin-PTEN interaction suppresses NF- κ B activation via inhibition of IKK phosphorylation**, *Biochem J*, **2016**, 473, 859 - 872
- Zhang N and Bevan MJ, **CD8⁺ T cells: foot soldiers of the immune system**, *Immunity*, **2011**, 35(2), 161 - 168
- Zhang Y et al., **Integrin signaling and function in immune cells**, *Immuno*, 135(4), **2012**, 268 - 275
- Zhou X et al., **Bystander cells enhance NK cytotoxic efficiency by reducing search time**, **2017**, *Sci Rep*, 2017, 7, 443 - 457
- Zou L et al., **Profilin-1 is a negative regulator of mammary carcinoma aggressiveness**, *Br J Cancer*, **2007**, 97(10), 1361 - 1371

7. Publications

1. Uijtdewilligen PJ, Versteeg EM, Gilissen C, van Reijmersdal SV, **Schoppmeyer R**, Wismans RG, Daamen WF, van Kuppevelt TH
Towards embryonic-like scaffolds for skin tissue engineering: identification of effector molecules and construction of scaffolds
J Tissue Eng Regen Med, **2016**, 10(1), E34-44 (Epub **2013** Mar 7)
2. **Schoppmeyer R**, Zhao R, Cheng H, Hamed M, Liu C, Zhou X, Schwarz EC, Zhou Y, Knörck A, Schwär G, Ji S, Liu L, Long J, Helms V, Hoth M, Yu X, Qu B
Human profilin 1 is a negative regulator of CTL mediated cell-killing and migration
Eur J Immunol, **2017**, 47(9), 1562-1572
3. Klein-Hessling S, Muhammad K, Klein M, Pusch T, Rudolf R, Schmitt J, Qureischi M, Beilhack A, Vaeth M, Kummerow C, Backes C, **Schoppmeyer R**, Hahn U, Hoth M, Bopp T, Berberich-Siebelt F, Patra A, Avots A, Müller N, Schulze A, and Serfling E
NFATc1 controls the cytotoxicity of CD8⁺ T cells
Nat Com, **2017**, 8(1), 511
4. **Schoppmeyer R**, Zhao R, Hoth M, Qu B
Lightsheet microscopy for long-term live 3D migration visualization of primary human cytotoxic T lymphocytes
JoVe, **2018**, in revision
5. Zhou X, Friedmann KS, Lyrmann H, Zhou Y, **Schoppmeyer R**, Knörck A, Mang S, Hoxha C, Angenendt A, Backes CS, Mangerich C, Zhao R, Cappello S, Bhat SS, Schwär G, Hässig C, Neef M, Buße B, Zufall B, Kruse K, Niemeyer BA, Lis S, Qu, Kummerow C, Schwarz EC, Hoth M
A Calcium Optimum for Cytotoxic T Lymphocytes and Natural Killer Cell Cytotoxicity
J Physiol, **2018**, accepted

8. Acknowledgements

I would like to thank

Prof. Dr. Markus Hoth - for allowing me to work on this wonderful project using state-of-the-art microscopy and methods and for constant support and help in almost every aspect related to work and beyond, for support towards a career in science

Dr. Bin Qu - for support, vivid conversation and discussions and a friendly working atmosphere

Dr. Renping Zhao - for providing data on the effect of collagen concentrations on CTL migration, for the fun we had, for exciting discussions and for sharing the frustration

Yan Zhou - for her hard work and determination on the profilin project, for showing me that will and determination can make everything possible

Dr. Wolfgang Metzger with who I could work on spheroids, for helping me with my further career, for producing a friendly and productive atmosphere and his infectious positivity

The Cytotoxicity group for vivid discussions

Dr. Eva Schwarz, Karsten Kummerow

Technical assistance

Gertrud Schwär, Cora Hoxha¹, Carmen Hässig², Janku Sandra, Sussane Renno

GS for qRT-PCR, RNA isolation, Western Blot shown in **Fig. 19**

CH¹, CH², JS and SR for cell culture of Raji, P815 cell lines

CH² and SR for PBMC isolation

CH² for bead-based cell isolations from PBMC

The Institute for *Clinical Hemostaseology and Transfusion Medicine* for providing donor blood

Personal acknowledgement

Friederike Stephani - words cannot describe

Ute Bernd und Jan Simon Stephani - for accepting me as one of their own

Dieter, Maria und Eva Schoppmeyer - for making it all possible

Sebastian Janzen - for staying a friend in troubled times

Funding

The PhD project was funded by

Deutsche Forschungsgemeinschaft (DFG) as part of the Sonderforschungsbereich
1027 (SFB 1027) Project A2 - Dynamics of T cell polarization

The profilin1 project was funded by

Chinesisch-Deutsches Zentrum für Wissenschaftsförderung GZ 857
Sonderforschungsbereich 1027 Project A2
National Science Foundation of China (81370065, 81372653 and 81172276)

The light-sheet microscope was funded by DFG (GZ: INST 256/4 19-1 FUGG)